UNIVERSITEIT VAN PRETORIA
UNIVERSITY OF PRETORIA
YUNIBESITHI YA PRETORIA

HP

Influence of an Igneous Intrusion on the Surrounding Coal Body

By

Thina Khwezi Buyisiwe Msomi

20002817

Submitted in partial fulfillment of the requirements for the degree
M.Sc: Geology
in the Faculty of Natural and Agricultural Sciences
University of Pretoria
2014

Declaration

I declare that this thesis is my own work, conducted under supervision of Dr R.J Roberts. No part of this research has been submitted in the past, or is being submitted, for a degree at any other university. It s being submitted for a degree of Masters in the Faculty of Agricultural and Natural Science, Department of Geology, Pretoria University, Pretoria.

_____

Thina Khwezi Buyisiwe Msomi

Abstract

On the north-western edge of the Witbank Coalfield, near the town of Delmas (Mpumalanga Province) a prominent and undulating sill is believed to affect quality of the coal in the seams mined in the area. The study area was separated into two subsections, Study Area A and Study Area B. In Study Area A the sill overlays the coal seams. The top of coal and the sill are separated by ~11 m thick sandstone with intermittent bands of shale, siltstone and carbonaceous shale. Study Area B, on the other hand, is located where the same sill underlies the coal seams. In this area, Dwyka tillites form the parting between the sill and the bottom coal seam. 51 composited samples were received from Study Area A and 26 uncomposited samples were received from Study Area B. In both areas, Seam 2 (bottom coal) was sampled due to its consistency and economic importance, as other seams were irregular over the complete area.

Three parameters were assessed and compared to the thickness of the sill and the distance between the sill and the bottom coal; i.e. volatile matter, calorific value and ash. The volatile matter behaviour was further investigated using an empirical equation postulated by an industry specialist to determine whether the samples had been devolatilised by an external mechanism, i.e. contact metamorphism. The experimental calculation, based on a regression slope in relation to the South African baseline, indicated that two very different events had occurred on the coal seam. In Study Area A, the calculation indicated that the coal in the area was not devolatilised, thus implying that the sill had no influence on the coal. Conversely the results of the experimental equation in Study Area B indicated that the volatile matter of the lower coal seam had been greatly reduced by an external factor and the coal was devolatilised.

Global studies of similar conditions point out that the content of volatile matter in the coal is the most affected variable during the intrusion of an igneous body into coal. This variability is governed by proximity to the sill, the shape of the intrusion, the thickness of the intrusion, orientation, location of the sill or lastly by the thermal conductivity of the country rock. In Study Area A the bottom coal seam was insulated from the heat conducted away from the sill by the presence of strata of different conductivities separating the sill intrusion from the bottom coal. On the other hand, in Study Area B heat was successfully transmitted to the bottom coal by highly conductive strata which separated the sill from the bottom coal.

Therefore the study concluded that the sill had a significant influence on the bottom coal when it was underlying the coal (Study Area B) and a conductive layer separated the sill from the coal. In addition, the results indicate that neither the distance from the sill nor the

thickness of the sill influence the effect which the sill had with the bottom coal seam in Study Area A.

Contents

Chapter 1: Introduction

The Witbank coalfield has for many years been a source for South Africa's energy production with its vast supply of accessible Karoo Supergroup coal. Over the decades good quality and structurally uncomplicated coal has been intensively mined throughout the coalfield and has ultimately left structurally and chemically complicated coal deposits of mainly lower quality than previously. Therefore a need for better understanding of the factors that affect the quality of the coal has arisen.

In the area of interest, the coal body has been found to occur in close proximity to an undulating dolerite sill. However when looking at the area locally, the sill behaves in such a way that in the western portion of the area it underlies the coal seams, while in the eastern portion the sill crosscuts the seams and overlies the seams.

1.1. Geological background

The Witbank Coalfield is one of South Africa's main producing coalfields. The coal seams occur within the Karoo Supergroup, a Late Carboniferous to Middle Jurassic sedimentary basin located in the central interior of South Africa (Figure 1 and Figure 2). The sedimentary sequence shows variations in facies that range from tillites, mudstone, shale and tills, to sandstones, reflecting the environmental changes which affected the Gondwana supercontinent, of which the Kaapvaal Craton and South Africa formed a part. The conditions prevalent in the Karoo range from glacial, deep marine, deltaic, fluvial to aeolian (Catuneanu et al., 1998).

The Karoo Supergroup is subdivided into the following:

a) Dwyka Formation

b) Ecca Group;

c) Beaufort Group; and

d) Drakensberg Formation.

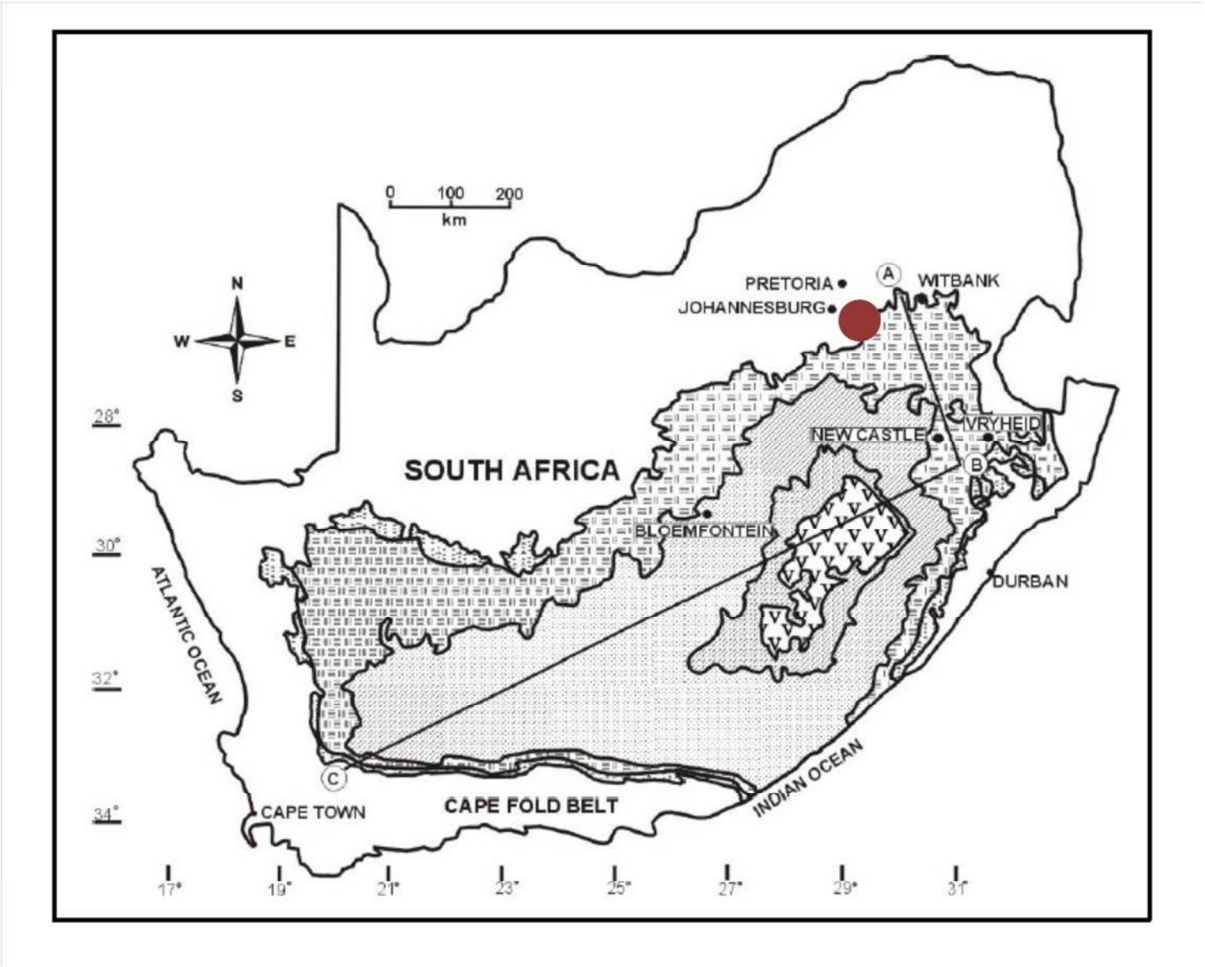

Figure 1. Plan view of the Karoo Basin in South Africa with study area indicated by the red dot (Du Plessis, 2008). Points A, B and C refer to the cross-section reproduced in Figure 2.

The lowermost Dwyka Formation is composed of glacial to periglacial sediments. The Dwyka Formation overlies the Transvaal Supergroup, which is the basement for the study areas. The formation is composed of glacial to periglacial sediments as mentioned above, that is mudrocks, sandstone, glaciolacustrine and fluvioglacial conglomerates, terrestrial moraines, lodgement tills and outwash tillites. The sediments display grading upwards into finer grained sediments (Catuneanu et al., 1998).

The presence of these particular sediments indicates glacial conditions prevailed during the Late Carboniferous to Early Permian (Snyman, 1998). The large glaciers scoured the surface, dragging sediments down the mountainous terrain into the fluvial plain to form moraines which later lithified to tillites (Falcon, 1977). In the distal (northern) depositional area where the study area for this investigation is sited, the depositional environment was controlled by the paleo-topography created by the scouring glaciers (Catuneanu et al., 1998). The surface profile of the Karoo during this period was said to be dipping in a

southerly direction, thus having a younger northern basin relative to the older southern basin (Catuneanu et al., 1998) (Figure 2)

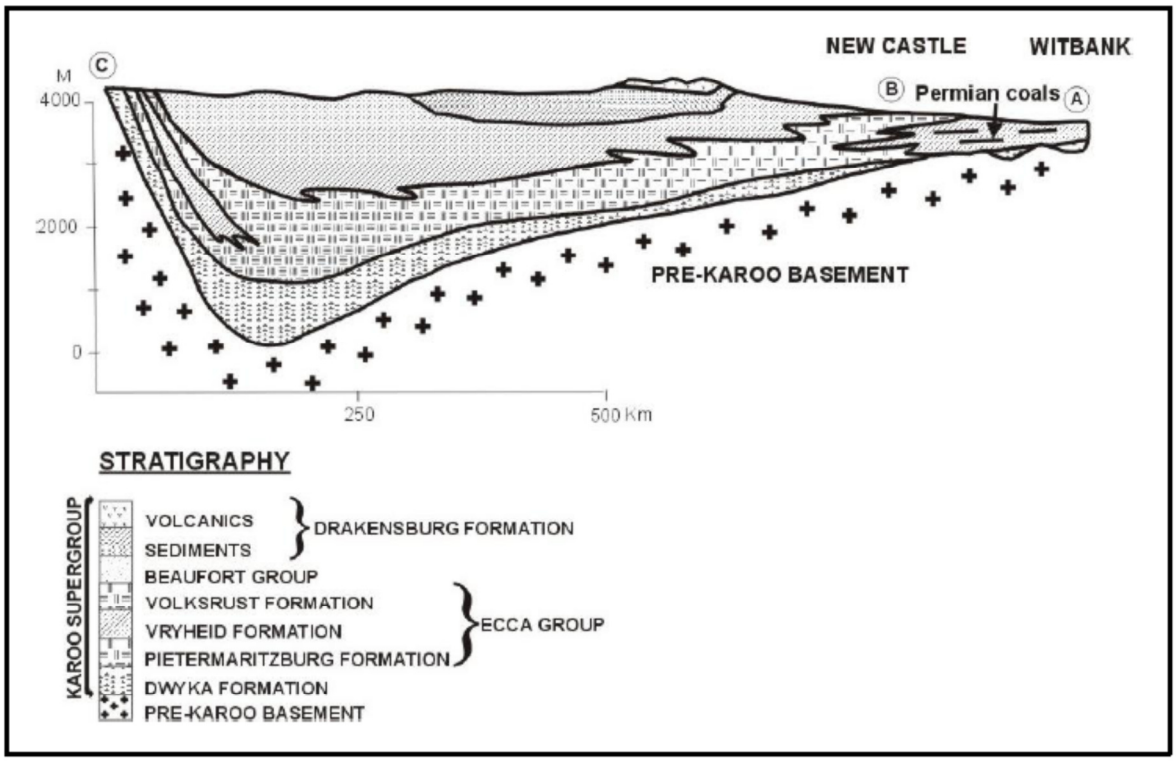

Figure 2. Cross-section of the Karoo Basin indicating the stratigraphy (Du Plessis, 2008)

Overlying the Dwyka Formation is the clastic Ecca Group. The Ecca Group hosts the Pietermaritzburg marine shale and mudstone formation, followed by the coal-bearing Vryheid Formation, which in turn is overlain by the Volkrust Formation. During the deposition of the Ecca Group, marine and non-marine conditions prevailed in the basin and the boundary between the Ecca and Dwyka is only clearly defined in the northern part of the basin. In the southern portion the Dwyka grades into the Ecca facies (Catuneanu et al., 1998).

The coal seams are present within the coal-bearing Vryheid Formation of the Ecca Group within the area of focus in this paper. The thickness of the formation varies between 0 and 500 m as seen in Figure 3, which displays the thickness isopach contours of the formation, where the thickness averages at 200 m within the coalfield. The Vryheid Formation is underlain by the glacial Dwyka Formation in the Witbank Coalfield and the Pietermaritzburg Formation is not present.

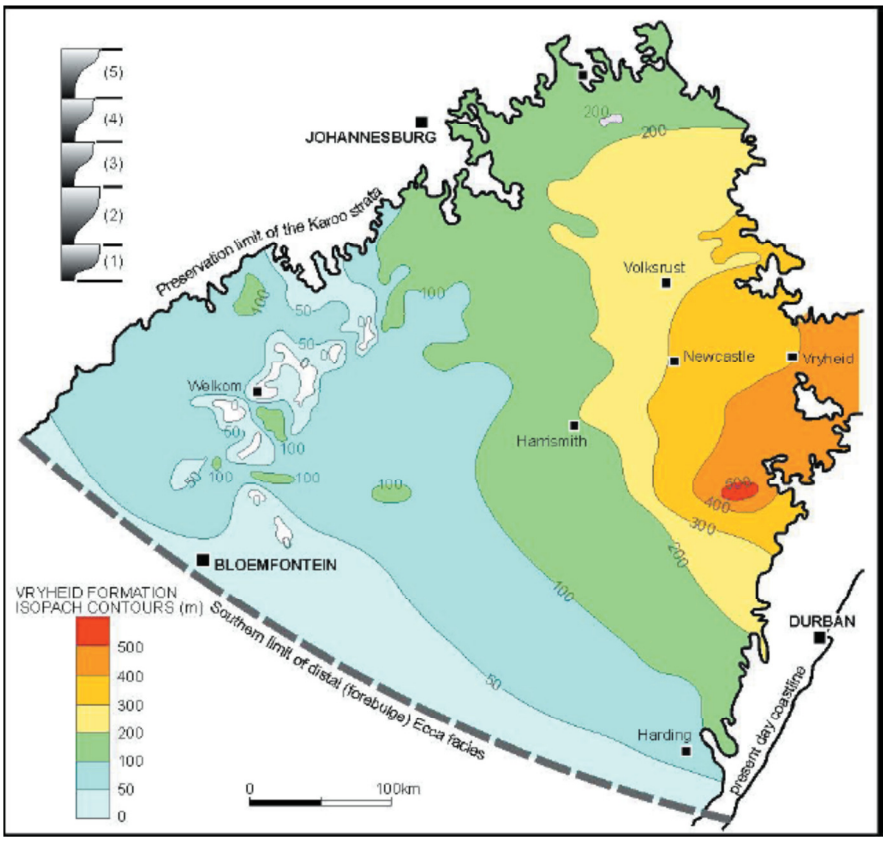

Figure 3. Isopach of the Vryheid Formation indicating thickness within the Witbank and Highveld Formation (Dekker, and van Wyk, , 2008)

The Vryheid Formation was deposited during the mid- to late Permian. The stacked assemblages of the Vryheid display upward coarsening in the lobate deltaic deposits and upward fining facies in the fluvial deposits (Cairncross, 2001). The result of the depositional conditions was interbedded shale, sandstone and coal. The formation formed initially when clastic sediments were deposited, which were followed on by peat formation and lastly finally marine transgressions (Cairncross, 2001). This is seen in three depositional intervals; lower fluvial dominated deltaic interval, middle fluvial interval and upper fluvial dominated deltaic interval. These intervals are approximately equivalent to the lower sandstones, coal zone and upper sandstones (Johnson et al., 2006). The coal initially formed in the terminal moraine formed by the melting ice sheets which contained fluvioglacial sediments within swamps in a cool temperate environment (Snyman, 1998 and Johnson et al., 2006). The peat formation is associated with delta plains, back barriers and fluvial environments with greater preference for fluvial environments (Johnson et al., 2006).

The Vryheid Formation overlies the Dwyka tillite succession which is very uneven and rugged due to the scouring effect of glaciers. This uneven topography characterised by palaeo-highs and lows created a sheltered environment that encouraged the development of peat swamps (Johnson et al., 2006). The typical environments created were ‘glacially

scoured valleys blocked by moraines and lagoons enclosed by islands of pre-Karoo rocks in conjunction with beach ridges or barrier bars' (Johnson et al., 2006). The variable topography has been said by many scholars as the controlling factor in the distribution of the lower coal seams (Cairncross, 2001), sedimentation and peat formation (Snyman and Barclay, 1989) and lateral extent, thickness and maceral content (Johnson et al., 2006).

Overlying the Vryheid Formation is the Volkrust Formation which has similar sediments as the Pietermaritzburg Formation as seen in Table 1. The formation is mostly dark shales with some mudstone, and formed in a deep to shallow marine environment (Catuneanu et al., 1998).

Table 1. Simplified stratigraphic tabling indicating the period and rock types of the Karoo Supergroup (Modified from Snyman, 1998 and Catuneanu et al., 1998)

Group	Formation	Age	Facies
Drakensberg Group		Middle to Early Jurassic (+- 187Ma)	Flood basalts
	Clarens	Early Jurassic (208-187Ma)	Aeolian sandstone
	Elliot	Late Triassic Early Jurassic (215-218Ma)	Red mudstone and sandstone
	Molteno	Late Triassic (237-215Ma)	Sandstone, mudstone
Beaufort Group		Early Triassic (250-237Ma)	Mudstone, shale, coarse to medium grained sandstone, coal
Ecca Group	Volkrust, Vryheid, Pietermaritzburg	Later to Early Permian (263-250Ma)	Shale and mudstone, Feldspathic sandstone, shale, mudstone and coal, Shale and mudstone
Dwyka Group		Early Permian to late Carboniferous (300-263Ma)	Tillite, fluvioglacial conglomerate, varved shale and drop stones.

The Beaufort Group reflects a change in the climate conditions as Gondwana continued to shift from the glacial conditions to hotter and more arid conditions. As the water table fluctuated, the oxidation process varied, and may be observed in the multi-colouring of

chemical sediments (Snyman, 1998). However, Johnson et al. (2006) suggest deposition under fluvial conditions was the cause of the multi-colouring of the group.

Overlying the Beaufort Group are the Molteno, Elliot and Clarens Formations. The Molteno is host to uneconomical and lower rank coal. The conditions during which deposition occurred for the formations became more and more arid as seen in the increasing sandiness (Table 1). The formations come to an end with the aeolian deposited Clarens Formation (Snyman, 1998).

Last is the Drakensberg Group which caps the Karoo basin and marks the end of the supergroup (Snyman, 1998, Rogers et al., 2004). The group is marked by minor sediments and followed on by a widespread outflow of basaltic lava. The outpouring of the lava was instigated by the breakup of Gondwana from Pangeae which lead to sills and dykes cross cutting the coal seams (Cairncross, 2001, Saghafi et al., 2008).

Witbank Coalfield

Five seams are found within the coalfield; however not all of them are present throughout the coalfield (Snyman, 1998). The seams occur in ascending order from 1 at the base to 5 at the top of the stratigraphy. The coal may be ranked from high-volatile bituminous to anthracite (Cairncross, 2001).

Seam 1 (S1) has approximately 2% mineable in-situ coal (Snyman, 1998). According to Falcon (1989) and Du Plessis (2008), the seam was formed in a stable shelf fluvial environment within peat swamps. The seam on average is between 1.50 and 2 m thick, and reaches an average of 2 m in Arnot. It is mainly composed of dull coal (Snyman, 1998).

Overlying S1 is Seam 2 (S2). This seam may be divided into Seam 2 Upper (S2U) and Seam 2 Lower (S2L). The seam is split by a clastic sediment lens. During the time of deposition, braided river systems meandered across the peat swamps and thus deposited the clastic sediment lens, which affected the coal's thickness and quality (Cairncross & Cadle, 1988). The seam constitutes 69% of in situ demonstrated resources relative to other seams in the coalfield (Snyman, 1998). The seam thickness varies from approximately 6.80m to 3 m from the central section of the coalfield to the eastern section respectively (Snyman, 1998) (Figure 4). S2 is characterised by increasing ash, decreasing volatile matter and decreasing calorific value in an upward direction through the stratigraphic column. Consequently S2 coal grades from brighter coal becoming duller into S2U(Cairncross, 2001).

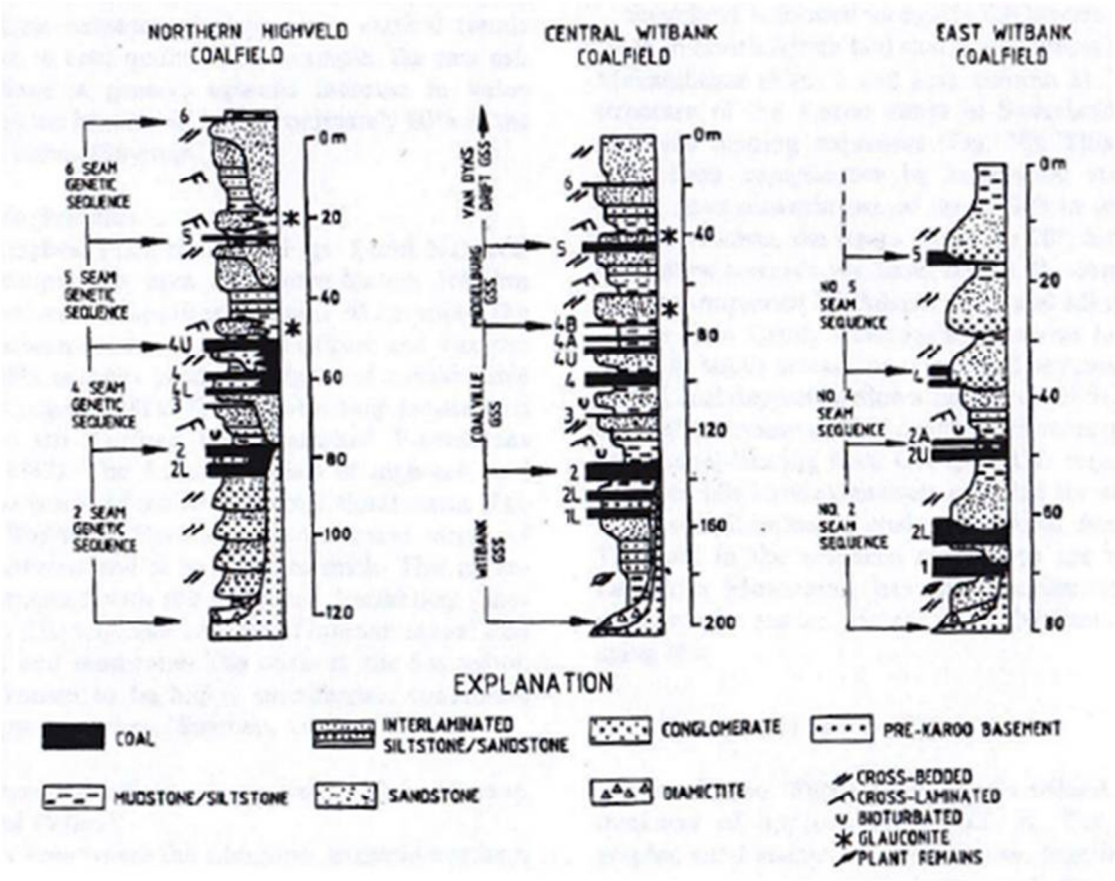

Figure 4. Stratigraphic profiles of the Witbank Coalfield and Highveld Coalfield (from Cairncross, 2001)

This is followed by the less economic Seam 3 (S3). S3 is separated from the underlying S2 by mudstone, mudstone and siltstone sediments which are indicative of the Vryheid Formation (Du Plessis, 2008). Seam 4 (S4) constitutes 26% of the coalfields resources (Snyman, 1998). The seam formed in an upper delta plain environment, in which fined grained sediments were deposited, followed by sandstone and shale simultaneously with the coal beds. The sandstone and shale deposition marks the seam parting which separates the coal seam into Seam 4 Lower (S4L) and Seam 4 Upper (S4U). The seams internally contain shale and sandstone partings. Economically the seam is mined to supply Eskom with coal for electricity generation (Du Plessis, 2008). The coal is mostly dull in appearance owing to a low proportion presence of vitrinite relative to high inertinite (Falcon, 1977, Falcon, 2012).

Lastly is Seam 5 (S5) which is located at the top of the stratigraphic column. Overall the seam is 1.50-2.0m thick; however it may be as thin as 0.50m and as thick as 2.50m (Cairncross, 1990). The seam is constitutes 4% of the in situ demonstrated resources (Snyman, 1998). The seam is commonly bright in appearance and pyrite-rich (Snyman, 1998).

1.2. Structural setting

The Karoo Supergroup overlies the Witwatersrand, Ventersdorp and Transvaal Supergroups. The Karoo Supergroup is deposited in three types of basins:

a) Retro-arc Foreland type such as the Karoo Basin in South Africa (Catuneanu et al., 1998)

b) InterCratonic rifts such as the Livingstonia in Malawi; and

c) IntraCratonic rifts such as the Waterberg Basin in South Africa (Cairncross, 2001).

Tectonically, the main Karoo Basin (KB) is a retro-arc foreland basin (Catuneanu et al., 1998). The basin underwent episodes of orogenic loading and offloading which are visual displayed in Figure 5 and 6. The loading and offloading of the basin was triggered by the formation of the Cape Fold Belt as the palaeo-Pacific plate subducted beneath Gondwana, resulting in the presence of thrust faults along the orogenic boundary.

For the duration of Dwyka deposition, the Craton was under compression and supracrustal loading was occurring, leading to uplift in the northern KB. The loading continued into the Ecca Group where unloading of the Cape Fold Belt occurred as seen in the sediments (Figure 5B). Loading began again (Figure 5C) and the process repeated as seen in Figure 5D to H. Southerly during the Stormberg group, orogenic activity decreased (Catuneanu et al., 1998).

In Figure 5, the initial orogenic loading is shown, during which the foredeep sequences (southern Karoo Basin) were deeper compared to the forebulge. With time the orogenic belt began to erode and deposited coarser facies; simultaneously a period of relaxation caused depositional foresag. In summary, the orogenic processes underwent first order orogenic loading between the Late Carboniferous and Middle Triassic and then first order orogenic unloading from the Late Triassic to Middle Jurassic, during which there were periods of relaxation (Catuneanu et al., 1998).

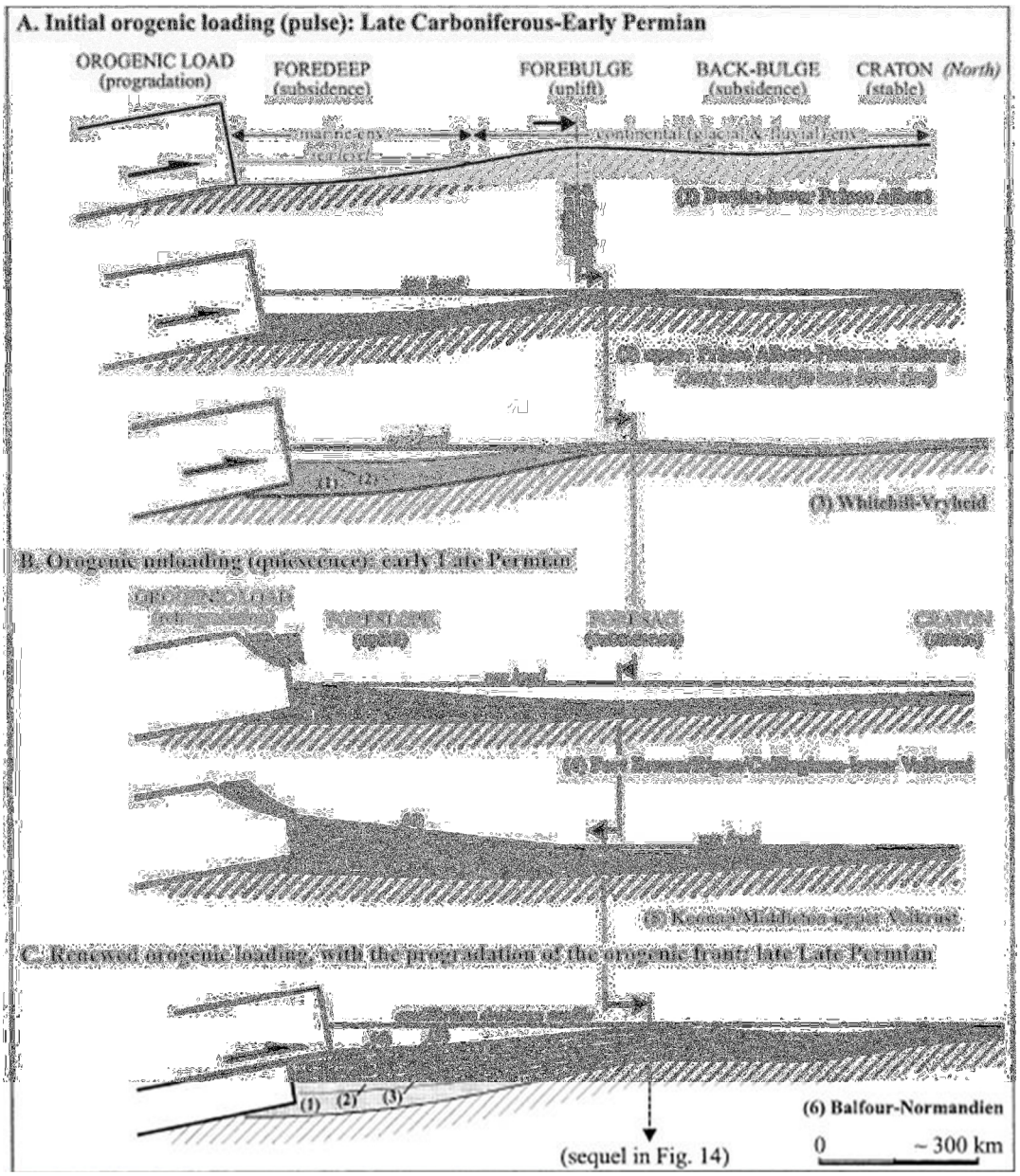

Figure 5. Loading with episodes of relaxation as described by Catuneanu et al. (1998).

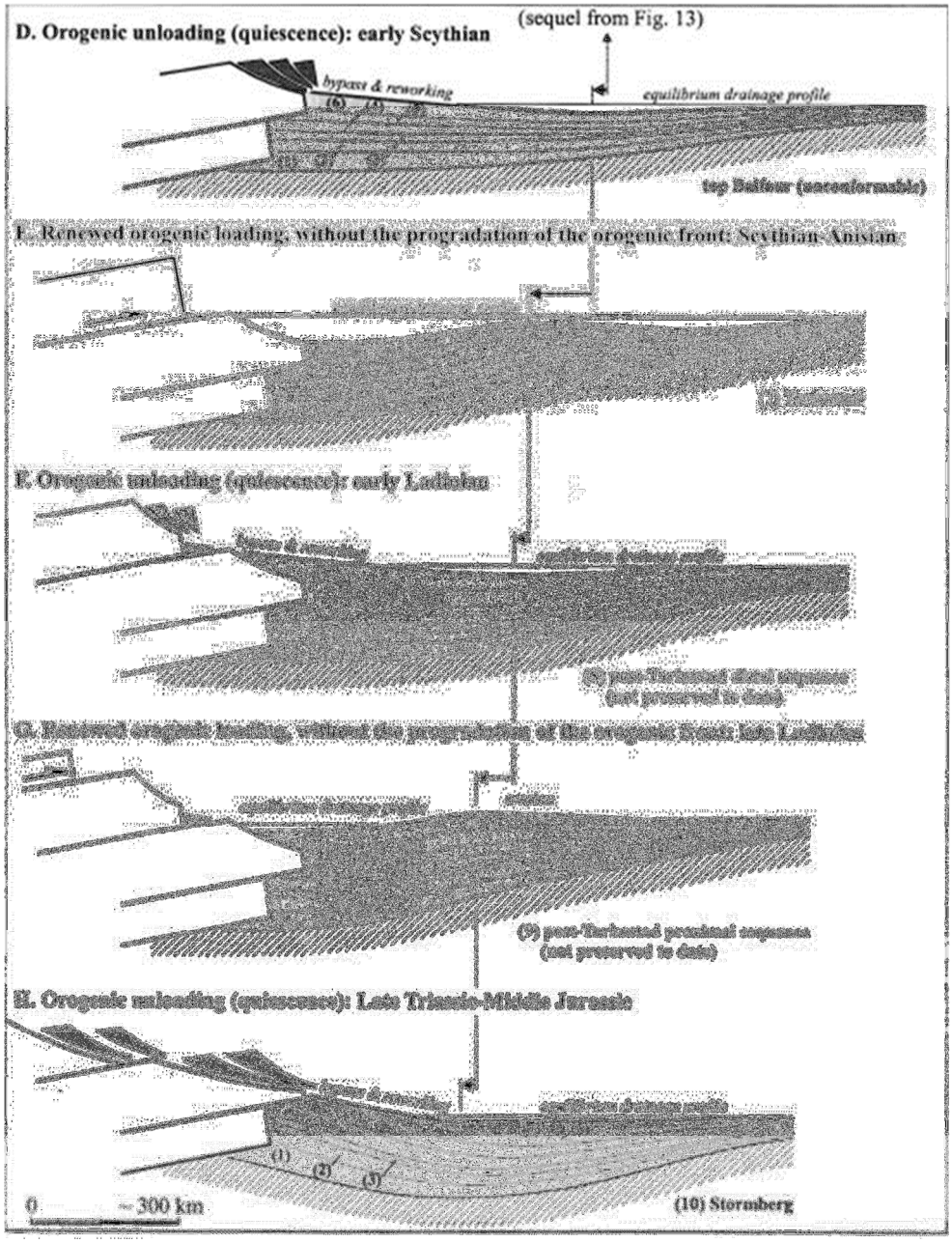

Figure 5. cont.

In late Permian to Triassic, amidst the process of loading and offloading, the breakup of Gondwana began. The tectonism came to a head during the eruption of the Drakensberg flood basalts during the Jurassic as Gondwana broke up. The volcanism is said to have continued into the early Cretaceous and resulted in the Karoo Igneous Province (Duncan and Marsh, 2006).

Witbank Coalfield Structural Setting

As the result of the Drakensberg flood basalt outpourings, numerous dyke and sill complexes spread through the coal seams. The sills were categorised by Snyman (1998) as

dykes, concordant sills and transgressive sills. Within the Witbank Coalfield, the most prominent feature from the magmatic event is that of the Ogies Dyke (Figure 6). The dyke strikes east-west from Ogies in the west to the Optimum/Arnot mine in the east (Du Plessis, 2008).

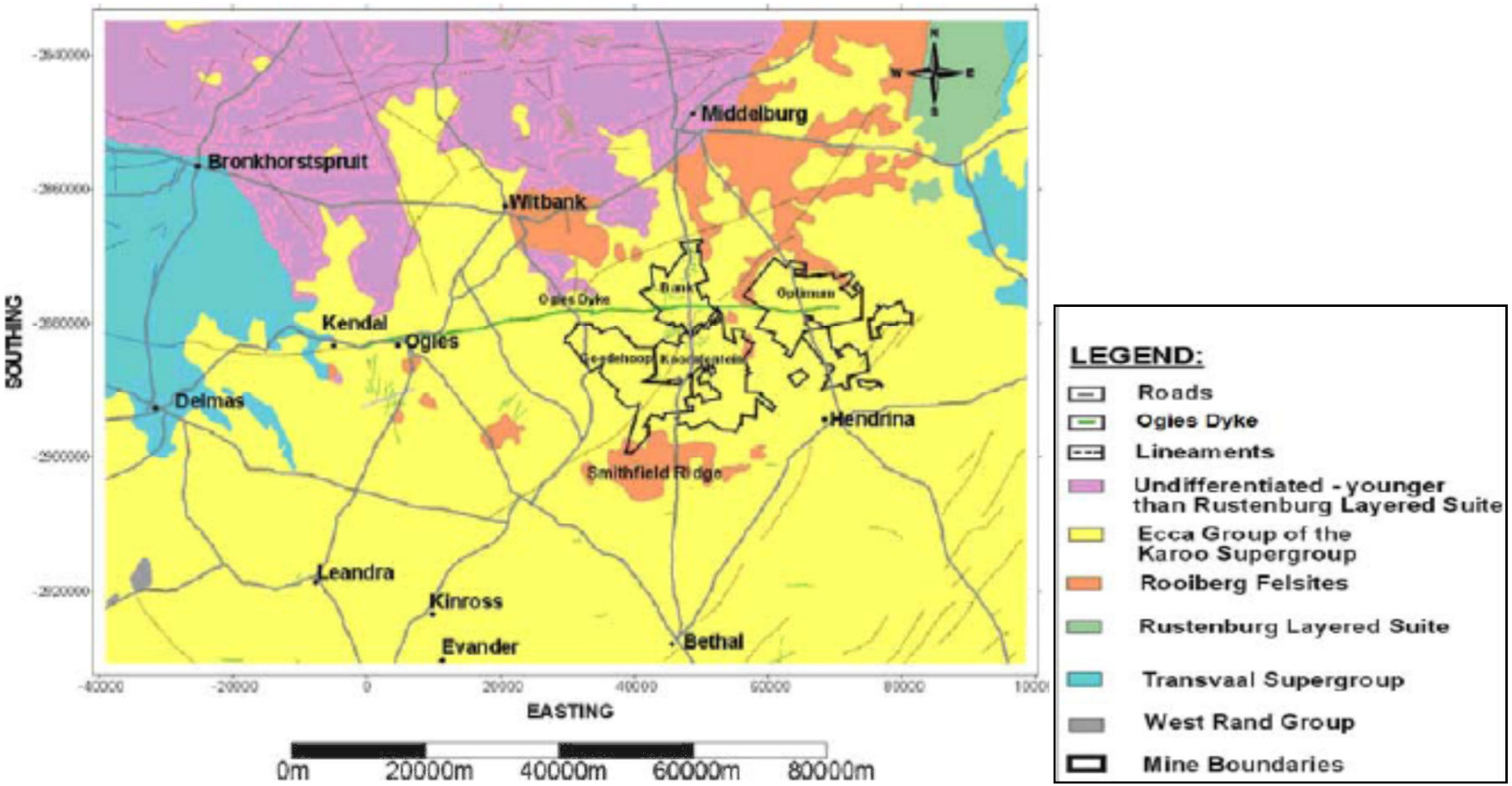

Figure 6. Witbank Coalfield indicating the Ogies Dyke and local geology (Du Plessis, 2008)

Highveld Coalfield Structural Setting

As the study area is located on the edge of the Witbank Coalfield, the Highveld Coalfield shall also be discussed. The Highveld Coalfield (Figure 7) is located south of the Witbank coalfield. It also has been inundated by sills to a greater extent than the Witbank Coalfield (Snyman, 1998). The coalfield lies on palaeo-topographical highs and lows, which control the distribution of the coal seams. The dykes range in thickness between 0.10 and 5 m, while the sills reach a maximum thickness of 40 m. In his research, Saghafi et al. (2008) found the dykes have been measured to having a north north-east strike and three dolerite sills have been identified in the coalfield: sill number 4 (B4), sill number 8 (B8) and sill number 6 (B6).

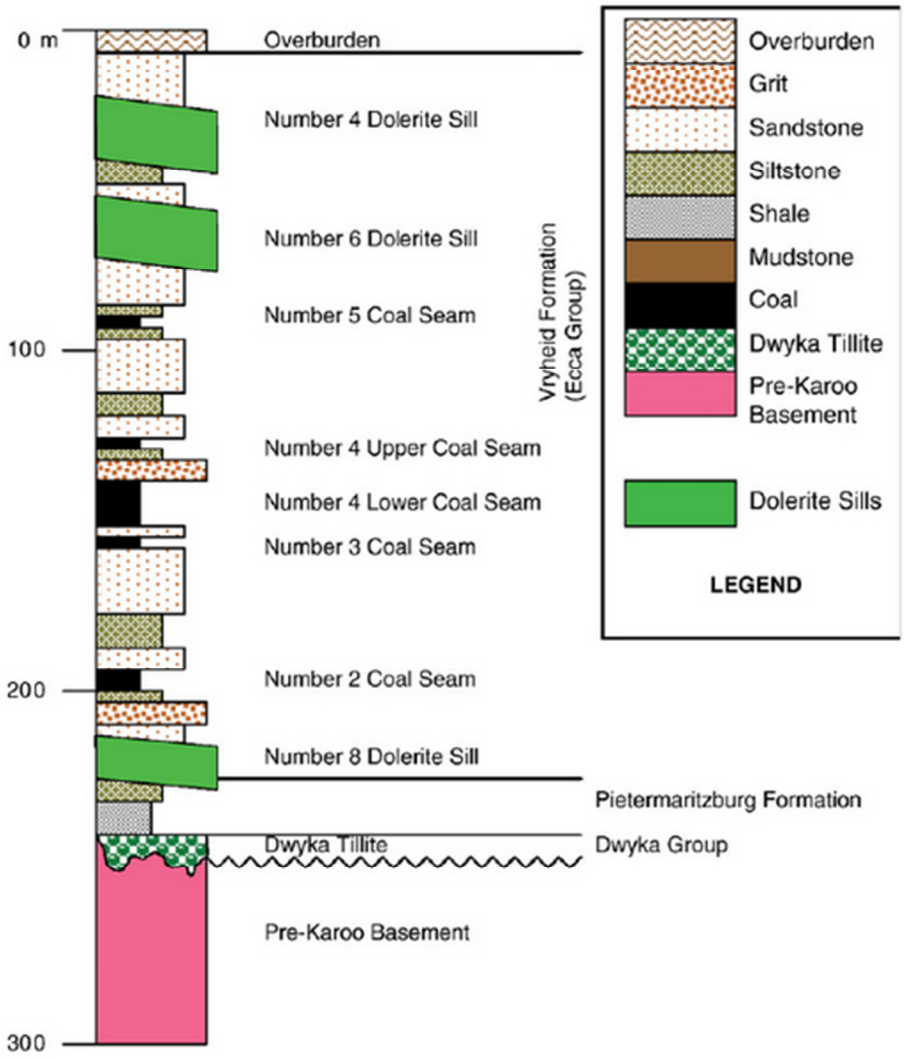

Figure 7. General stratigraphic column of the Highveld Coalfield (Saghafi et al., 2008)

The oldest and thickest sill in the coalfield is the number 4 (B4) sill. The sill is located closest to the surface where it has weathered and lies below the coal, and has resulted in

displacement but little devolatilisation of the coal. In terms of age, number 8 (B8) sill is younger than B4. The sill is 15 to 20 m thick and studies have indicated that it has created most of the devolatilisation in the coalfield relative to number 4 (Saghafi et al., 2008). Lastly the youngest sill is the roughly 0.50 m thick number 6 (B6) sill. It is not a continuous feature in the coalfield. Structurally the coalfield is bound by an east-west graben structure (Snyman, 1998). The joints and faults which are present have been intersected by the sills (Saghafi et al., 2008).

1.3. Study areas

The area of interest is located on the north-western edge of the Witbank Coalfield. It is further separated into Study Area A and Study Area B. It is bounded by the South Rand Coalfield and Highveld Coalfield, south-west and south-east respectively (Figure 8).

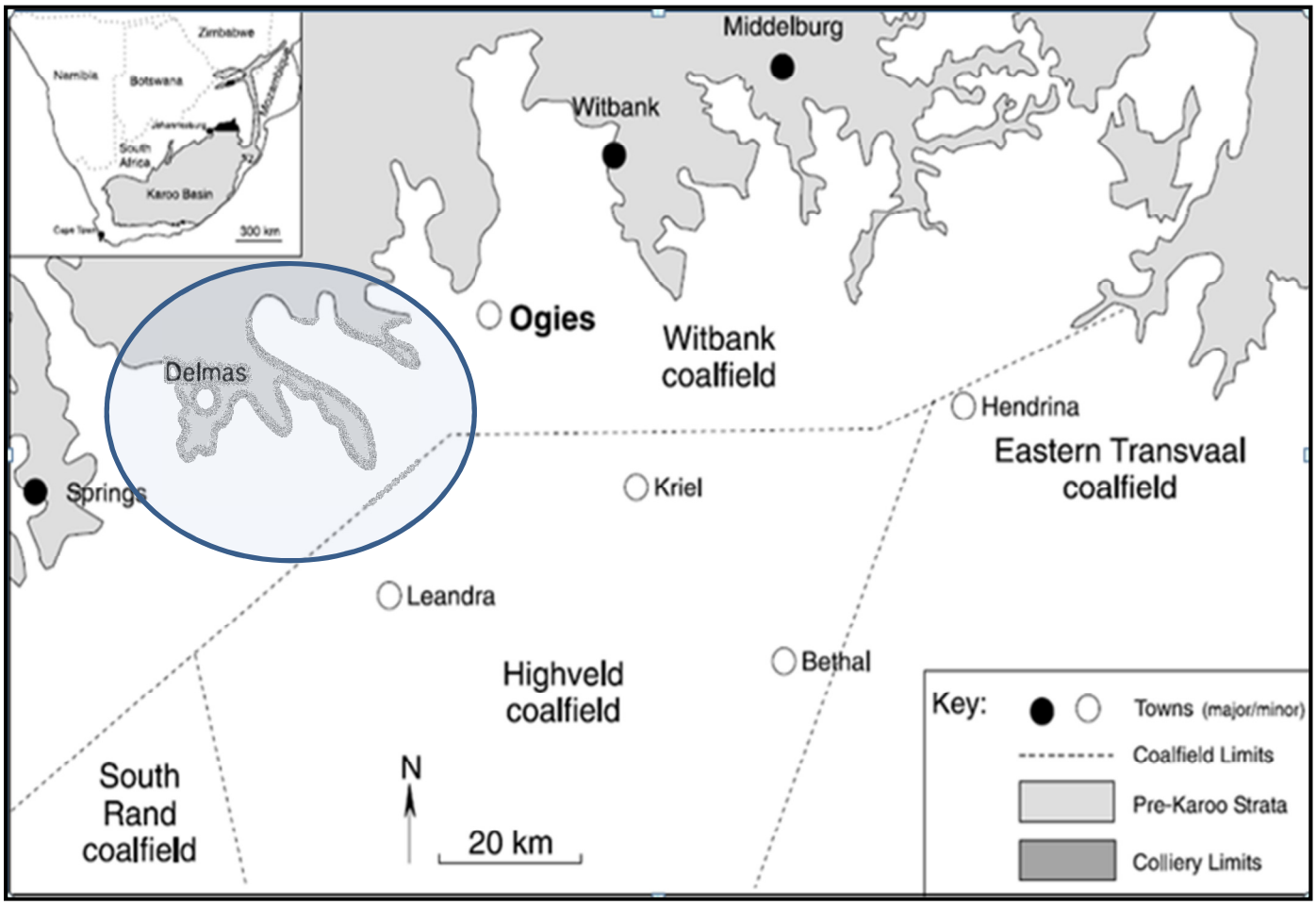

Figure 8. Map indicating the location of study area with respect to the Witbank, Highveld and South Rand Coalfields (Du Plessis, 2008).

In the mine area, the coal is intruded by numerous dolerite intrusions. The main intrusion is a large sill which initially intrudes the floor tillites to underlie the coal and as it moves in a

southerly-easterly direction it traverses through the coal and overlies the coal seams. Past studies have suggested that the sill present in the study area is the same number 4 (B4) sill which is present in the Highveld Coalfield (Dekker and van Wyk., 2008, SRK Consultancy, 2006). Within the mining area, thin dolerites dykes are present which cut through the coal seams.

The Witbank coalfield is subdivided into coal seams 1 to 5 as mentioned above; however in the study area the seams are further separated into bottom coal and top coal. These names can be roughly correlated with the Witbank seams. The bottom coal (BC) may be correlated to S2, and the top coal (TC) to S4 and S5 in the study area (Figure 9) (per. comm. F. Schutte).

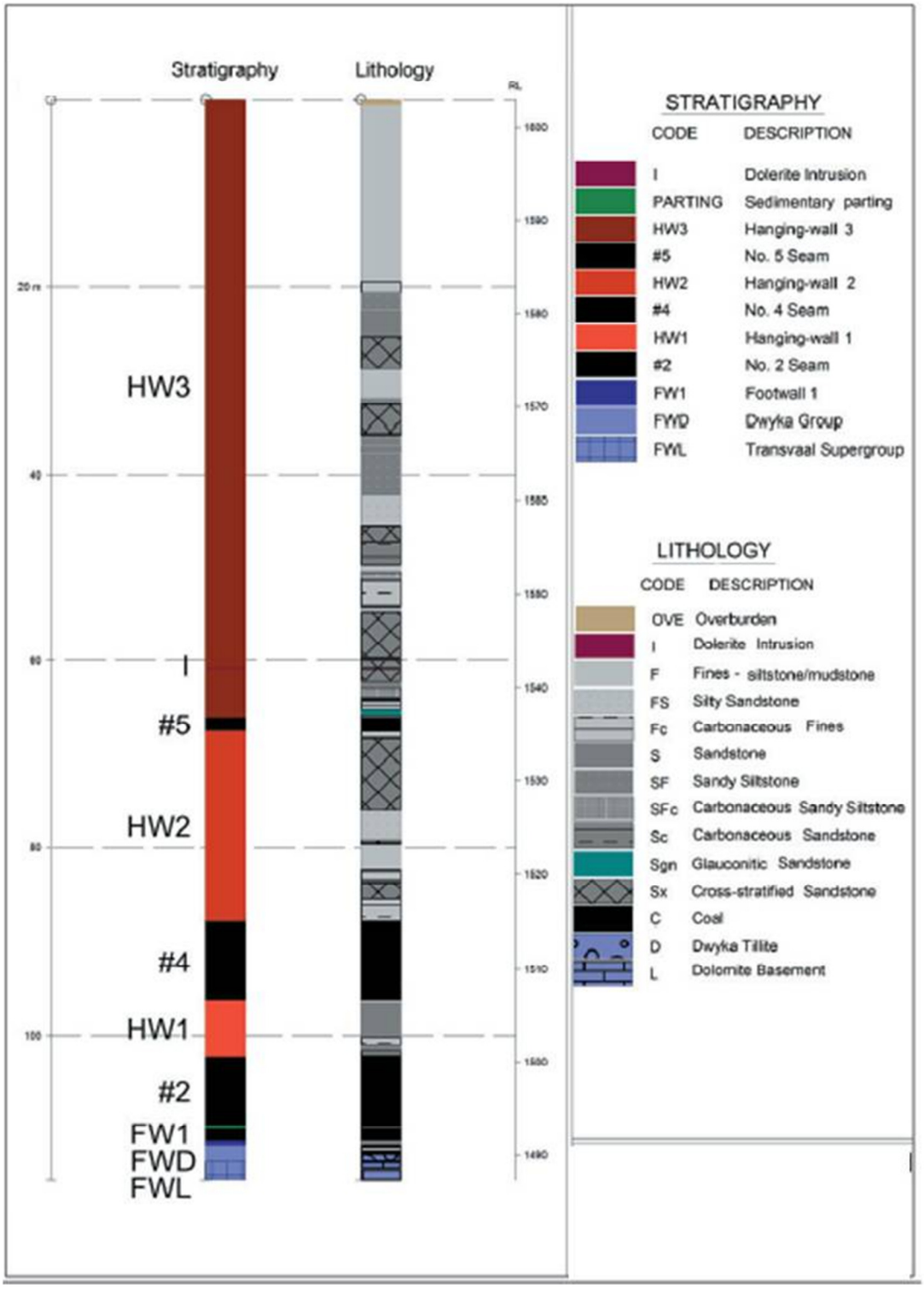

Figure 9. Generalised stratigraphic column of Delmas area (Dekker, and van Wyk, 2008)

Seam 2 within the Witbank Coalfield is subdivided into S2U and S2L and is separated by a clastic sediment lens. However within the study areas, no seam parting is present and is defined on differences in volatile content, that is medium volatile or low volatile (Figure 10).

Overlying S2 is a shale band, locally called the O-shale. The shale has an average thickness of 0.40 m. The shale is used as the marker which separates S2 from S4 (Figure 10).

Seam 4 is subdivided into S4U and S4L (Figure 10). S4L is a 3 to 4 m thick. It is higher in ash relative to S2L and is mainly dull in appearance. Overlying the S4L is the X-shale, which is approximately 0.40 m in thickness as well. S4U shares similar characteristics as S4L, and both are mainly mined for power generation.

Seam 4U is followed by the BB-shale, which is in the region of 0.30 to 0.40 m in thickness. This is finally overlain by S5, which is not present throughout the study area; where present it has a thickness of 0.50 m (Figure 10). It is mainly composed of bright coal, but is rich in pyrite as observed in drill holes and opencast workings (per comm. C. Van Ryneveld).

In Study Area A, S5, S4U and S4L, S2U and S2L are present, while in Study Area B, S4U and S4L, S2U and S2L are present. However S2U does not occur consistently throughout the Study Area B and will thus not be considered for the investigation which therefore means the BC will be only samples of S2L.

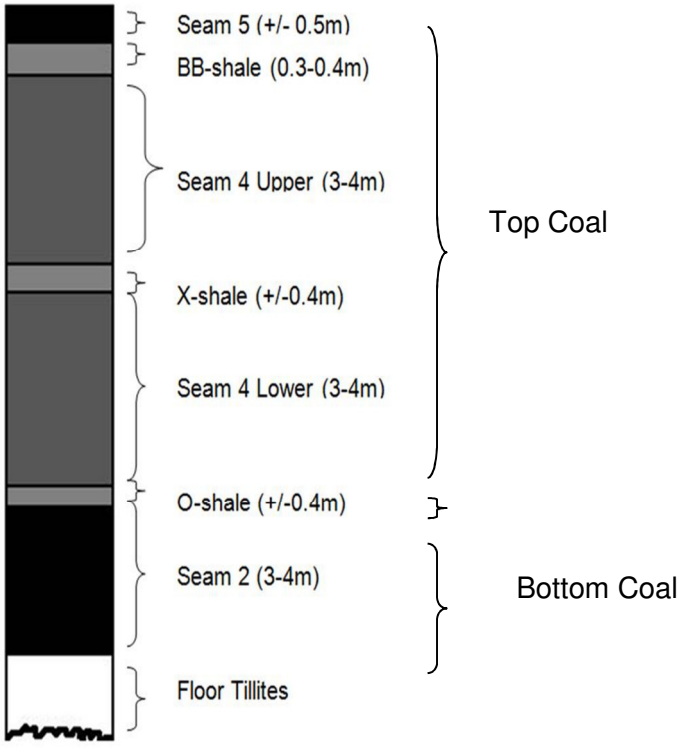

Figure 10. Simplified stratigraphic column of both study areas.

1.4. Influence of dolerite intrusions on coal

Literature review

Dolerite intrusions are a common feature within the Karoo Basin (Duncan and Marsh, 2006). The intrusions have been linked to the breakup of Gondwana from Pangaea in the Early Jurassic. In the main basin, in South Africa, the intrusions have manifest themselves as extensive cross cutting dykes or displacing sills as seen in Figure 11. Where the intrusions interfere and interact with the country rock, thermal contact metamorphism occurs. The intrusions not only affect the quality and characteristic of the coal (Van Alphen, 2012), they also have a direct influence on mining processes (Du Plessis, 2008).

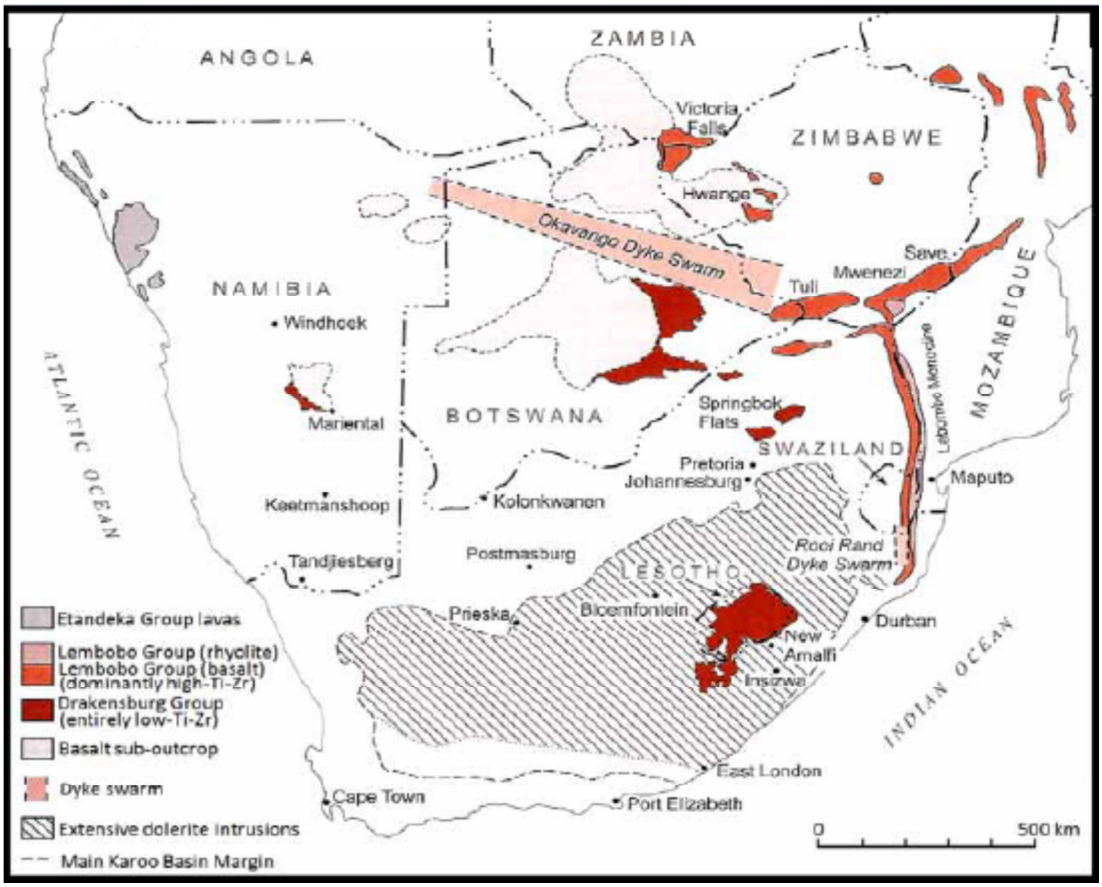

Figure 11. Location of Karoo age intrusions (Duncan and Marsh, 2006).

In the study area, the intrusions not only cause transformation of the coal; they also have an influence on the physical characteristics of the coal as well as the combustion characteristics (Van Alphen, 2012; Melenevsky et al., 2008). Along the contact between the intrusion and the coal, transformation of the coal is seen visually where the coal may appear to be burnt. Analytically the coal may be devolatilised; that is, the volatile matter original present has been driven off by the high temperatures. If the temperatures are high enough the coal may be converted to a higher ranking such anthracite and coke (Falcon, 2012; Melenevsky et al., 2008).

Many studies have been undertaken in order to understand the influence of sills on the surround country rock, with particular focus on coal and organic matter rich sedimentary rocks. In their study of a lamprophyric sill which underlay a coal seam, Crelling and Dutcher (1968) discovered that the coal had been thermally altered, noting the highly contorted bed, the natural coke and the prismatic fracturing of the coal zone. It was also deduced that the sulphur content of the coal was not influenced by the sill and had no relation to the sill. However volatile matter was found to have been influenced by the sills. The volatile matter was highest at the seam margins and as the distance between the seam and sill decreased, the volatile matter showed an increase. Crelling and Dutcher (1968) attributed this finding to either the release and re-absorption of the volatile matter, or the volatile matter was never released initially during heating.

Snyman and Barclay (1989) deduced that the early Jurassic intrusions that cross cut the Karoo sediments affected the coal by 0.60 to 2 times the thickness of the intrusion (variable distance). They also deduced that the rank of the coal outside the contact aureole did not play a role in the distance with which the intrusion had an effect. According to Cairncross (2001) the higher rank anthracite deposits of the KwaZulu Natal Coalfields were induced by the additional heat introduced by the early Jurassic sills, resulting in the devolatilisation of the bituminous coal.

Saghafi et al. (2008) concluded that the bituminous and sub-bituminous coal of the Highveld Coalfield had been adversely affected by the dolerite intrusions (sill and dykes). The coal had been devolatilsed and displaced as a result of the intrusions. From the study it was concluded that metamorphism of the coal had increased the coal's gas storage capacity (CO_2) and that the dolerites were capable of storing and trapping gas.

Melenevsky et al. (2008) investigated the influence of a 6.75 m thick dolerite dyke which intruded a sheet of coal. The investigation showed that the bituminous coal that was in contact with the dyke was altered to anthracite. It was also reported that most of the volatile matter in the coal was released during the first stage of contact metamorphism.

Studies conducted on the metamorphic effect of dolerite intrusions have indicated various outcomes. Arnes et al. (2010) noted that when a sill interacted with the Ecca Group, the organic matter was converted to hydrocarbons and dehydration reactions were observed. Yao et al. (2011) concluded that intrusions affected the coal quality, rank and adsorption capacity depending on the following:

a) The emplacement temperature during intrusion;

b) The style of heating transfer as well as the thermal properties of the surrounding rock;

c) The form, size and shape of the intrusion; and

d) The distance from the contact boundary.

1.5. Aim and objectives

The aim of the study is to investigate the effect of the undulating sill on the coal within its immediate vicinity and the implications this relationship has on the volatile matter, ash and calorific value of the coal.

The objectives of the study are to acquire data concerning the study area from the mine and extract relevant parameters from the data received. These parameters are then to be interpreted in order to deduce the results. The results are then compared to a hypotheses related to the effect which dolerite intrusions have on surrounding coal.

2. Methodology

2.1. Data source

Data for the research originated from the mine's database, and is historical data from previously drilled drill holes that were logged by the mine's geologist and analysed by an SABS approved laboratory.

In addition to database data, two drill holes were personally logged for the study. The drill holes were logged, photographed and sampled for the purpose of understanding the historical dataset that was used for this study.

2.2. Drill hole logging

Logging is generally conducted by the mine geologist. The drill holes are drilled vertically with an azimuth of zero degrees (0°) and a dip of 90°. No inclined boreholes area drilled in the area. The drill holes are piloted to below the soft sediments and, thereafter the diamond core drilling proceeds. The hole is drilled through the overlying sedimentary strata into the coal and commonly terminates where it intersects the tillite floor.

The following coal seams are present in the study area: S5, S4 and S2. The seams are further broken down to S4 and S4L, S2U and S2L. The following naming conventions for describing the lithology are used:

a) Shale;
b) Shaley coal;
c) Coal shaley;
d) Coal dull;
e) Coal mixed dull;
f) Coal mixed; and
g) Coal bright (though it is not found in this study).

The S4U and S4L are logged as mainly coal dull with bands of coal shaley and shale coaly. S2 is a combination of coal mixed dull, coal dull and coal mixed with intermittent coal shaley.

During logging the following features are identified:

a) Lithology;
b) Mineralization;
c) Intrusions;
d) Sedimentary features; and
e) Structures.

Features are measured on a centimetre scale basis and descriptions are included. The colour, weathering and texture are noted on a log-sheet. Once the drill holes have been logged and sampled, the data is then captured onto soft copy and stored in a database. Such information is utilised for geological modelling as is the case in the study.

2.3. Sampling

After the drill holes have been logged according to the mine's standards, the coal is then sampled. The coal was sampled the following way:

a) Coal must be sampled irrelevant to its length;
b) Shale is sampled individually, unless the shale is thin and is interbedded with the coal;
c) Dolerite is not sampled;
d) Each sample bag is tagged with the following information: drill hole identification and the meters at which it was sampled; and
e) The bags are sealed and documented on the log sheet.

The sample information is also captured onto the data management software and later the wash information is captured onto it.

2.4. Analytical method

Once the coal has been logged and sampled, it is then sent to a SABS approved laboratory for analysis. Coal is traditionally analysed by proximate analysis, ultimate analysis, and calorimetry. Proximate analysis records the following parameters:

a) Ash content (ash);
b) Volatile matter (V.M);
c) Fixed carbon content (F.C);and
d) Inherent moisture content (I.M).

Ultimate analysis is that of total sulphur (T.S) and phosphorus, whereas calorimetry measures the calorific value (C.V) of the coal. Phosphorus is conducted on per request basis and is not a standard analysis like the other analysis parameters

The method used to determine the parameters is sink float analysis which is based on the Relative Density (R.D) of the sample (Falcon, 2012). Relative density is defined as the 'ratio of the mass of a certain volume of coal (or rock) to that of an equivalent volume of water' (SANS 10320, 2004).

During the sequential sink float method the coal is processed through a number of liquids of different relative densities: 1.40, 1.50, 1.60, 1.70, 1.80 and 3.00 (Figure 12).

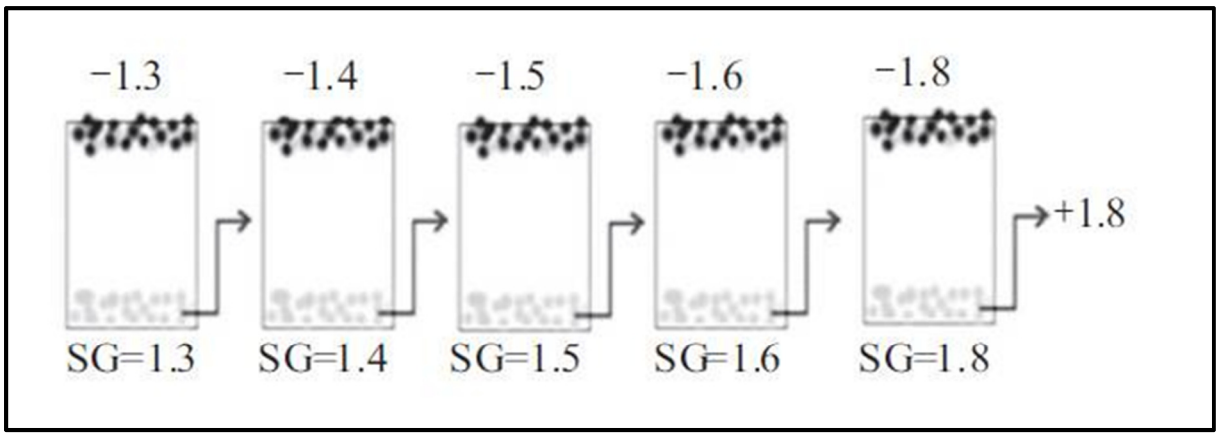

Figure 12. Diagram displaying the sink-float process (Hamidreza et al., 2012).

During sink float analysis, a sample of coal is placed in the lowest density liquid; the material which floats is washed and analysed for the above mentioned parameters, and the remaining material is then placed in the next liquid of higher density liquid (Figure 12). This is continued until a density of 1.80 R.D. is reached. The remaining material is considered mostly inorganic material with a density greater than 3.00 R.D. It is commonly reported as the 'sink'.

Other types of analyses available assess the physical nature and condition of the coal. They assess the size distribution, calorific value, the abrasiveness of the coal and lastly the hardness or grindability of the sample (Johns, 2012).

The third group of analyses are rank related which focus on the basic properties of the coal. During this the petrography is investigated, coking tests are conducted such as CNS, Roga Index, plastometer and dilatometer (Johns, 2012).

Lastly the combustion and heating capabilities of the sample are explored. The combustion kinetics, TGA combustion, volatile release curves are plotted and drop tube furnace tests are some of the important tests available (Johns, 2012).

2.5. Analyses presentation

The analytical data is reported as the drill hole identification (BHID), R.D1 and R.D2, the raw R.D, yield measured at that R.D, I.M, ash, V.M, T.S and C.V (Table 2)

Table 2. Analytical data reporting format

BHID	R.D1	R.D2	RAW R.D	Yield	I.M	Ash	V.M	T.S	C.V
A1	0	1.4	1.64	0.10	2.00	19.20	8.20	0.60	26.80
A1	1.4	1.5	1.64	0.30	2.20	20.70	8.00	0.50	26.10
A1	1.5	1.6	1.64	0.90	2.10	23.10	7.90	0.50	25.00
A1	1.6	1.7	1.64	2.50	2.60	25.10	7.70	0.40	23.90
A1	1.7	1.8	1.64	6.80	3.50	27.80	9.50	0.30	21.80
A1	1.8	9.9	1.64	100.00	4.30	57.40	10.10	0.20	8.90

Included with the analytical results in the database are the coordinates as surveyed after drilling has completed. Thus the results include drill hole I.D, final coordinates and qualities of the sample.

2.6. Data received

The original data received for this study consist of analyses of cumulative data as well as fractional data; however no raw analysis was conducted on the coal samples for both study areas. Fractional data is data collected during sink-float analysis at different relative densities, for which both proximate and ultimate analysis for each fraction is reported. Cumulative data is data determined through cumulating the fractional data to 100% of sample matter recovered (known as the yield). The final category for the cumulative data is the sink, which has a value of 3.00. The sink represents all the material present in the coal that does not float at R.D's less than 1.80. By comparison, raw analysis is the data collected by crushing the entire coal sample to the relevant size and analysing it without beneficiating the coal through sink flotation. In raw analysis, the coal is analysed along with the inorganic material present in the partings in the coal seam, whereas in fractional and cumulative data, only the coal and its contents is analysed.

2.7. Sample data

In total 51 samples from Study Area A were utilised for the study and 26 samples in Study Area B. The samples were all analysed according to the parameters above. A typical drill hole logged by the mine's geologist found within Study Area (A) is seen in Figure 13.

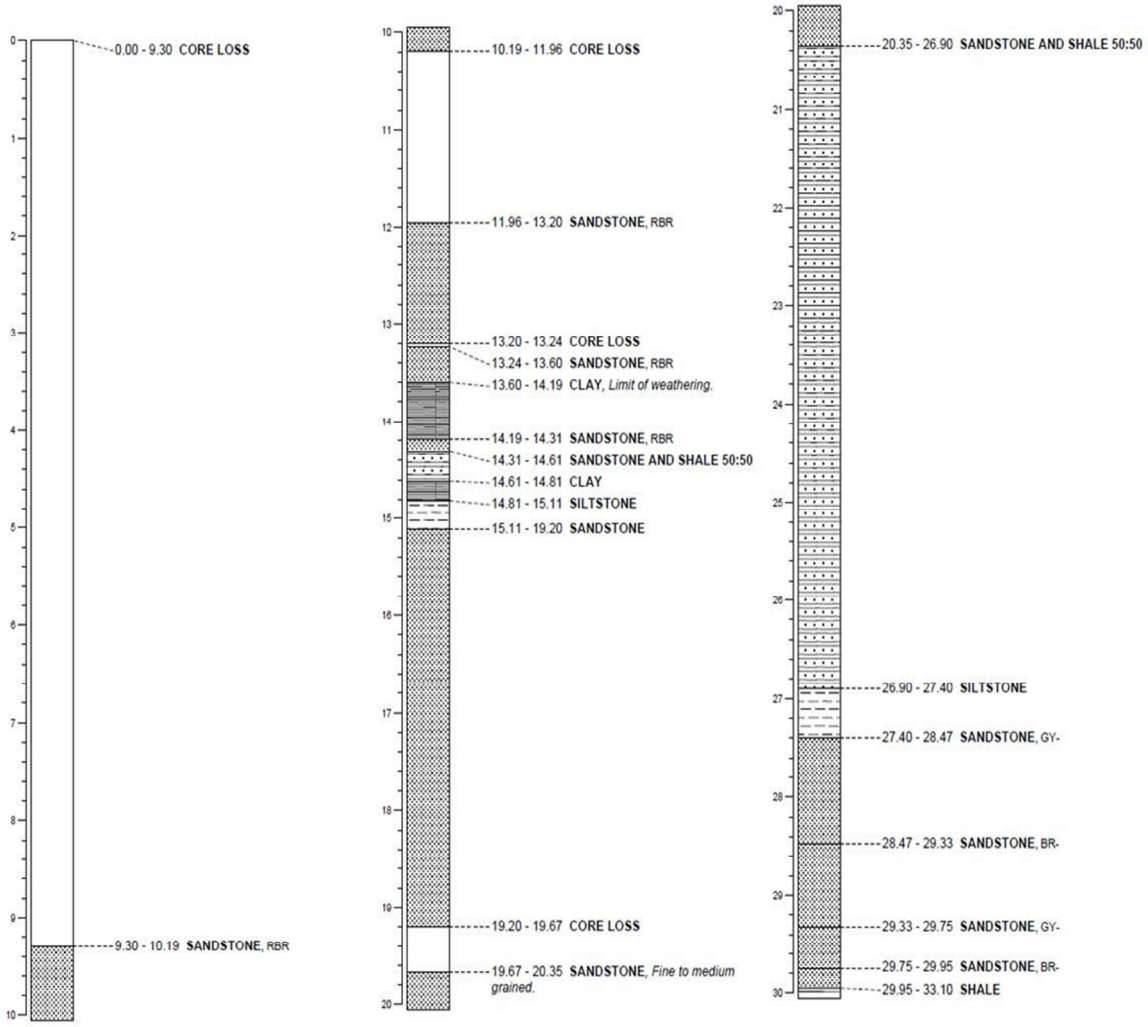

Figure 13. Drill hole A1 from Study Area A as logged by the mine's geologist.

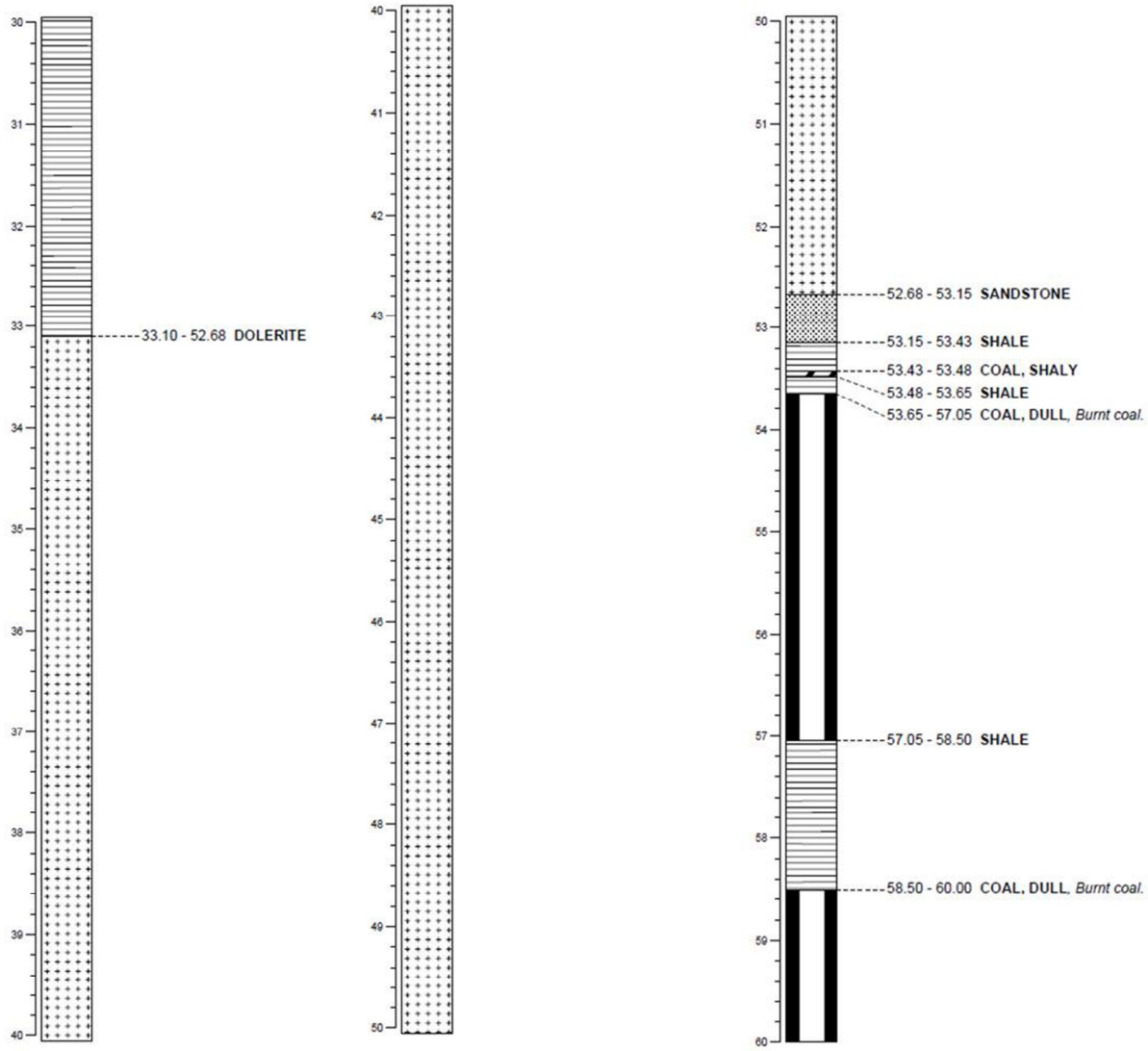

Figure 13. Continuation of drill hole A1.

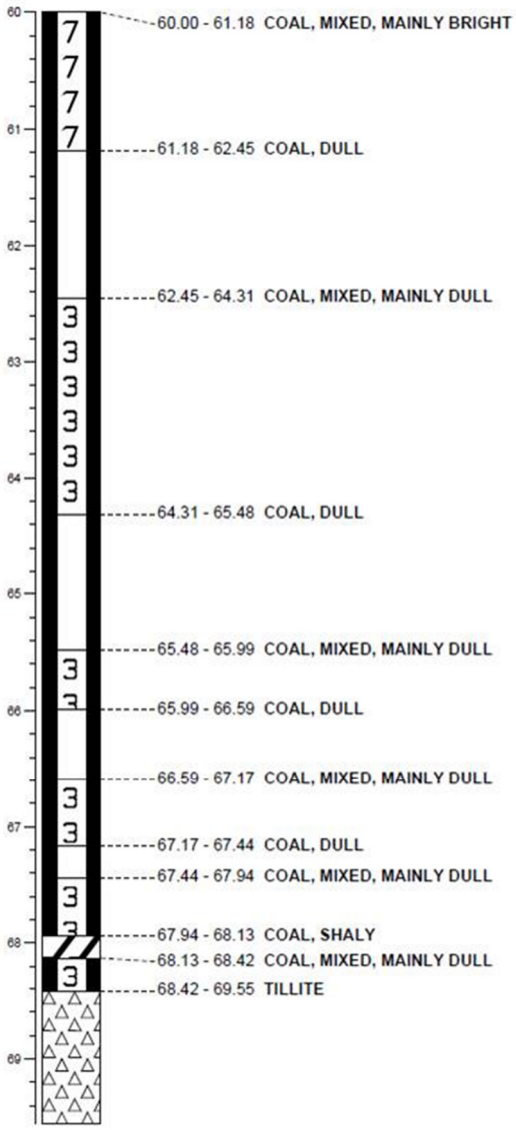

Figure 14. Continuation of drill hole A1

2.8. Data preparation

From the two study areas, data preparation was conducted prior to any work on the data. The following steps were taken:

a) Data validation;
b) Exclusion of data;
c) Selecting the sink qualities (R.D of 3.0);
d) Calculation of thickness of sill and distance from the bottom coal to the sill's floor; and
e) Populating the data into excel worksheets.

Validation and exclusion of data

During validation the data was assessed for a number of constraints. During which the relationship between the various parameters was examined.

The relationship between calorific value with increasing relative density in cumulative wash data was evaluated through 'IF' statements. The equation used is **=if (cv above> cv below, true, false).** Similarly, evaluation of the relationship between ash with increasing relative density was conducted through 'IF' statements. Simultaneously the relationship between cumulative yield and increasing relative density was evaluated through 'IF' statements on Excel. That is **=if (ash above<ash below, true, false)** and **=if (yield above < yield below, true, false)**, respectively. Data which reported a false was checked in the original data received and also with the lithological logs of the samples.

Graphical validation was conducted on the data set. That is the relationship between calorific value and ash. Scatter graphs were plotted for the two parameters. Similarly, graphical relationship was plotted for the relationships mentioned in the above paragraph.

Drill hole collars were plotted in space to determine the spatial relationship of the data points received.

Lastly the sample boundaries were checked that they correlated with the lithological boundaries.

The consequence of validation was that erroneous data is detected. Therefore once data was found to have errors the original data was checked if it was correct and no typing errors may have been present during validation. Once that was confirmed and the error did not lie in typing error, the analysis of the sample was assessed to the lithology of that particular sample. The assessment aimed to ascertain if there was a correlation between lithological data and analytical data. The assessment was based on typical qualities of types of coal.

According to Falcon (2012) each lithotype of coal is composed of microlitotypes which is further broken down to macerals (Figure 15). That is, bright coal is high in vitrain that gives the appearance of a glossy shine which has >65% vitrinite. Such coal has characteristic qualities, one of which is that it floats at R.D<1.45, it has low ash and volatile matter of approximately 30% (Figure 16).

Banded coal is a combination of vitrinite, inertinite and liptinite. These macerals are present in various ratios and when combined they form microlithotype called clarite. In the logs such coal is called coal mixed dull and if sampled with a shale parting or shale lens, as is the case in our study area, typical qualities are approximately 14% ash and 24% volatile matter.

Dull coal is higher in inertinite, with inertinite being over 56%. Once such coal is sampled with an inorganic material such as any sedimentary rock, the qualities expected (once beneficiated) are approximately 25% ash and a lower volatile of 14% (Figure 16).

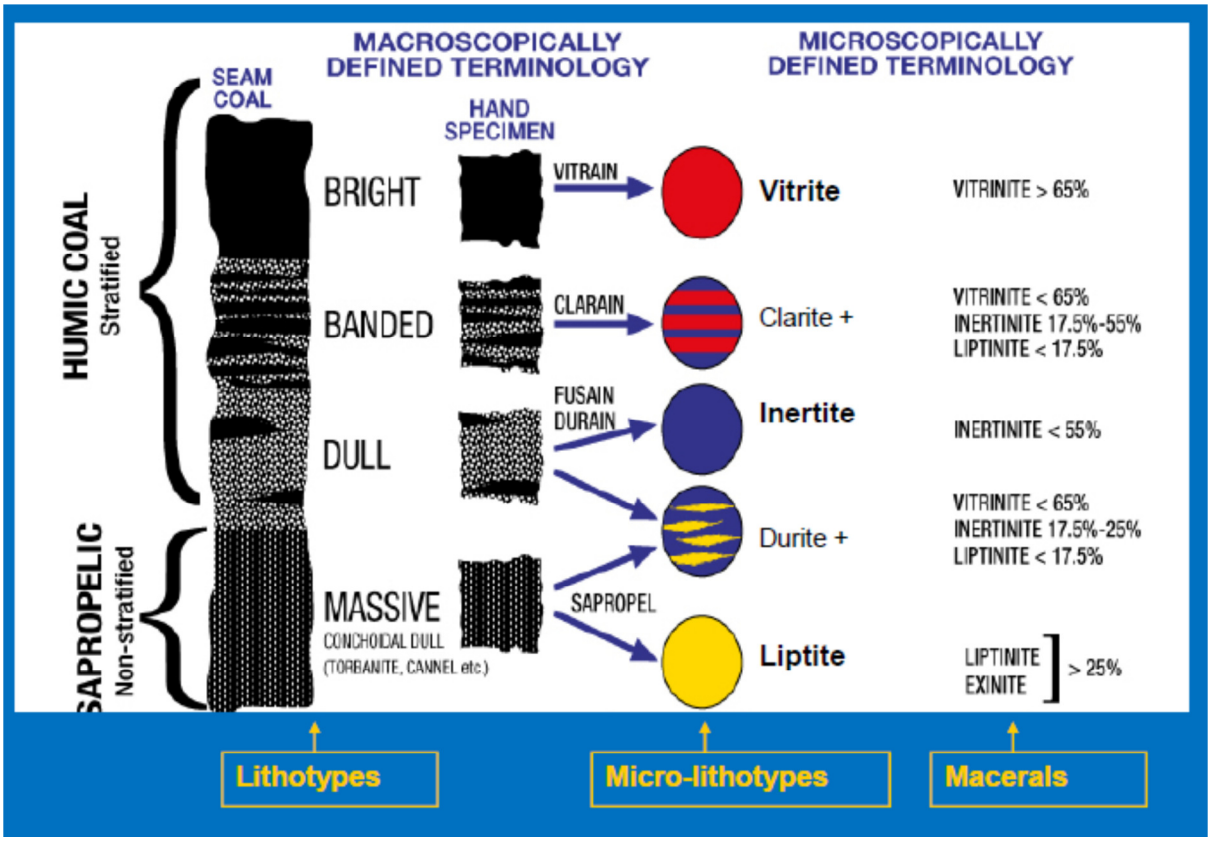

Figure 15. Breakdown of a coal seam and the macerals which they may be composed of (Falcon, 2012).

Therefore the criterion above, in conjunction with the lithological logs, assists in finalising which data is to be excluded.

Selecting sink qualities

As no raw analysis data was received, the sink is used as raw analysis in conjunction with the raw relative density, which on the other hand had been received. Sink data, which has 100% yield, is the total of all the fractions cumulated to 100%.

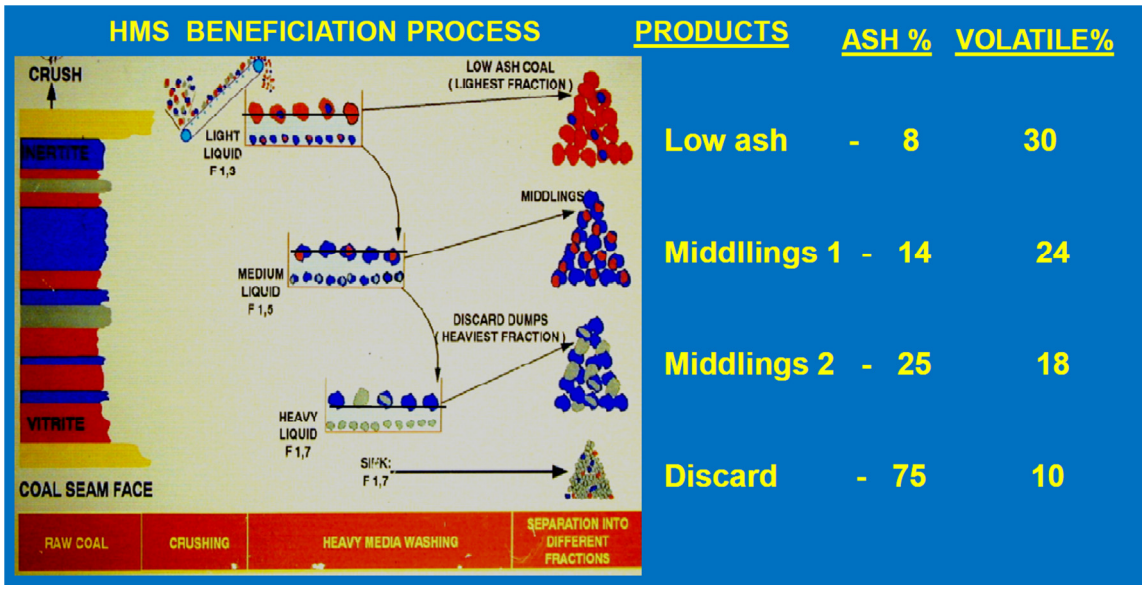

Figure 16. Example of typical qualities produced after beneficiation of a seam (Falcon, 2012)

Consequently if the sink's yield is 100% of the sample, it is then comparable to the raw results as mentioned in the previous section that the raw results are results determined from analysing the entire sample of coal instead of through sink float analysis. However during the analysis of the raw sample, part of the sample is lost in the form of fines which are weighed and reported by the laboratory. When the sink, raw and fines are compared, the difference is minimal. In some cases where no fines were reported, but raw analysis information as well as cumulative information is available, the difference is no greater than 0.1. Nevertheless the fines should be considered when the data is present. Therefore all graphs are based on the sink analysis and raw R.D information on air dry basis.

Calculation of thickness of sill and distance from the bottom coal to the sill's floor

Calculations were conducted to ascertain the:

a) The distance between the dolerite sill and the bottom coal seam; and
b) The thickness of the dolerite sill.

The distance between the dolerite sill and the lower coal seam was determined by subtracting the floor depth of the sill from the roof depth of the lower coal seam. The results were reported in meters.

The thickness of the seam was determined by subtracting the roof depth of the dolerite sill from the floor depth of the sill. The calculations were also reported in meters.

2.9. Limitation of data

In Study Area A, 51 samples were taken for the lower coal seam. No raw analytical data was received for the study. The data set used had been composited together by the mine geologist into the lower coal sample. On the other hand Study Area B, due to mine constraints, had only 26 samples available which were not composited on a sample by sample bases. Due to the size of the population, bias in the results may be present. The bias would be due to a smaller sample population which would greatly skew the results. In addition to the biasness, another factor to be considered is that the drill holes were not drilled into the sill by the mine. The drill holes were only drilled to the Dwyka tillites, however from previous aeromagnetic information (which cannot be used for the study) of the mine as well as the qualities of the samples received, the sill has been interpreted to exist below the Dwyka tillites. This will be further investigated in this study.

3. Study Area A

In Study Area A the sill is overlying the coal seams and in this area two main seams are present, S4 and S2. Seam 2 (bottom coal seam) is the main economic seam as it contains minimal to zero in-seam partings relative to S4. For all further discussions in the study, S2 will be called the bottom coal seam.

3.1. Data received and terminology

In order to determine the effect of sill proximity on the coal in Study Area A, statistical investigation has been conducted on the received data. The original data received consists of cumulate data as well as fractional data. As no raw analysis data was received, the sink is used as raw analysis in conjunction with raw R.Ds received. Therefore all graphs are based on the sink analysis and raw R.D information on air dry basis.

3.2. Logged drill hole: A52

In Study Area A, 51 drill hole geological logs and analytical data were received, covering the entire study area. One drill hole was logged but not analysed for the study. The images of drill hole A52 are found below in Figure 17, Figure 18 and Figure 19. The original log is located within the appendix. The drill hole was piloted by air flushing method to the depth of the harder sandstone material. The sandstone is light grey to cream in the colour, the grain sizes grade from fine to medium grain. Siltstone laminations are interlaminated with the sandstone at shallower depths of the stratigraphy. As the depth increases pyrite occurs sporadically, during which the sandstone displays signs of being burnt.

Underlying the sandstone layer is dolerite. The dolerite is greenish-grey to grey in colour. The grain sizes varying between coarse, medium and gradually grades to a fine texture towards sandstone contact. The dolerite has calcite-filled fractures that cross cut diagonally to the drill core. In addition, calcite veins and calcite filled fractures are present throughout the intrusion.

Underlying the dolerite intrusion is 18.43 m thick sandstone. The sandstone displays downward coarsening as it grades from fine to medium grained texture. The sandstone exhibits alternating sandstone/siltstone lamination structures and lenticular laminations. Furthermore wavy laminations area observed as seen in Figure 17. The colour fluctuates from light grey to grey, becoming darker and more carbonaceous with the presence of siltstone laminations.

Figure 17. Site drill hole indicating the contact between the sandstone parting and the top coal (40% core loss).

Continuing along the stratigraphic column, a gradual contact continues to the underlying coal seam of S5. Sixty five centimetres of coal mixed dull is logged which displays banding and is broken with some core loss (10%) (Figure 18). In order to use the data set for the study as well as to build a geological model, at least 90% of the sample must be present.

Figure 18. Sharp contact between the overlying sandstone and the top seam of the area.

Underlying the coal is a shale parting followed by 3.46m of fractured and slickensided coal dull, coal mixed dull and coal shaley interbedding. The coal is separated from another seam of coal by a 0.40m shale marker band. The coal is mainly coal mixed dull interbedded with shale lenses and is characterised by increasing siderite content to towards the contact with the siltstone parting.

The bottom seam of the area is spilt into an upper and lower seam, the upper seam is characterised by coal shaley, shaley coal and shale. Structurally fractures are present at the contact with the overlying siltstone/sandstone parting and minor slickensides towards the bottom.

No precise contact between the upper and lower seam is present. However the grade of the coal improves to more vitrinitic coal interbanded with dull coal, but culminates with a coal shaley band at the contact with the tillite floor. The presence of slickensides increases into the lower seam, where the slickensides are characterised by calcite filling. Overall the bottom seam is 10.55m thick with the upper and lower seams equalling 2.67m and 7.88m thick respectively.

Figure 19. Sharp contact between the lower portion of the top coal seams and the sandstone/siltstone parting separating to and bottom coal.

3.3. Classic statistics

Initially, classic statistics were calculated for the data set, producing histograms, correlation coefficients and descriptive statistics. The statistics were conducted on the distance from the sill, the thickness, V.M, ash and C.V.

Histogram and descriptive statistics

The following was observed:

a) The V.M histogram displays three possible populations (Figure 20). A larger number of samples are present between 19-28% V.M, with two smaller groups of lower V.M of between 6-9% and 12-16%, respectively. The average V.M present is 22.88% with samples skewed to the right negatively.

b) Calorific value statistics indicate one population is present with an outlier with a low C.V of 10.21MJ/kg (Figure 22. Histogram and descriptive statistics of ashFigure 21). The data displays right hand side skewness. The samples mostly range between 20-26.69MJ/kg as per the historgram with a mean of 23.96MJ/kg the median is 24.29MJ/kg, standard deviation is 2.39 and the skewness is -4.01. 51 samples were used.

c) The ash histogram (Figure 22) displays left hand side skewness, in contrast to the V.M and C.V histograms. In total, 51 samples are used and no samples have been excluded. The mean is 21.55% with a median of 20.57%, standard deviation of 5.85% and a positive skewness of 4.17%. Maximum ash present is 55.48% and a minimum of 15.95%.

d) The maximum thickness of the dolerite in the study area is 29.70m which decreases to a minimum of 2.87m (Figure 23). The mean of the thickness is 13.48m with a medium of 12.40m and a standard deviation of 6.17%.

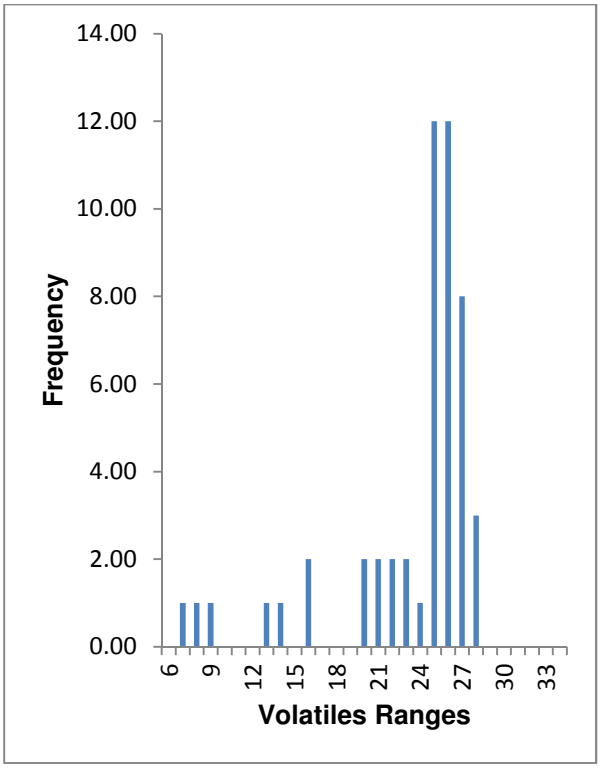

Volatile Matter	
Mean	22.88
Standard Error	0.72
Median	24.77
Mode	24.77
Standard Deviation	5.17
Sample Variance	26.73
Kurtosis	3.14
Skewness	-1.94
Range	21.48
Minimum	6.03
Maximum	27.51
Sum	1166.90
Count	51.00
Largest(1)	27.51
Smallest(1)	6.03
Confidence Level (95.0%)	1.45

Figure 20. Histogram and descriptive statistics of V.M

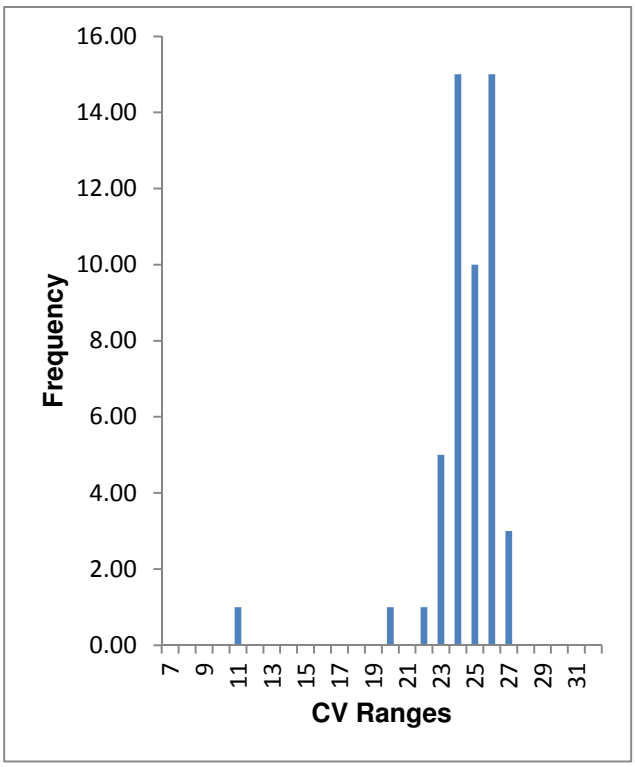

Calorific Value	
Mean	23.96
Standard Error	0.33
Median	24.29
Standard Deviation	2.39
Sample Variance	5.70
Kurtosis	22.05
Skewness	-4.01
Range	16.48
Minimum	10.21
Maximum	26.69
Sum	1221.78
Count	51.00
Largest(1)	26.69
Smallest(1)	10.21
Confidence Level (95.0%)	0.67

Figure 21. Histogram and descriptive statistics of C.V

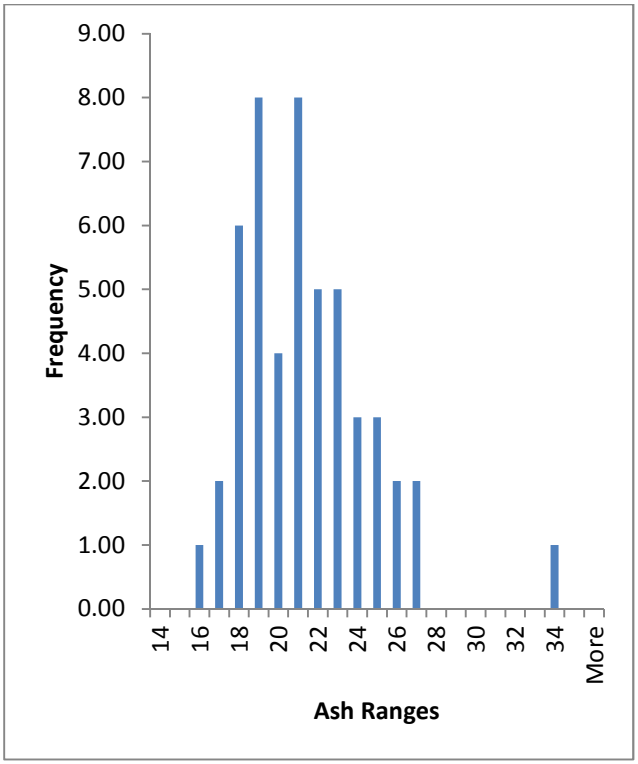

Ash	
Mean	21.55
Standard Error	0.82
Median	20.57
Mode	#N/A
Standard Deviation	5.85
Sample Variance	34.24
Kurtosis	22.86
Skewness	4.17
Range	39.53
Minimum	15.95
Maximum	55.48
Sum	1 099.06
Count	51.00
Largest(1)	55.48
Smallest(1)	15.95
Confidence Level (95.0%)	1.65

Figure 22. Histogram and descriptive statistics of ash

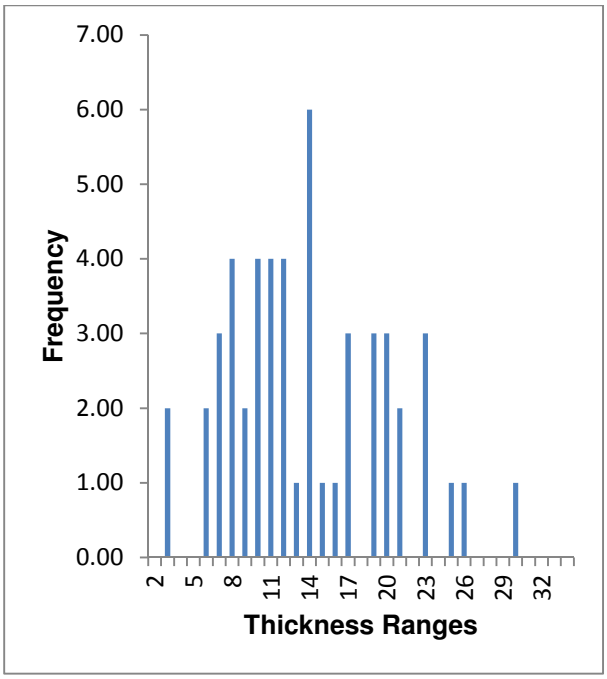

Dolerite Thickness	
Mean	13.48
Standard Error	0.86
Median	12.40
Mode	20.90
Standard Deviation	6.17
Sample Variance	38.10
Kurtosis	-0.25
Skewness	0.54
Range	26.83
Minimum	2.87
Maximum	29.70
Sum	687.54
Count	51.00
Largest(1)	29.70
Smallest(1)	2.87
Confidence Level (95.0%)	1.74

Figure 23. Histogram and descriptive statistics of the dolerite sill's thickness

Lastly the statistical assessment of the distance between the bottom coal and the dolerite sill was assessed through a histogram. Three populations are present in data set according to the histogram (Figure 24). The data lies to the right with a negative skewness of -0.24. On average the coal is 22.51m away from the sill where the median is 25.31 and the standard deviation is 10.86. The maximum distance between the coal and dolerite sill is 42.01m, while the minimum is 0.00m.

Population one contains samples that range with 5-13m, population two between 18-33m and lastly population three between 37-42m based on the histogram (Figure 24). The populations are looked at individually in Figure 25, Figure 26 and Figure 27. The first population displays two internal populations (Figure 25). The second population contains two peaks in thickness, possibly creating two additional populations within the population (Figure 26). Lastly population three contains too few data points to be statistical relevant (Figure 27).

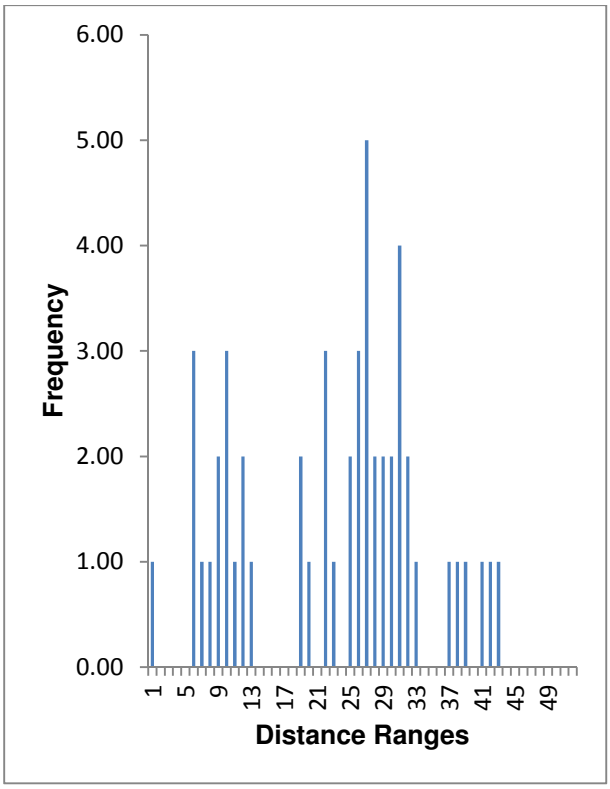

Distance	
Mean	22.51
Standard Error	1.52
Median	25.31
Mode	26.22
Standard Deviation	10.86
Sample Variance	117.89
Kurtosis	-0.87
Skewness	-0.24
Range	42.01
Minimum	0.00
Maximum	42.01
Sum	1148.25
Count	51.00
Largest(1)	42.01
Smallest(1)	0.00
Confidence Level (95.0%)	3.05

Figure 24.Histogram and descriptive statistics of the distance

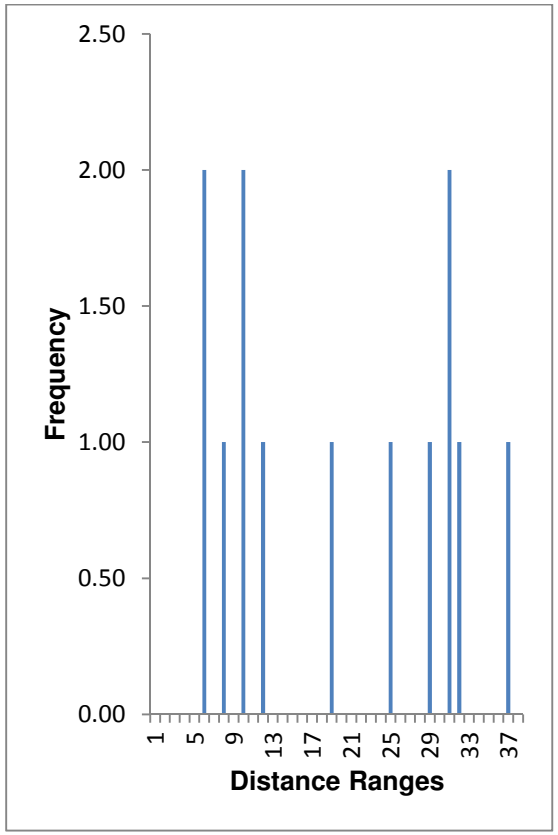

Figure 25. Histogram of the distance for population 1

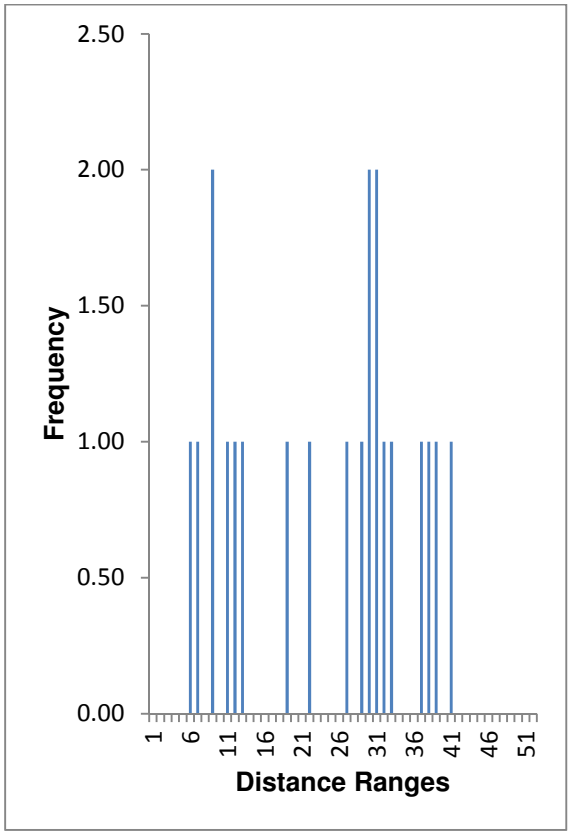

Figure 26. Histogram of the distance for population 2

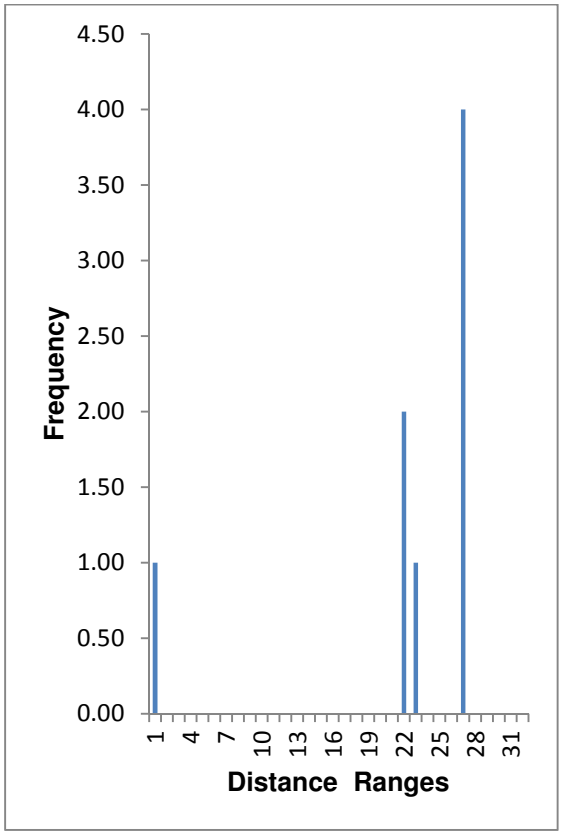

Figure 27. Histogram of the distance for population 3

3.4. Correlation statistics

Correlation between each of the parameters is assessed to determine if the parameters are independent or interdependent of each other. The data is summarised in Table 3. Furthermore the above mentioned correlations are assessed graphically through scatter plots in the subsequent sections.

Table 3. Correlation statistics table of Study Area A

	THICKNESS	DISTANCE	RD	VM	ASH	CV
THICKNESS	1.00					
DISTANCE	-0.47	1.00				
RD	-0.50	0.23	1.00			
VM	-0.55	0.75	-0.70	1.00		
ASH	0.18	0.21	0.86	-0.68	1.00	
CV	0.02	-0.47	-0.78	0.46	-0.94	1.00

The summary table indicates that the distance and thickness have a -0.47 correlation, distance and V.M a correlation of 0.75, distance and ash a correlation of 0.21 and lastly distance and C.V a correlation of -0.47. Thickness has a correlation of -0.55 with V.M, 0.18 with ash and 0.02 with C.V. Furthermore the above mentioned correlations are assessed graphically through scatter plots in the subsequent sections.

3.5. Distance from sill to coal seam and its effect on coal quality

Visual correlation

The main relationship under investigation is the relationship between the sill and the coal. In order to ascertain the influence the sill has on the coal body, distance versus V.M, Ash and C.V scatter graphs are plotted (Figure 28). In addition to the distal graphs, scatter graphs are displayed for the influence of the sill's thickness on V.M, Ash and C.V.

The distance between the sill and the lower coal seam was determined by subtracting the floor depth of the sill from the roof depth of the lower coal seam. The thickness of the seam is determined by subtracting the roof depth of the sill from the floor depth of the sill.

A non-linear relationship is observed between the V.M and the distance between the sill. A rapid increase in V.M occurs from approximately 5 m from the sill until 15 m from the sill; thereafter the V.M remains moderately unchanged.

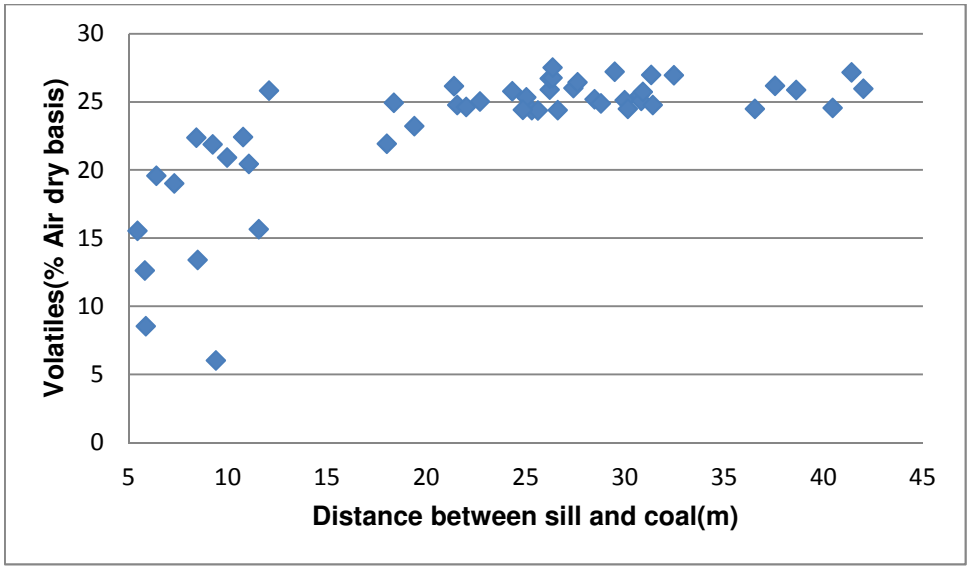

Figure 28. Relationship between V.M and distance between the sill and the coal roof

The distance is calculated in the same manner to determine the relationship between the ash and the sill-seam separation. In Figure 29, the data points display that with increasing distance from the sill, the ash remains. The ash varies between 15.95 and 26.43% Ash with an R^2 of 0.2, which implies no relation to the two parameters. An exception to the variation in ash is found in drill hole A36 which records 33.68% Ash.

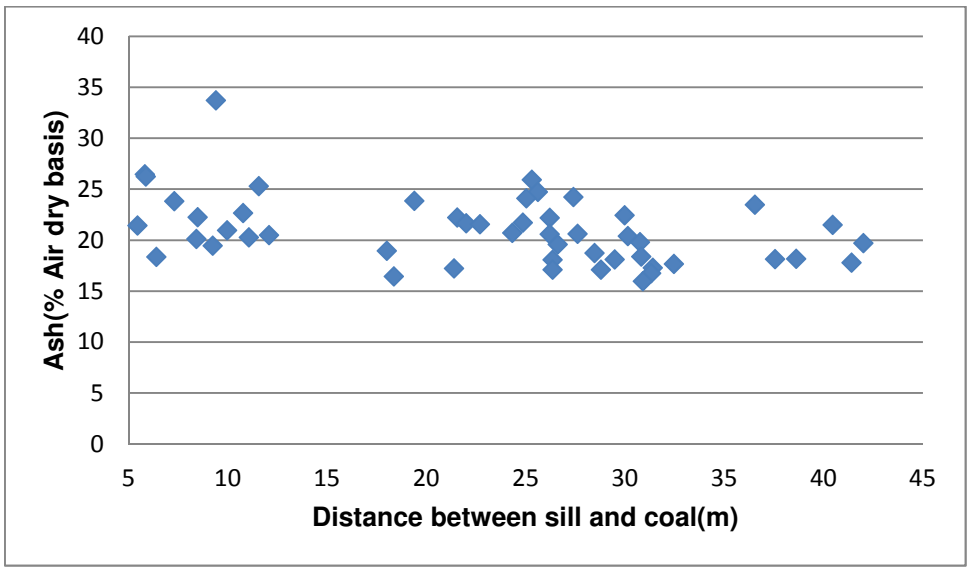

Figure 29. Relationship between the ash and distance from sill

Lastly the relationship between the calorific value and the distance between the sill and coal is graphically displayed below (Figure 30.). The data points display no relationship between the distance from the sill increases and the C.V. The C.V varies between 20MJ/kg and 27MJ/kg with an exception of 19MJ/kg for A36, the same sample has ash of 33.68%.

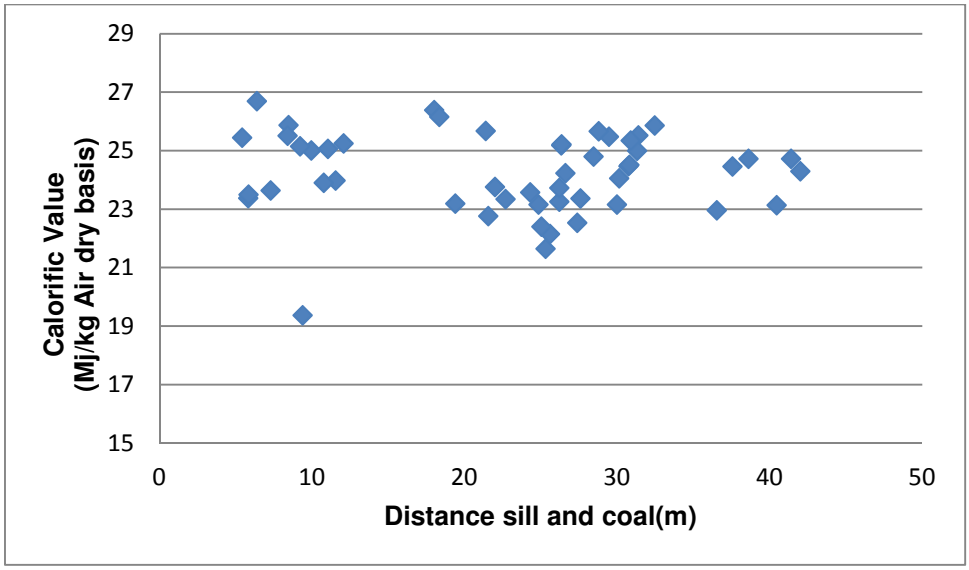

Figure 30. Relationship between calorific value versus distance from sill

The graph exhibits a mirror image to the ash graph in Figure 29; however the outliers identified above appear inverted (A36). This is expected due to the relationship between calorific value and ash in coal. Traditionally, the calorific value of coal is controlled by the organic matter that forms part of coal, but coal is a combination of organic carbon material as well and inorganic matter. In the Karoo Supergroup, inorganic material may be shale, sandstone, siltstone, mudstone-type which underwent coalification simultaneous with the organic material.

During combustion of coal, the organic material is released and what remains is ash- an inorganic substance. Thus if coal releases a high amount of ash, the amount of inorganic material was greater than organic material and therefore less energy is present in that sample. Therefore it may be deduced that the higher the ash percentage, the lower the calorific value of the sample. Thus the two parameters display an inverse relationship.

Variograms

Experimental variograms were determined through GS+ Geostatistics for Environmental Sciences. The four isotropic models are available on the software:

- Gaussian;
- Spherical
- Exponential and
- Linear.

Data was imported into the software, where model build is run prior to building the variogram model. Variograms have been built for ash, C.V, V.M, R.D, distance and thickness.

The V.M variogram's best near fit model is that of the Gaussian model (Figure 31). The data displays that it does not begin at the origin. The data thus has a discontinuous origin. No nugget effect is apparent visually. In terms of perfect fit to the Gaussian model, the data has an R^2 value of 0.79. This implies the data deviates from the model and is not a perfect fit. Other models were tested and only the Gaussian model has a near fit.

An experimental model for the distance between the dolerite sill and the lower coal seam has the best fit with that of the Gaussian model (Figure 32). The data deviates slightly from the model as is reported by the R^2 value of 0.96. The data displays smooth continuous behaviour with the exception of the discontinuous origin which may be explained in that no zero values are present in the data. This is commonly seen in data such as topography according to Vann (2008), thus its good fit with the distance data.

A Gaussian model is also used in the variogram of thickness as it offers the best fit for the dataset (Figure 33). The data nevertheless deviates from the model as reported by the R^2 value of 0.75. Discontinuous origin is present as the data does not begin at zero.

Ash as well as C.V best fits into a Gaussian model with R^2 values of 0.39 and 0.73, respectively. Neither of the parameters fit perfectly into the models available.

Lastly the R.D is plotted into a variogram. The data points are scattered and display no particular trend. The closest model, in which the data fit in, is that of the exponential model. The deviation is great and is reported at an R^2 value of 0.20.

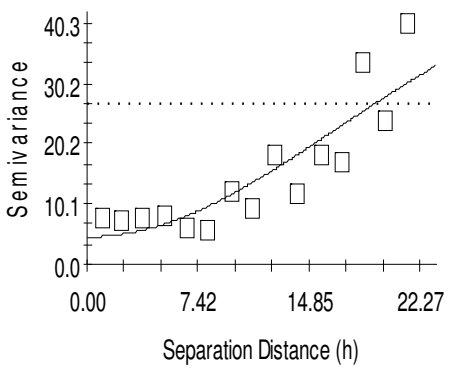

Gaussian model (Co = 4.60000; Co + C = 50.20000; Ao = 23.47; r2 = 0.789; RSS = 330.)

Figure 31. Gaussian model which is best near fit model for V.M

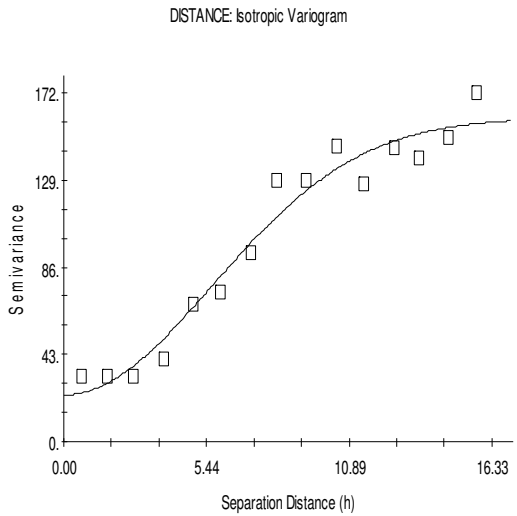

Gaussian model (Co = 23.00000; Co + C = 159.70000; Ao = 8.00; r2 = 0.961; RSS = 1371.)

Figure 32. Gaussian model which is best near fit model for distance

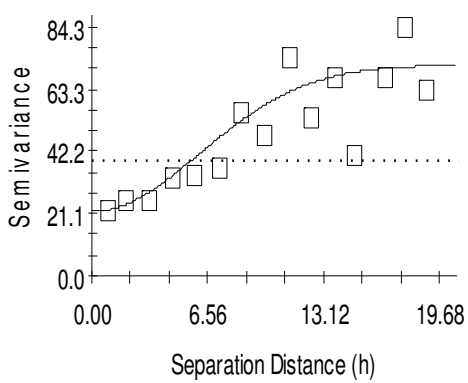

Gaussian model (Co = 21.80000; Co + C = 71.62044; Ao = 8.59; r2 = RSS = 1563.)

Figure 33. Gaussian model which is best near fit model for thickness

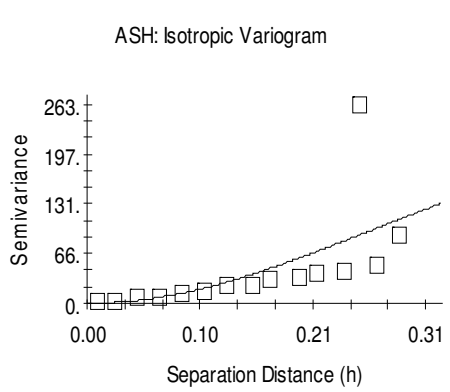

Gaussian model (Co = 0.10000; Co + C = 239.70000; Ao = 0.36; r2 = 0.391; RSS = 35995.)

Figure 34. Gaussian model which is best near fit model

for Ash

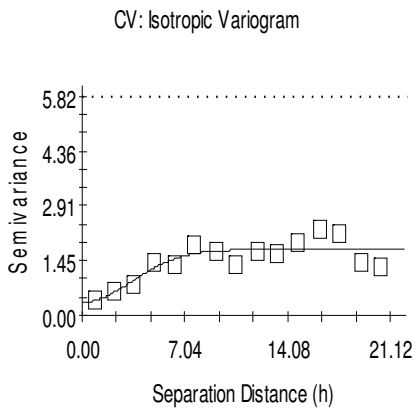

Gaussian model (Co = 0.34900; Co + C = 1.74900; Ao = 4.77; r2 = 0.730; RSS = 1.07)

Figure 35. Gaussian model which is best near fit model for C.V

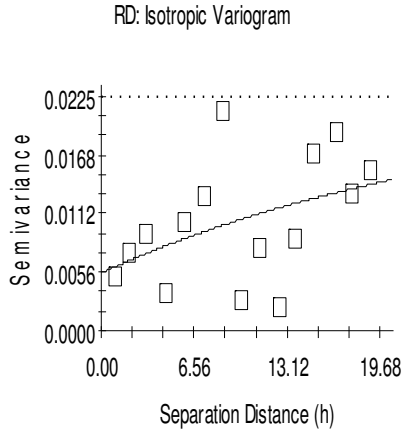

Exponential model (Co = 0.00556; Co + C = 0.02232; Ao = 27.04; r2 = 0.202; RSS = 3.856E-04)

Figure 36. Gaussian model which is best near fit model for R.D

3.6. Influence of the thickness of the sill

The influence of the sill thickness on the coal quality is assessed graphically through three graphs. Firstly the relationship between the thicknesses is assessed through a scatter plot as seen in Figure 37.. An unclear relationship is observed. Increased variability in the V.M is observed at sill thicknesses between 15-30 m, while limited variability is observed at sill thicknesses between 0 and 15 m.

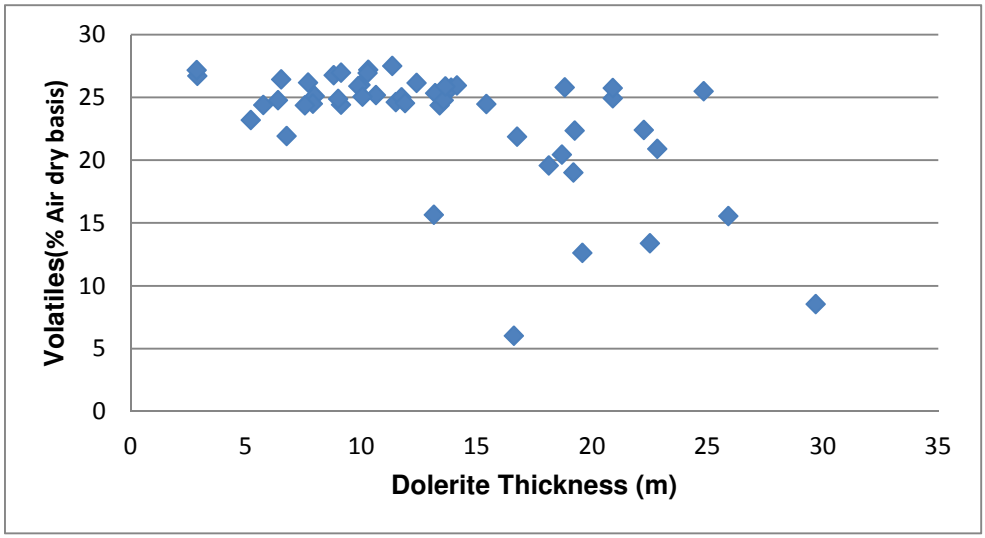

Figure 37. Relationship between the volatile matter and thickness of the sill

Secondly the relationship between the thickness of the sill and the ash is evaluated below (Figure 38.). The ash remains unchanged no matter the thickness of the sill, excluding A36. The ash varies between 15.94% and 33.43% Ash.

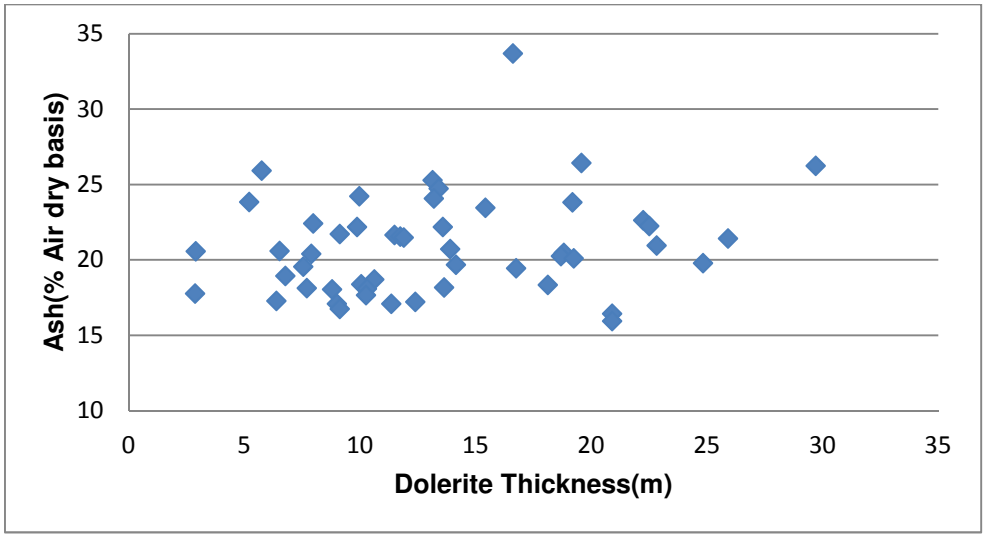

Figure 38. Relationship between ash and thickness of the sill.

Lastly the correlation between the calorific value and thickness is determined in the figure below (Figure 39.). No significant variations are observed. The calorific value remains largely constant with the exception of A36.

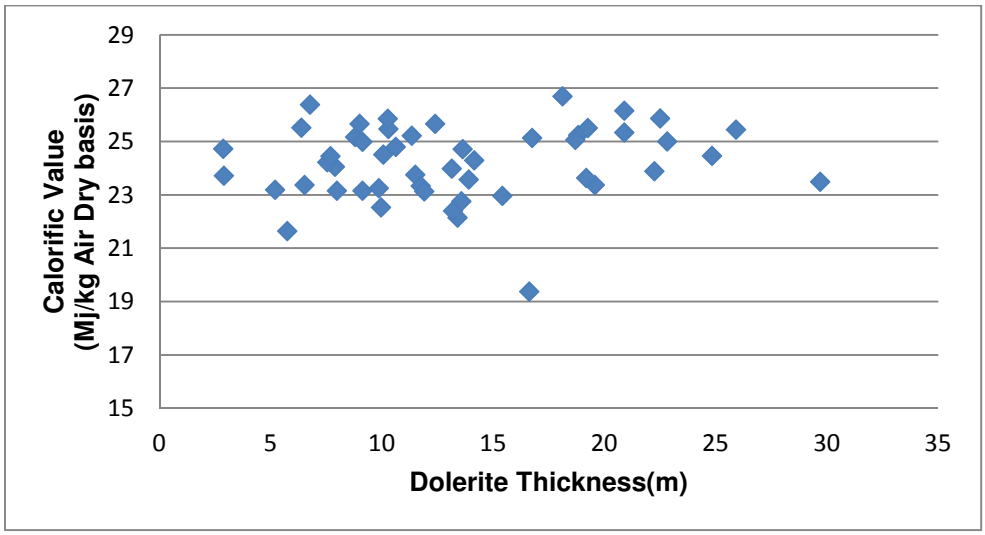

Figure 39. Relationship between calorific value and thickness of the sill

3.7. Comparison between the influence of distance and thickness on the volatile matter

The V.M data, which was plotted against the distance and thickness, respectively is now combined in the following graph (Figure 40). The graph displays similar clustering as the previous graphs above. The data points are scattered, with an unclear trend at the lower V.M. As the V.M continue increase to above 25, the points cluster vertically. In the previous graphs of the individual parameter (distance and thickness), the plots display no variations at the higher V.M.

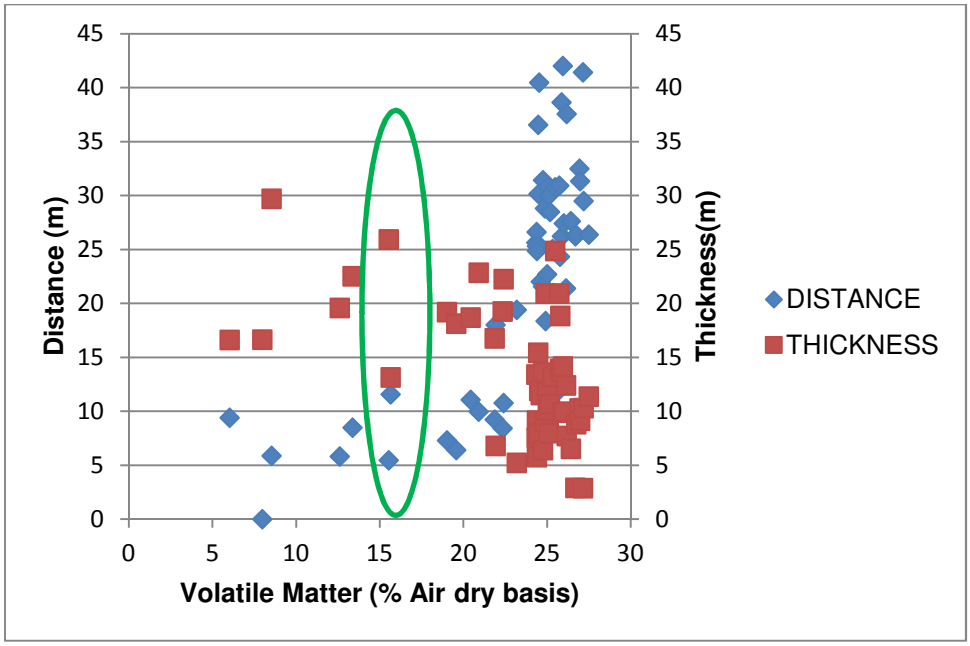

Figure 40. Distance and thickness plotted simultaneously against the V.M. Four points with the same V.M. value are circled to show the range in thickness.

Four data points have been encircled in Figure 40. The data points all report a V.M of approximately 15% at different thicknesses and distances. The finding above is visually assessed through the cross section in Figure 41 and Figure 42, comparing two of the drill holes with similar V.M. values. The cross section displays that in drill hole A33 the sill is thinner relative to drill hole A2 and it is further away from the bottom coal seam. The two drill holes are approximately 56m apart.

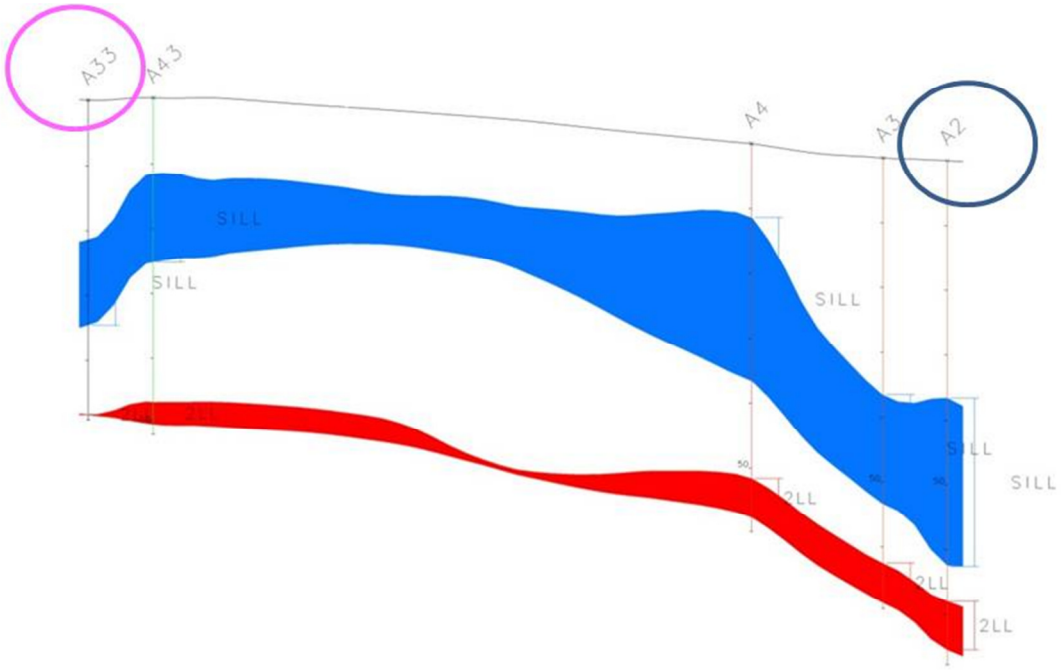

Figure 41. Cross section of drill holes A2 and A33 which have the same V.M (10 times exaggerated) (Blue: sill and Red: bottom coal)

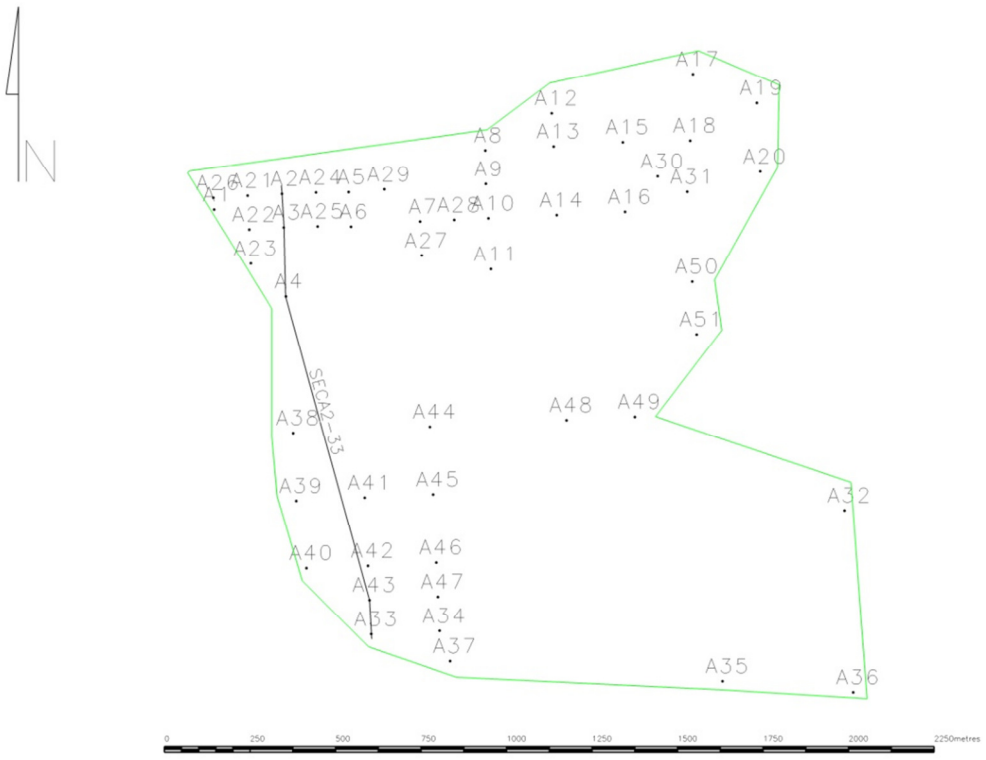

Figure 42. Plan view of the cross section between drill hole A2 and A33

3.8. Correlation to the relative density

Once the physical relationship between the coal and the sill has been assessed, the correlation between the above parameters versus the raw R.D can be examined.

In Figure 43, a clustering of data points is observed. The data points cluster between R.D 1.45 and 1.65. A gradual decline of V.M is seen towards R.D 1.85.

The nearest fit trend line, calculated on MS Office Excel, is that of a polynomial to the power trend line. The R^2 value is 0.66, a value that indicates the data deviates from the exponential line. The equation used to calculate the value is as follows:

Equation 1: $\mathbf{y = -1E\text{-}06x^6 + 0.0001x^5 - 0.0049x^4 + 0.1049x^3 - 1.206x^2 + 6.8934x - 13.344}$

When plotted with a linear equation, R^2 is 0.49 indicating no linear relationship is present between the V.M and the R.D. Similar finding are found in the regression graph produced on GS+ Geostatistics software (Figure 44).

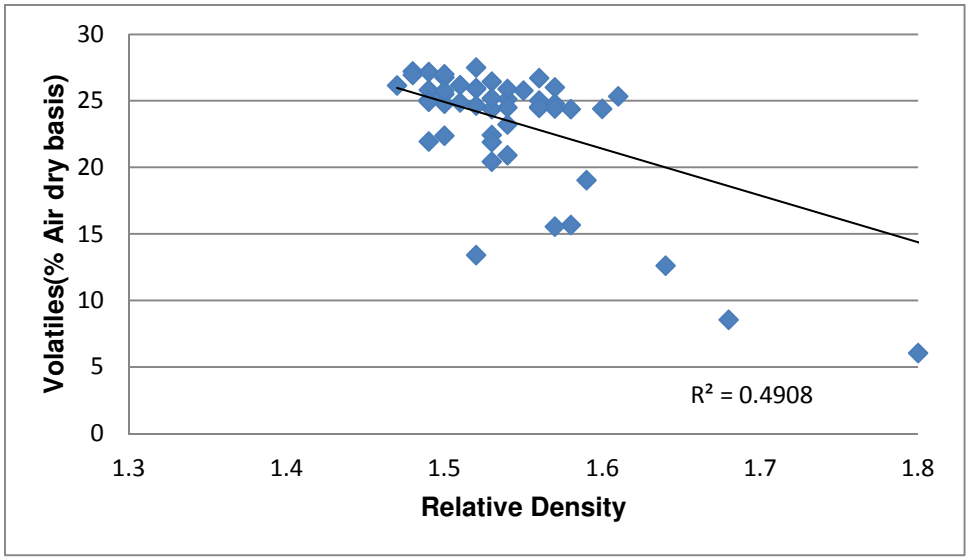

Figure 43. Correlation between Volatile matter and Raw R.D

The regression graph produced on GS+ Geostatistics software (Figure 44) reports that the R^2 value is equal to 0.002. Thus there is no correlation between the V.M and the R.D.

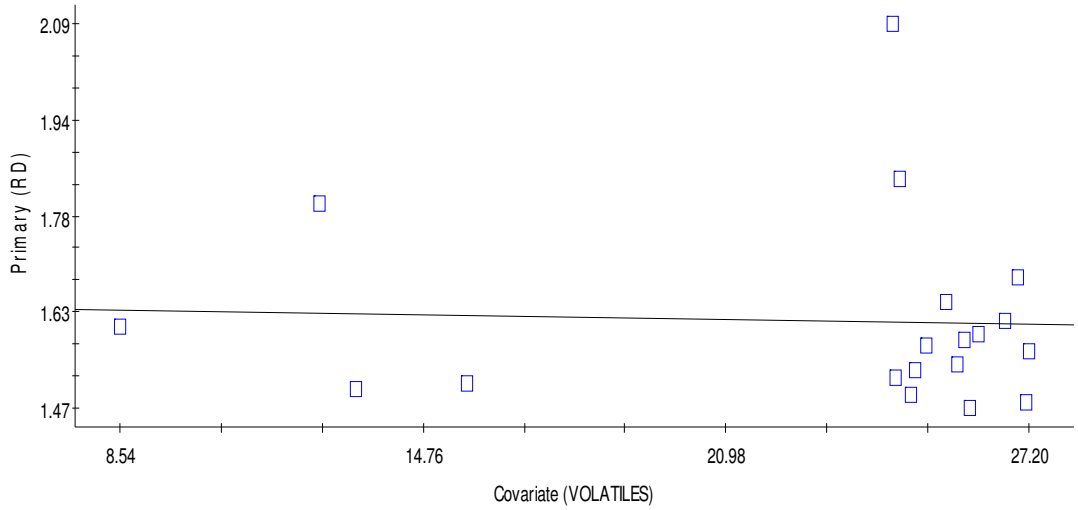

Figure 44. Regression cross correlation of R.D and V.M

The relationship between the ash and the R.D's for the bottom seam is also assessed in Figure 45. The two parameters are plotted against each other and a linear trend line is plotted over the data set.

The data points display a clustering with increasing Ash and increasing R.D between R.D 1.45 and 1.65. The R^2 value for the plotted linear trend is equal to 0.73. The value implies that the data points have a partial linear trend, but deviate from the trend line. An outlier is present at near 1.75-1.85 R.D. The outlier is determined visually as it deviates from the trend line. When the outliers have been removed, the R^2 value remains unchanged for the ash; therefore it remains included in the figure.

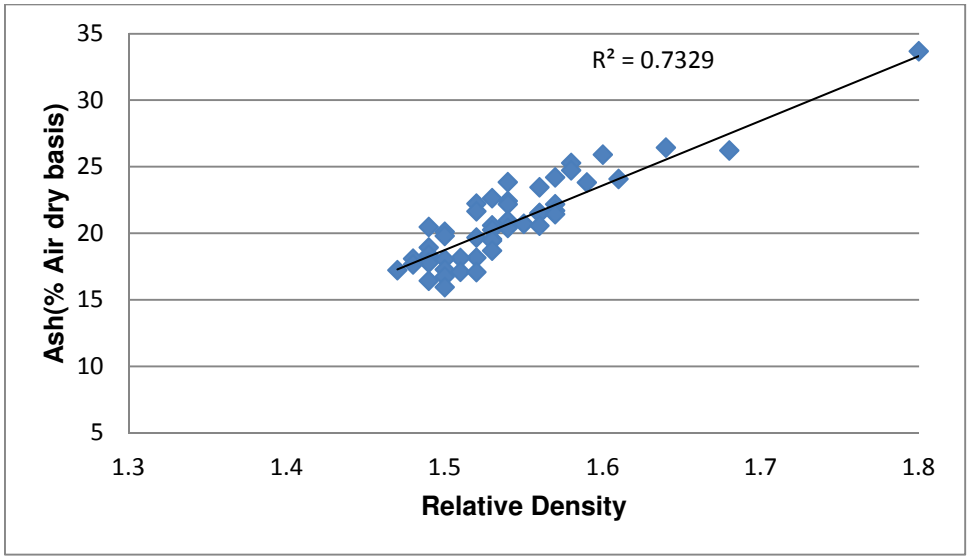

Figure 45. R.D versus ash regression plot plotted on MS Excel

The regression plot plotted in GS+ Geostatistics reports similar results (Figure 46). The R^2 value is calculated to be 0.71 with a regression coefficient of 0.02. The data displays a relationship between the R.D and Ash which appears to increase with increasing R.D, though it deviates and is not precisely proportional to each other.

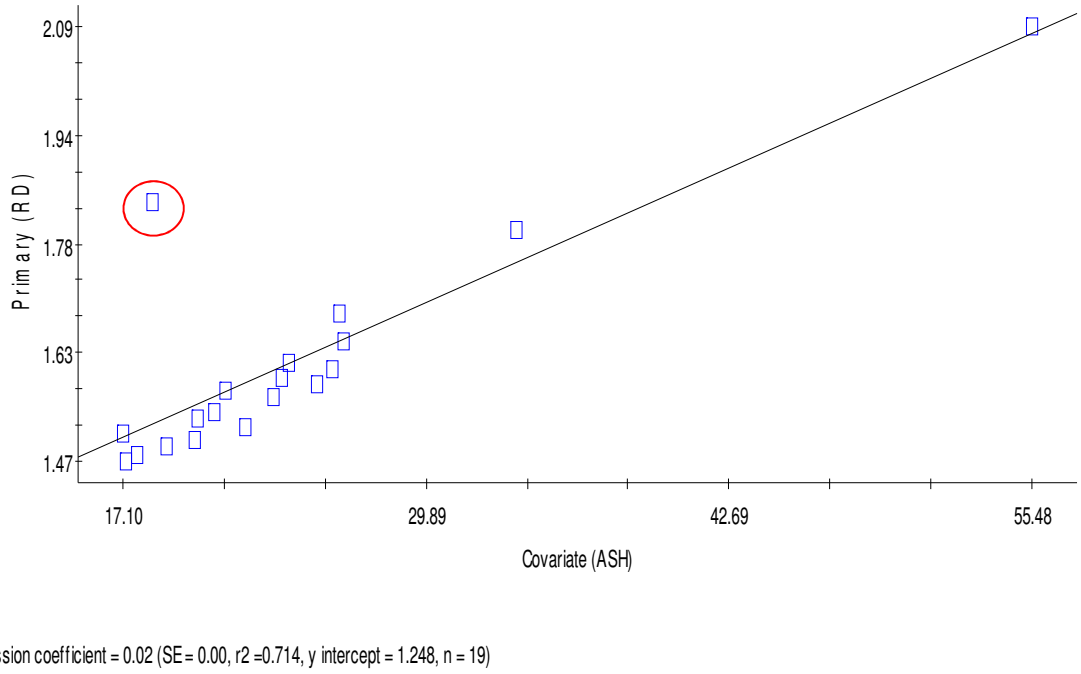

Figure 46. Regression correlation between R.D and Ash

The last relationship assessed with respect to the R.D of the bottom coal is that with the C.V (Figure 47).The data points cluster between R.D's of 1.45 and 1.65 as observed in the

previous volatile versus R.D and ash versus R.D graphs. Two noticeable outliers are present.

The closest fitting trend line to the dataset is the logarithm trend line, with $R^2 = 0.62$, where many points deviate from the trend line. However the general trend present indicates the C.V decreases with increasing R.D. This relationship is the opposite to that of the ash versus R.D. Similarly the exclusion of the outliers makes no difference the R^2 value, thus is displayed in the graph.

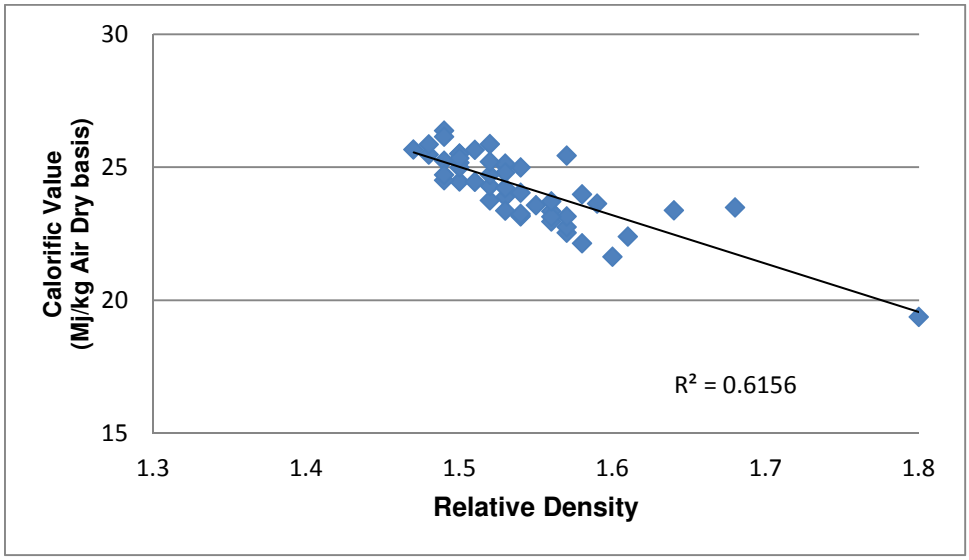

Figure 47. Correlation between C.V and Raw R.D

Regression assessment indicates the data is partially linear with a similar R^2 value of 0.66. The calculated regression coefficient is 0.03.

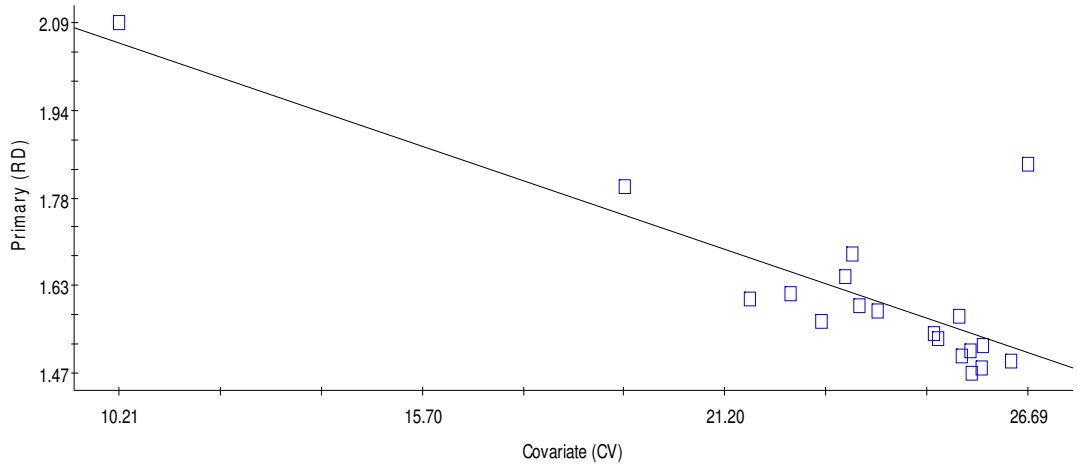

Figure 48. Regression correlation between R.D and C.V

Above it is noted that the relationship between the ash and R.D to that of C.V and R.D are opposite to each other. Therefore the relationship between ash and C.V is interrogated through a scatter plot. The results are shown in Figure 48.

The data indicates the two parameters have a near inverse relationship. The C.V decreases with increasing ash. The R^2 = 0.89, which is not perfect, but nevertheless close to the ideal value of one. When A36 is excluded on the basis of having ash content greater than 30% which made it an outlier to the general population, the R^2 values also remain unchanged.

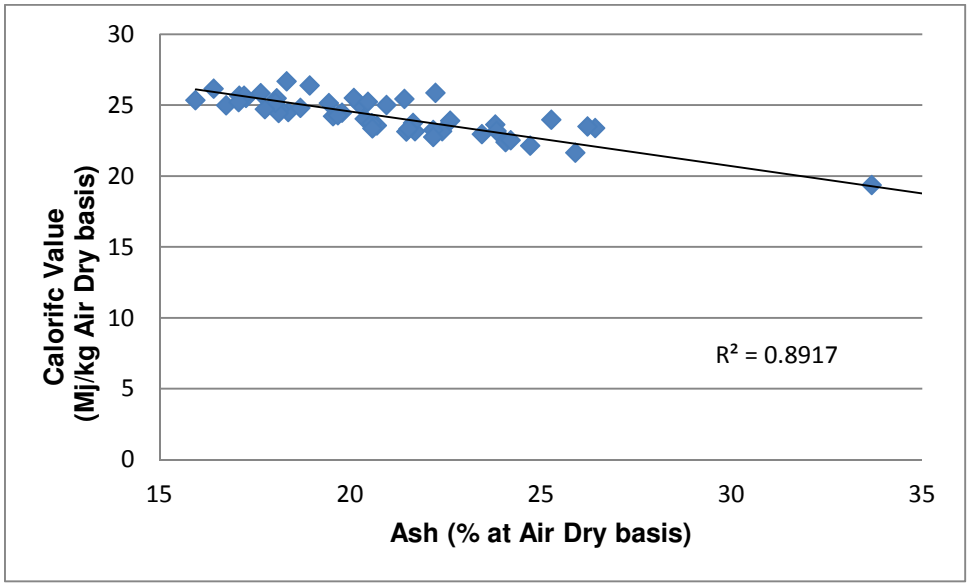

Figure 49. Relationship between ash and C.V

3.9. Volatile matter relationship

As the main objective of the study is to determine the influence of the sill on coal, the impact of the sill on the V.M is further investigated. According to Van Alphen (2012) the theoretical V.M of coal can be calculated from the ash at dry basis. The calculation is as follows:

Equation 2: ***Devolatilised V.M=-0.19082 x Ash (dry basis) + 25.2077***

It then follows that a comparative study can be done using calculated V.M against the actual measured V.M as per the data received and the calculated V.M determined with the above (Equation 2). Graphically this is displayed in the figure below (Figure 50).

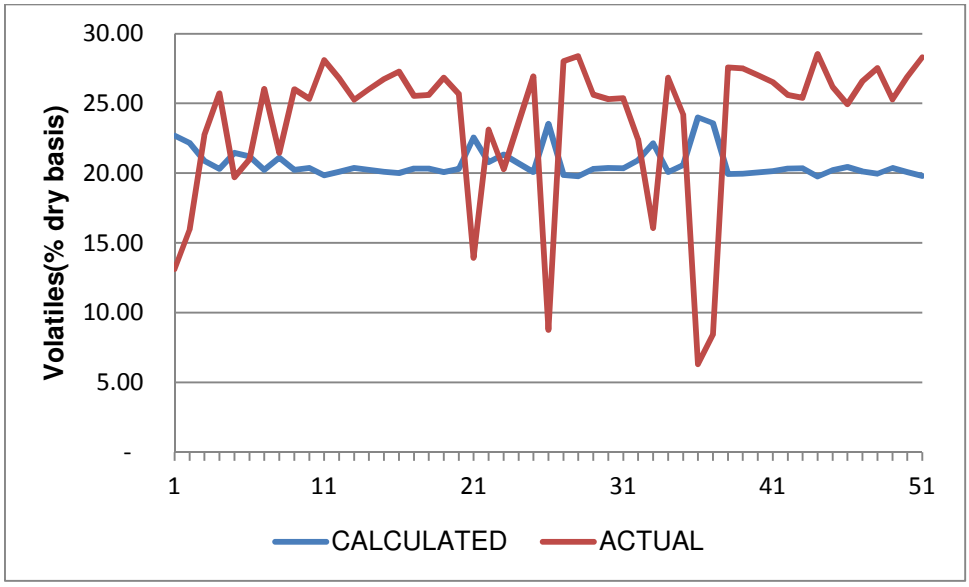

Figure 50. Graphical comparison between calculated V.M and measured V.M for Study Area A

In the above graph, Figure 50., the calculated V.M based on Van Alphen's equation (blue) is compared with the measured V.M (red). The Y-axis represents the V.M and the X-axis represents the number of samples. Overall the calculated V.M is less than that which is actually measured. Seven exceptions are visually identified where the measured V.M is less than that of the calculated V.M.

In conclusion, the relationship between Ash and the V.M is assessed in Figure 51. The data points are clustered between ash of the high teens and 30%. Dataset below in Figure 51 displays no particular trend. The closest trend observed is that of an exponential trend. The R^2 value calculated is equal to 0.47 and visually the points vary substantially to the trend line and display poor correlation between the V.M and Ash.

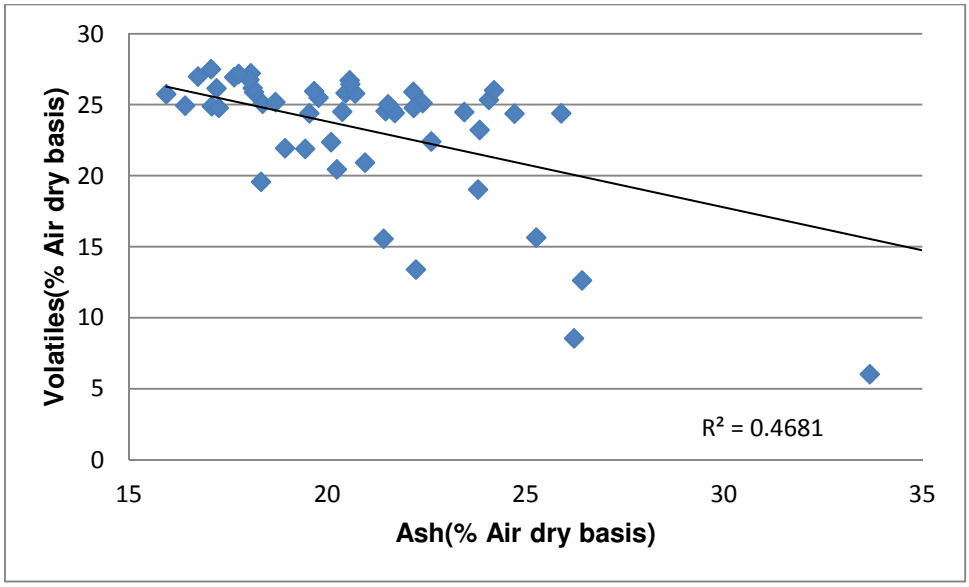

Figure 51. Correlation between Ash and V.M

3.10. Geological model information

The data received which included the lithological logs and qualities was used to produce a seam model of the sill and the bottom coal seam. Spatially the drill holes are plotted to visually assess their relationship to each other (Figure 52).

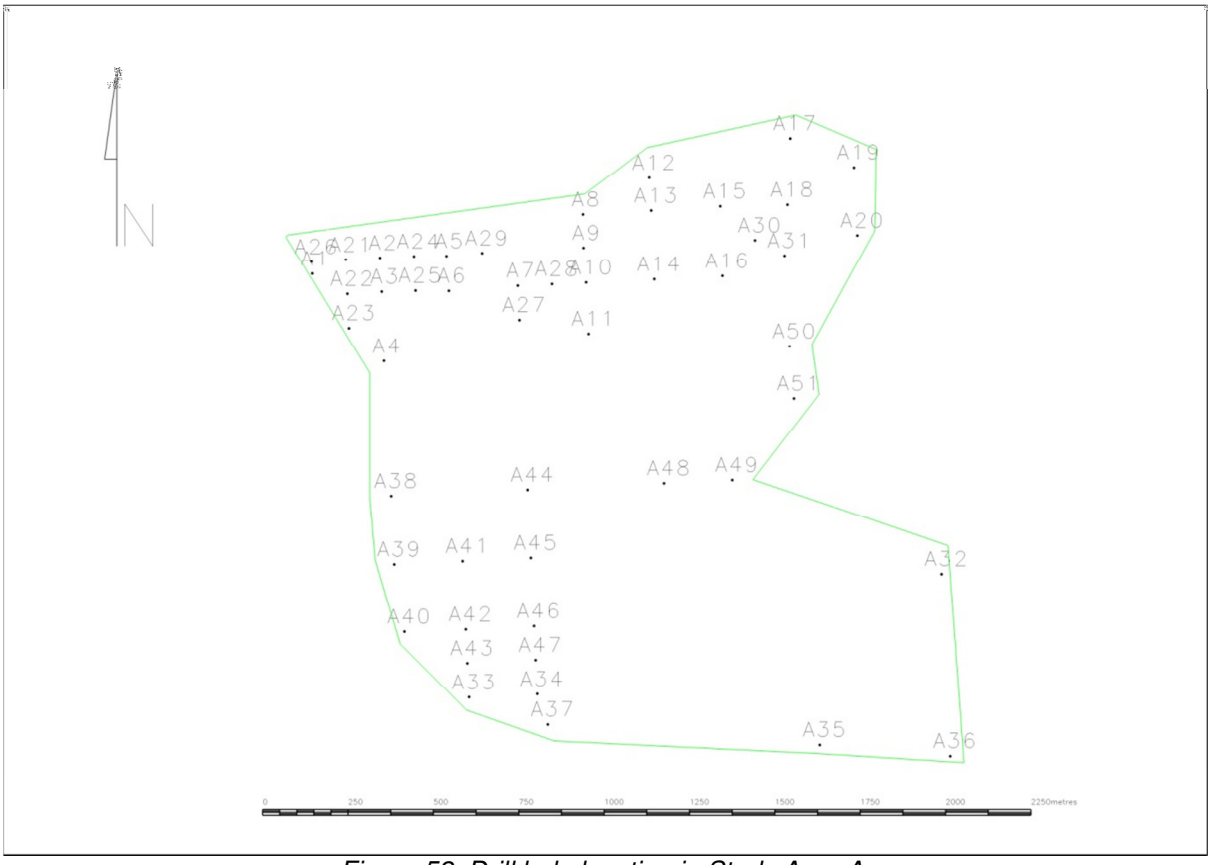

Figure 52. Drill hole location in Study Area A

Cross sections of the area indicate the sill undulates in the study area. Cross sections were drawn through the Study Area and the plotted sections are displayed below (Figure 53).

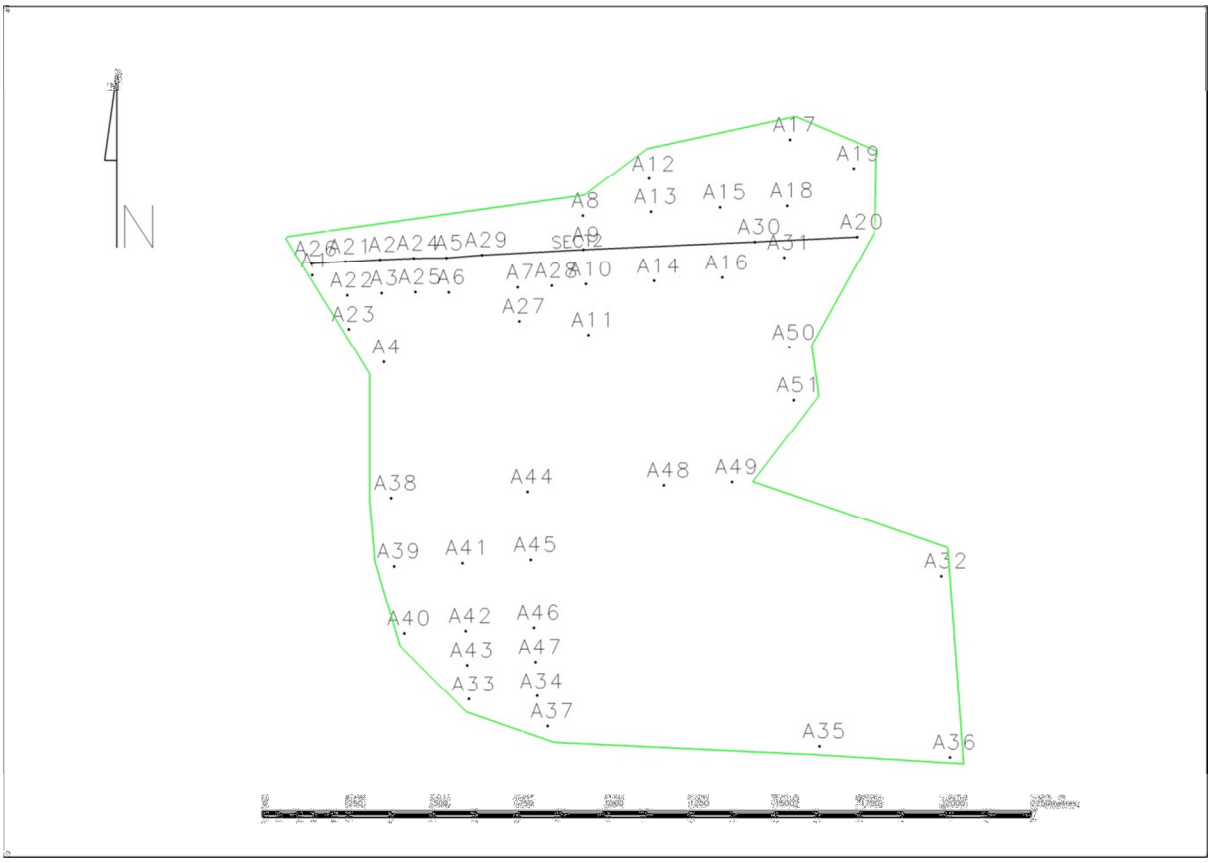

Figure 53. Location of section one cross sections in Study Area A

Section one navigates in an east-west direction through the study area (Figure 54). The sill (blue) in the section undulates, slightly mirroring the coal seam (red). The sill thickness also varies, moving from its thickest in the west and gradually becoming thinner in the east. The qualities of the eastern end (A26) and western end (A20) are as follows: 24.80% V.M, 17.30% Ash and 8.50% V.M, 26.2% Ash, respectively.

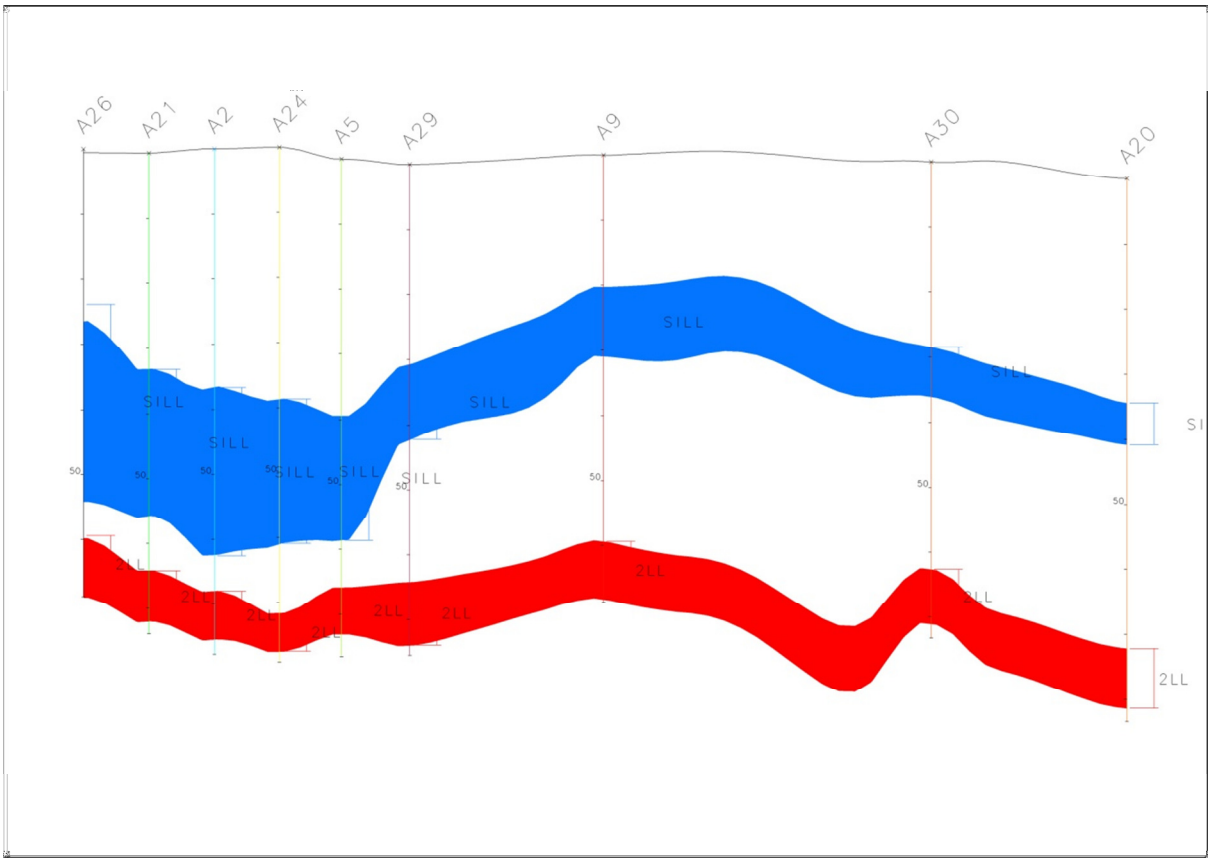

Figure 54. Section 1 moving in an east-west direction (10 times exaggeration)

In a north-south direction, a second cross section is plotted which intersects where the sill is zero distance from the coal seam (Figure 55). At drill hole A37, the sill intersects the coal and the qualities report that the coal has 7.90% V.M and 55.50 % ash. These qualities are indicative of a coal that has experienced high temperatures and “burnt” *in situ* (per. comm. H van den Berg).

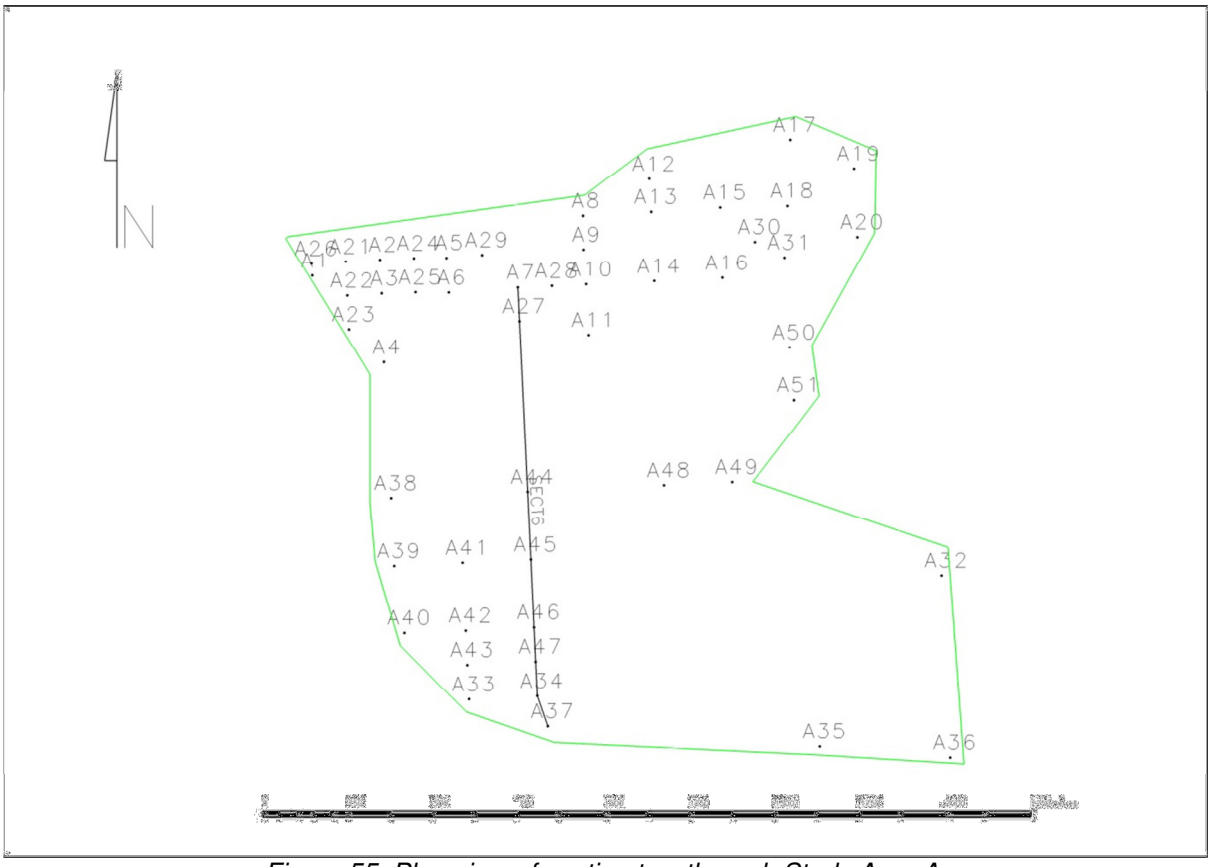

Figure 55. Plan view of section two through Study Area A

The cross section demonstrates the sill experienced a rapid drop in elevation at drill hole A37 (Figure 56). The sill maintains a similar thickness to the preceding drill holes in the section.

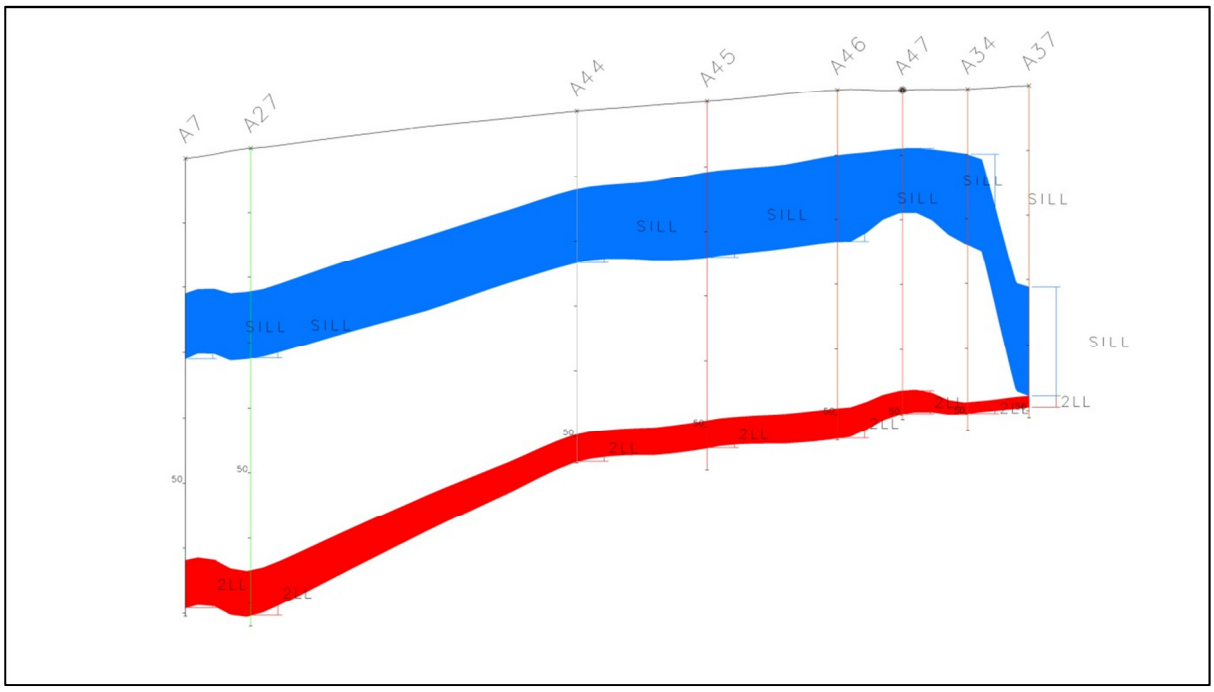

Figure 56. Coal and sill intersection cross section at drill hole A37 (10 times exaggeration)

As mentioned above the V.M rapidly decreases at drill hole A37. A shaded contour of the V.M grid is shown in Figure 57. Grids were built using the growth algorithm method of Minex, using a mesh size of 25 x 25 Mesh and a scan distance for information of 2000m.

Overall the V.M range between 25.0% and 29.2%, however in the north east and south east lower V.M are present.

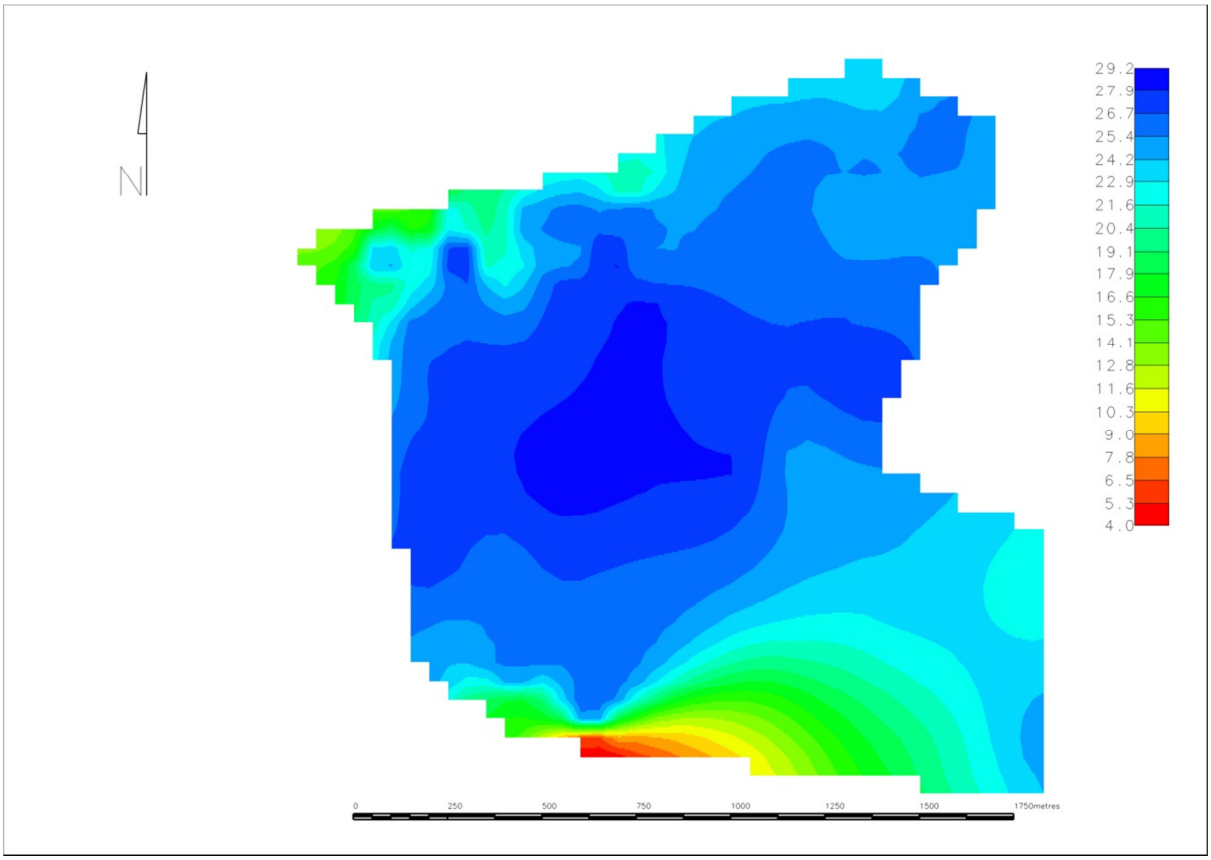

Figure 57. Shaded contour of the V.M

Similar shaded contour plan is present for ash and C.V (Figure 58). Very low Ash is present in the south east edge of the area. The ash is greater than approximately 40%. This is an outlier to an area where overall the ash is between 15.0% and 21.8%.

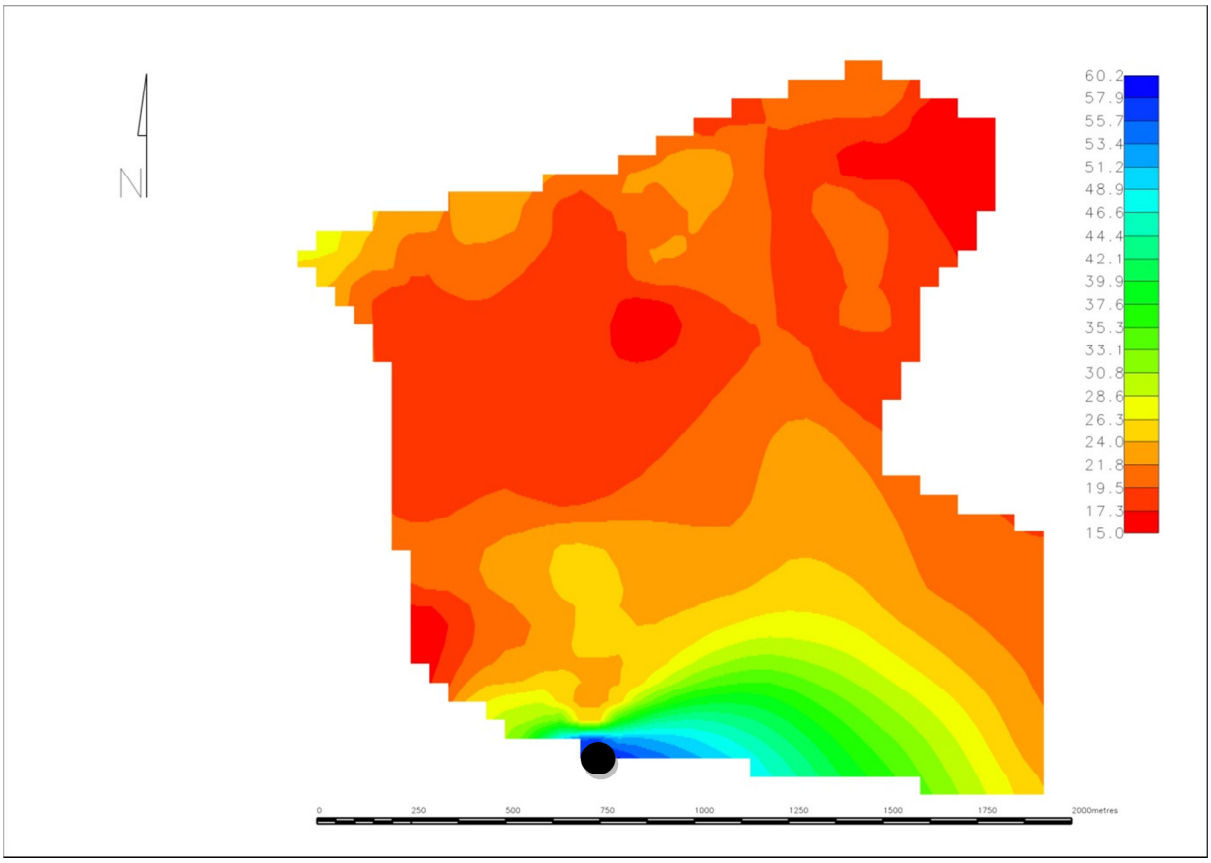

Figure 58. Shaded contour of the ash (A37 represented by a black dot)

Lastly the shaded contour is assessed. The C.V mainly lies between 22MJ/kg and 26.3MJ/kg, however at A37 the conditions differ. The C.V decreases to below 10MJ/kg. Thus in areas where the sill is in contact with the coal, the V.M and C.V decrease while the ash increases.

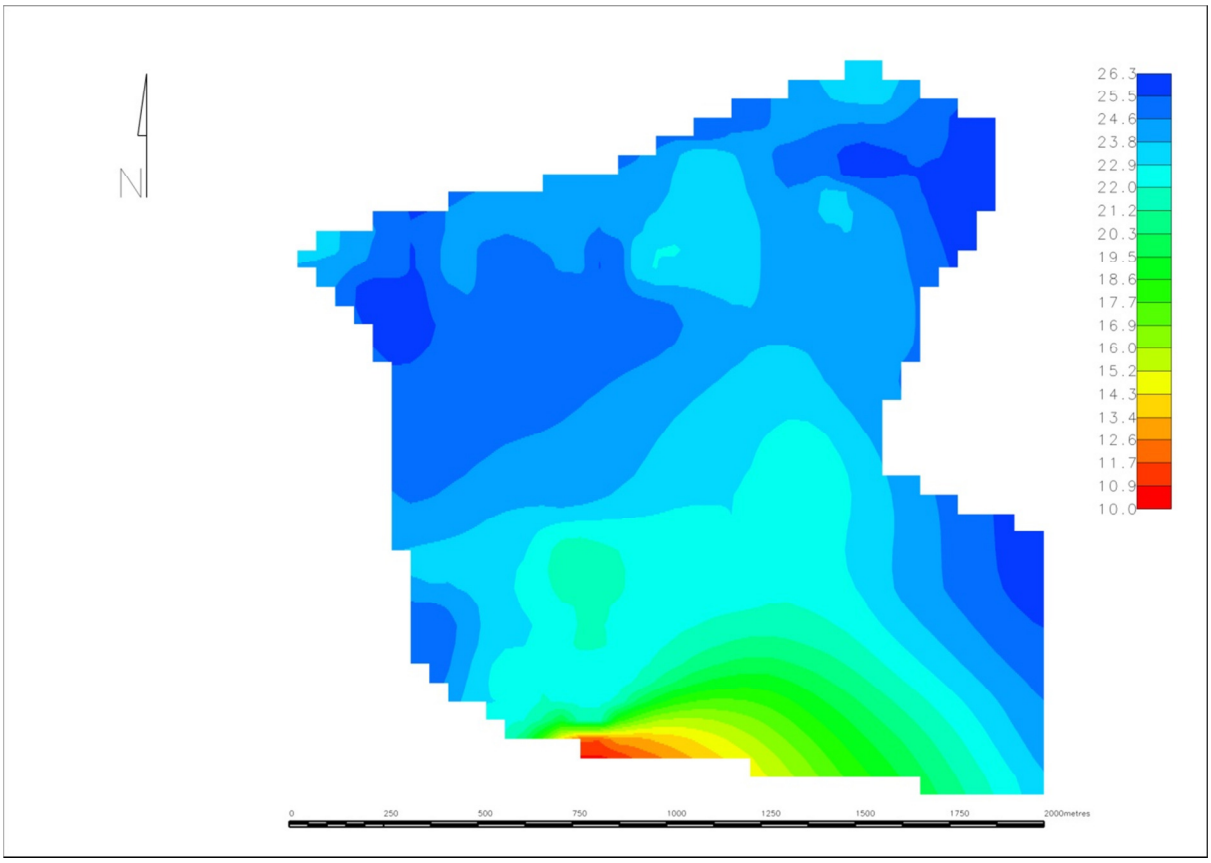

Figure 59. Shaded contour of the calorific value

4. Study Area B

Study Area B is an area where the sill underlies the coal seams in contrast to the conditions which prevail in Study Area A. In order for appropriate comparison, the lower coal seam is assessed using the same statistical tools as in Study Area B. However as the aim of drilling was to ascertain the depth limit of the coal, no actual depths for the sill are present. Aeromagnetic studies conducted in the area by the mine, indicate the sill continues into the study area (Mahanyele, 2008) (Figure 60). However recommendations from the study were that a confirmation drill hole be drilled to confirm presence of sill.

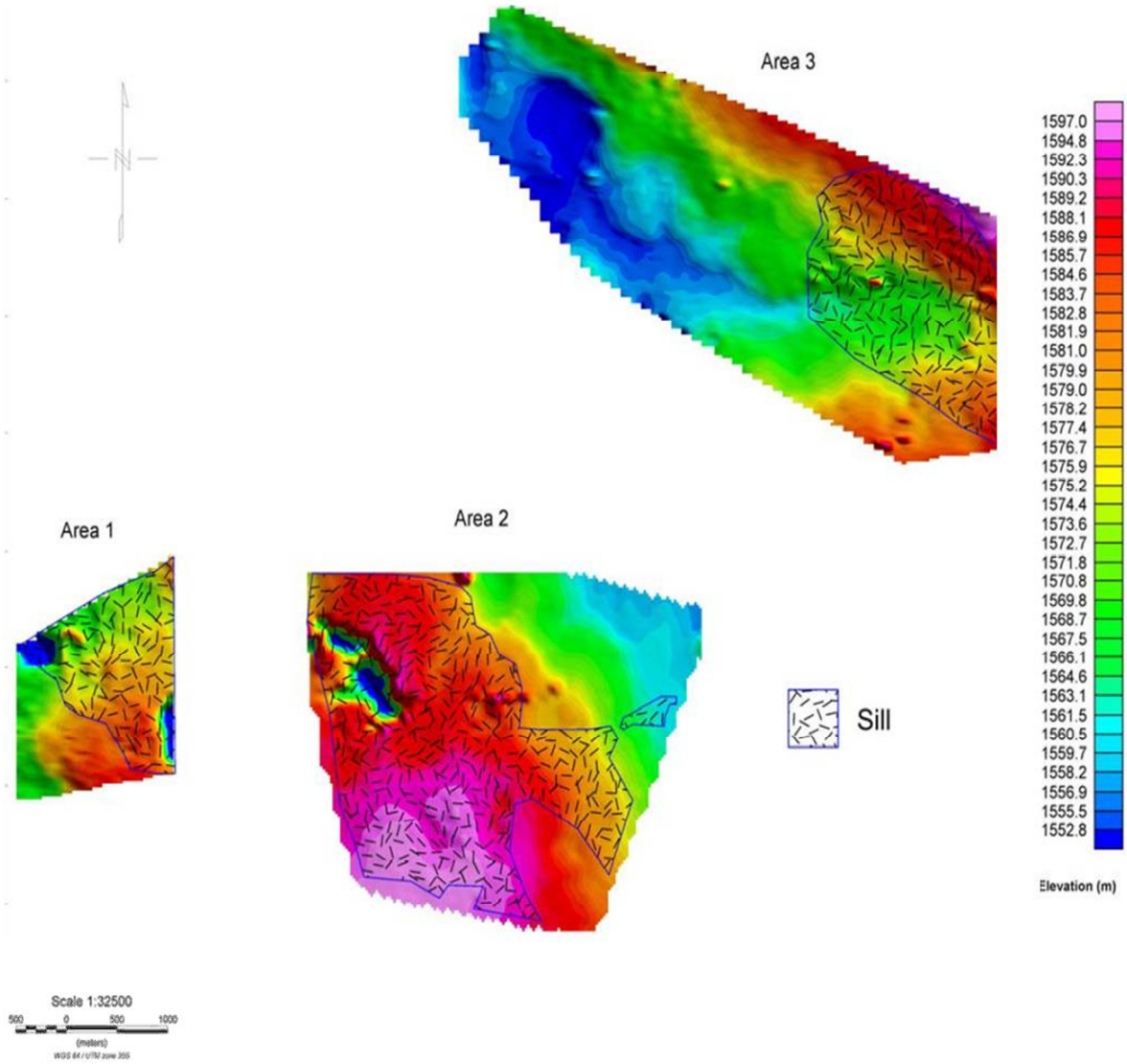

Figure 60

Also according to SANS 10320 (2004) *'devolatilized coal: bituminous coal that has a dry ash-free (3.16.15) volatile content of less than 24 % (by massfraction on a dry ash-free*

basis) but more than 16,5 % (by mass fraction on a dry ash-free basis)due to the thermal effect of igneous intrusions' the area has been interpreted by the mine as having been influenced by an igneous intrusion. Therefore the parameters which best relate to the V.M will be used to determine influence of the sill and no distance from sill and thickness of sill graphs will be plotted.

4.1. Data received

In terms of data received, Study Area B similarly has fractional data, cumulative data and raw R.D data at air dry basis. Sink analysis is used in place of raw analysis to determine the various relationships in the dataset.

4.2. Classic statistics

Histograms and descriptive statistics

Histograms are presented for V.M, Ash, C.V and R.D. The 26 composited samples have been assessed though a histogram and descriptive statistics, two samples were later excluded as they were outliers with very low V.M. Therefore only 24 counts are indicated in Figure 61. The same samples were excluded for Ash, C.V and R.D.

The average V.M for Study Area B are 10.32%, the median is 8.04, the standard deviation 4.93 and skewness 1.30. The minimum V.M present are 6.15%(8.42 DAF) reaching a maximum of 21.31% (42.42 DAF). The data indicates most of the data contains less than 13% V.M with a smaller population between 14-15% V.M with the remaining samples with higher V.M greater than 19% V.M.

The C.V data has a mean of 25.54MJ/kg where the data is mainly less than 26MJ/kg and greater than 22MJ/kg. A lesser number of samples have C.V greater than 28MJ/kg.

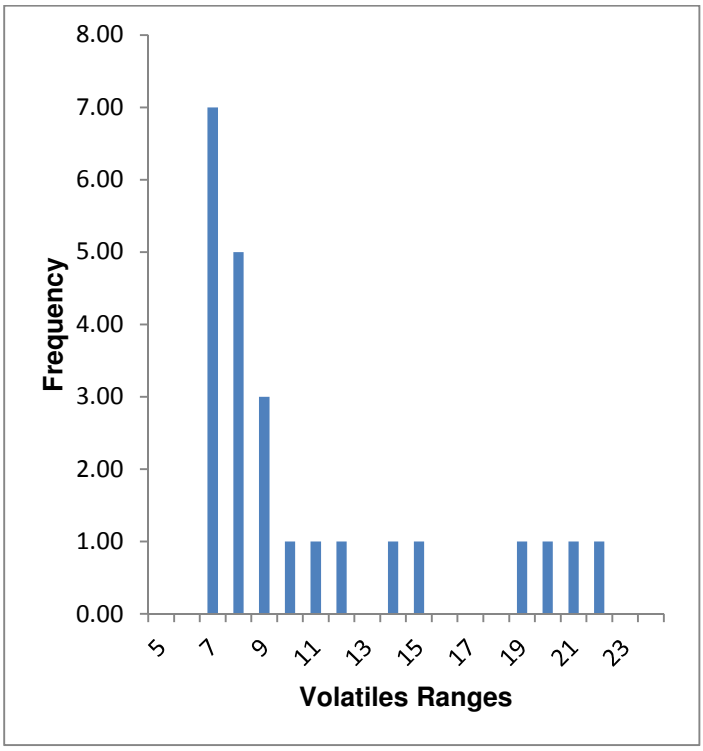

Volatile Matter	
Mean	10.32
Standard Error	1.01
Median	8.04
Mode	#N/A
Standard Deviation	4.93
Sample Variance	24.30
Kurtosis	0.34
Skewness	1.30
Range	15.16
Minimum	6.15
Maximum	21.31
Sum	247.59
Count	24.00

Figure 61. Histogram and descriptive statistics of V.M

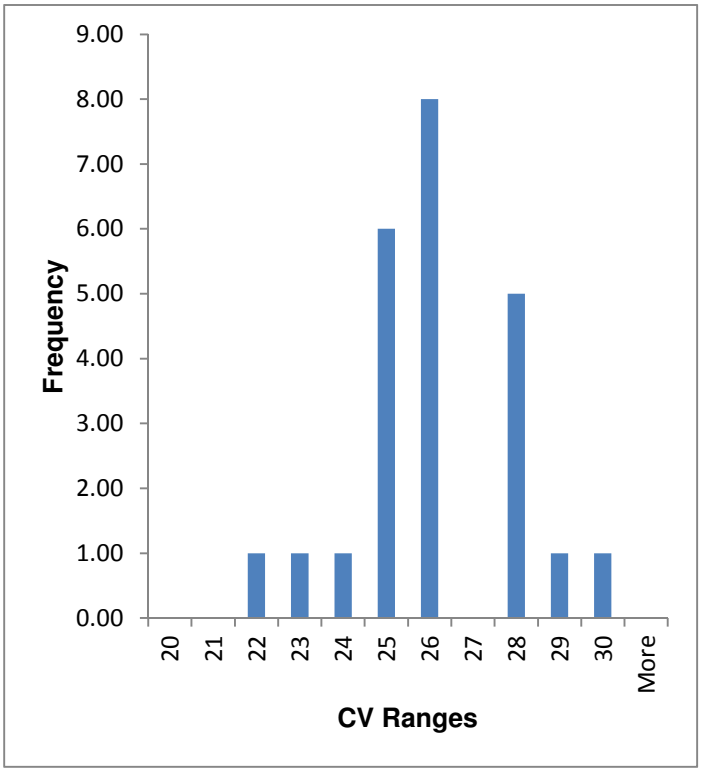

Calorific Value	
Mean	25.54
Standard Error	0.37
Median	25.28
Mode	#N/A
Standard Deviation	1.79
Sample Variance	3.21
Kurtosis	0.49
Skewness	0.17
Range	7.88
Minimum	21.79
Maximum	29.66
Sum	612.95
Count	24.00

Figure 62. Histogram and descriptive statistics of C.V

The ash histogram is skewed to the right with a negative skewness of-0.23. The ash has a mean of 20.94% where most of the samples range between 15-25%. The lowest Ash present is 9.09% and the remaining samples are greater than 27% ash.

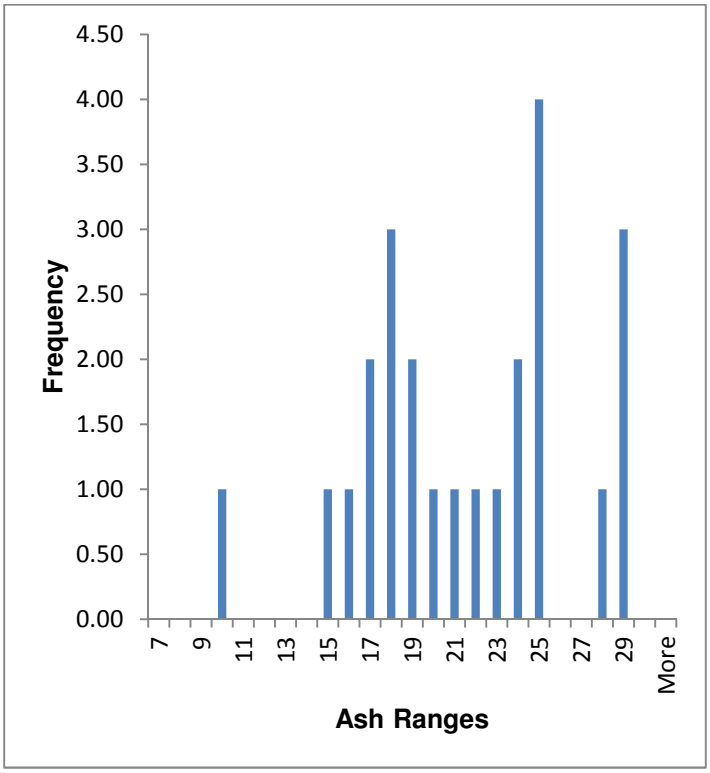

Ash	
Mean	20.94
Standard Error	1.01
Median	20.73
Mode	#N/A
Standard Deviation	4.95
Sample Variance	24.46
Kurtosis	-0.06
Skewness	-0.23
Range	19.87
Minimum	9.09
Maximum	28.95
Sum	502.46
Count	24.00

Figure 63. Histogram and descriptive statistics of ash

Lastly the R.D histogram is displayed. The data is skewed to the right hand side with a negative skewness of -0.12 reported. The mean R.D is 1.50, median 1.50 and standard deviation 0.06. The maximum R.D is 1.61 and minimum R.D is 1.37. The data set mainly occurs between 1.5 R.D and 1.65 R.D with most points at 1.50 R.D. Fewer samples are present at low R.D's of 1.37 R.D to 1.50 R.D

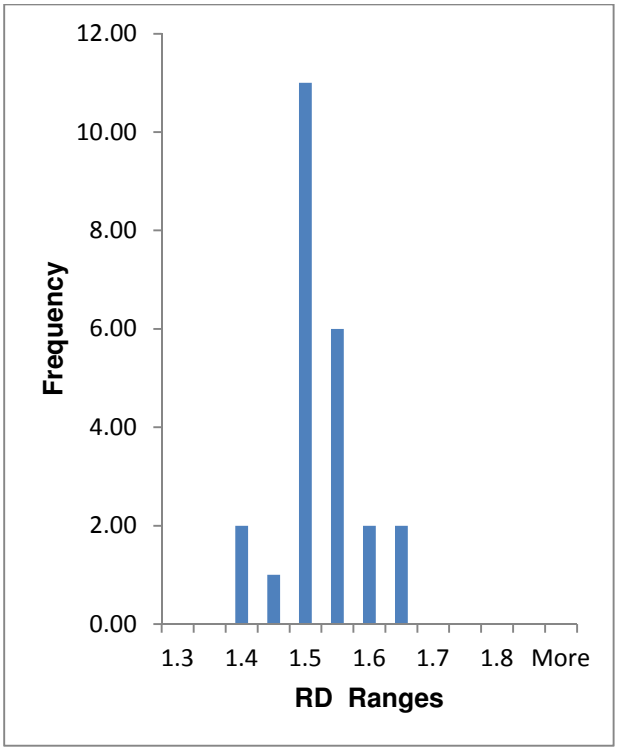

R.D	
Mean	1.50
Standard Error	0.01
Median	1.50
Mode	1.47
Standard Deviation	0.06
Sample Variance	0.00
Kurtosis	0.01
Skewness	-0.12
Range	0.24
Minimum	1.37
Maximum	1.61
Sum	36.07
Count	24.00

Figure 64. histogram and descriptive statistics of R.D

4.3. Correlation statistics

Correlation between each of the parameters is assessed to determine if the parameters are independent or interdependent of each other. The data is summarised in Table 4 below. The summary table indicates that the R.D has a -0.95 correlation with C.V, 0.99 with ash and -0.35 with the V.M. The C.V has a correlation of -0.96 with Ash and 0.16 with V.M. Lastly Ash has a -0.31 correlation with V.M. Furthermore the above mentioned correlations are assessed graphically through scatter plots in the subsequent sections.

Table 4. Summary of correlations

	R.D	*C.V*	*ASH*	*V.M*
R.D	1.00			
C.V	-0.95	1.00		
ASH	0.99	-0.96	1.00	
V.M	-0.35	0.16	-0.31	1.00

4.4. Relative density relationships

Basic scatter graphs are plotted to determine if the parameters correlated with the R.D. A correlation graph is plotted for ash and R.D (Figure 65.); a linear trend line is also plotted for the data.

The graph indicates that much of the coal floats between 1.35 and 1.65 R.D, with two outliers greater than 1.85 R.D with an Ash greater than 50% Ash. The two outliers were excluded, as Ash of that magnitude nature is indicative of shale-like material. The ash increases with increasing density; therefore a directly proportional relationship between the ash and the R.Ds is displayed by the trend line.

The R^2 value calculated equals to 0.98, a value very close to a perfect fit which suggests very few points lie off the linear trend line and a good correlation between the two parameters. This includes the high Ash outliers encircled in red. With the two outliers excluded, the R^2 value remains 0.98, thus the two boreholes have been in kept in Figure 66.

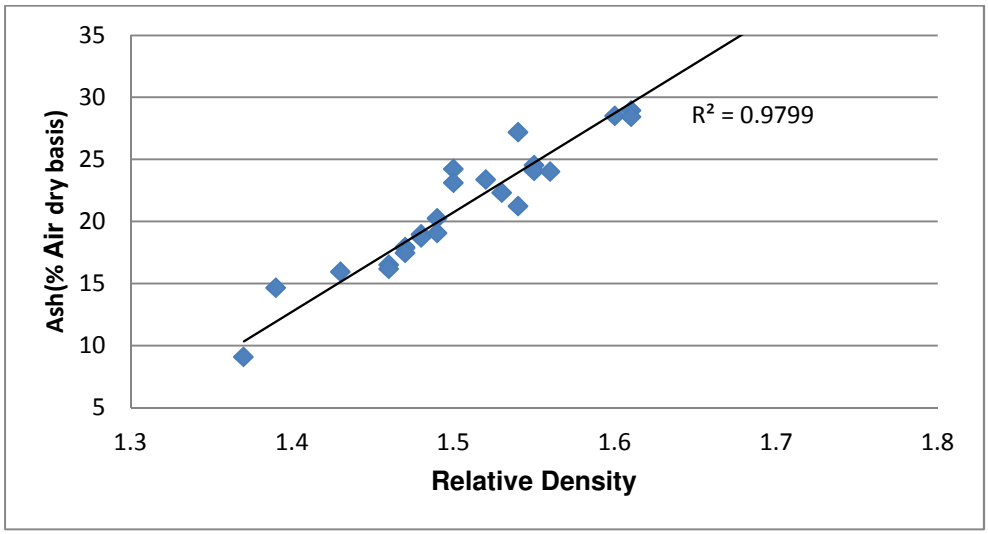

Figure 65. Correlation graph between ash and the raw Relative Density

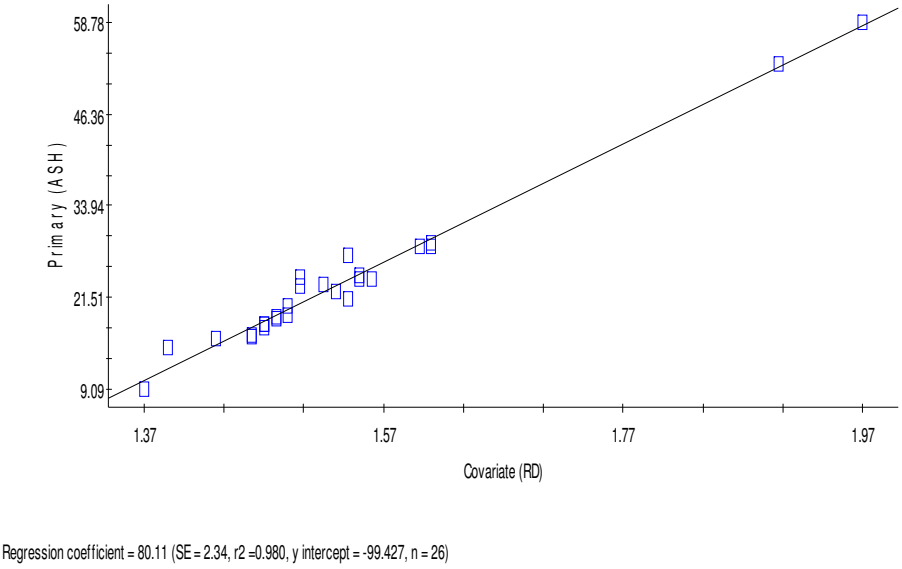

Figure 66. Regression plot for R.D and ash

The relationship between the C.V of the coal samples versus the reported R.D's is displayed below. The data points mainly lie in the lower and varying between 20-30MJ/kg, the same outliers were excluded as in other diagrams (Figure 67).

The two parameters have a linear relationship observed in the linear trend line superimposed on the data points. R^2 is just less than 1 at a value of 0.91. The value is interpreted as the data points closely lying on the linear trend line and displays good correlation between ash and R.D. As the data less the two drill holes produces the same R^2 value of 0.91, the points have been kept in Figure 68.

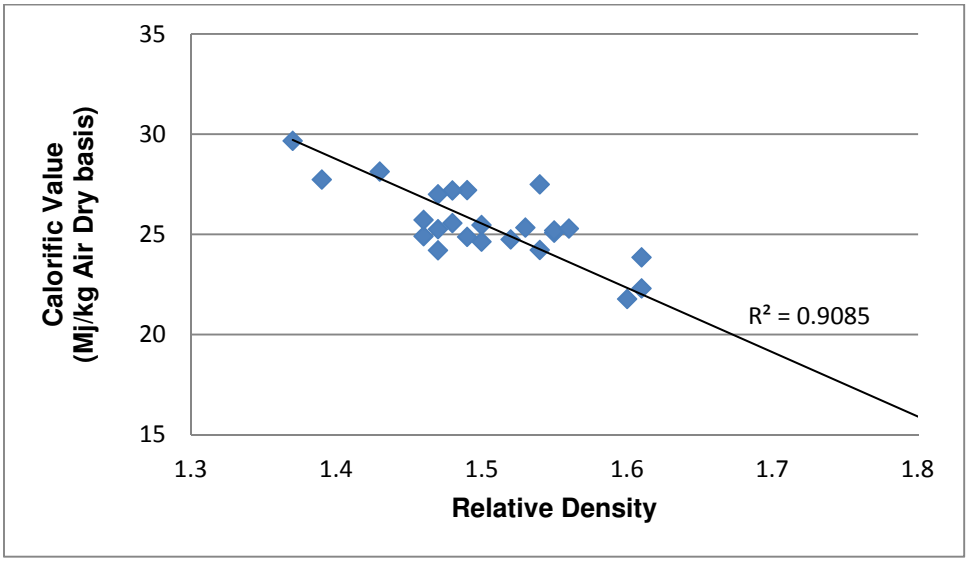

Figure 67. Correlation between calorific value and raw R.D

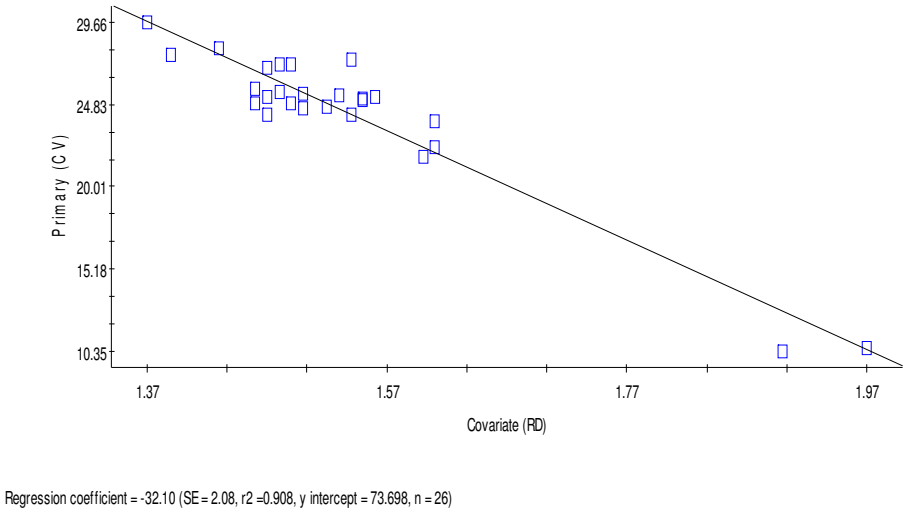

Figure 68. Regression plot for R.D and C.V

Lastly the V.M and R.D relationship is plotted (Figure 69). The graph presents a non-linear relationship between the two parameters. The V.M varies between 5% and 22% at R.D's of between R.D 1.35 and 1.65. The data points display large variation in V.M in the lower R.D's (<1.50). Thereafter at R.D's >1.50 the variation between points decreases.

A trend line is superimposed on the graph to determine any trends. The closest fitting trend line is that of a linear line. The data points are non-linear based on visual assessment. In addition to the assessment, the R^2 is 0.22 polynomial relationships. Such a low value suggests a no relationship exists. With the points included, it is apparent a poor correlation is present (Figure 70).

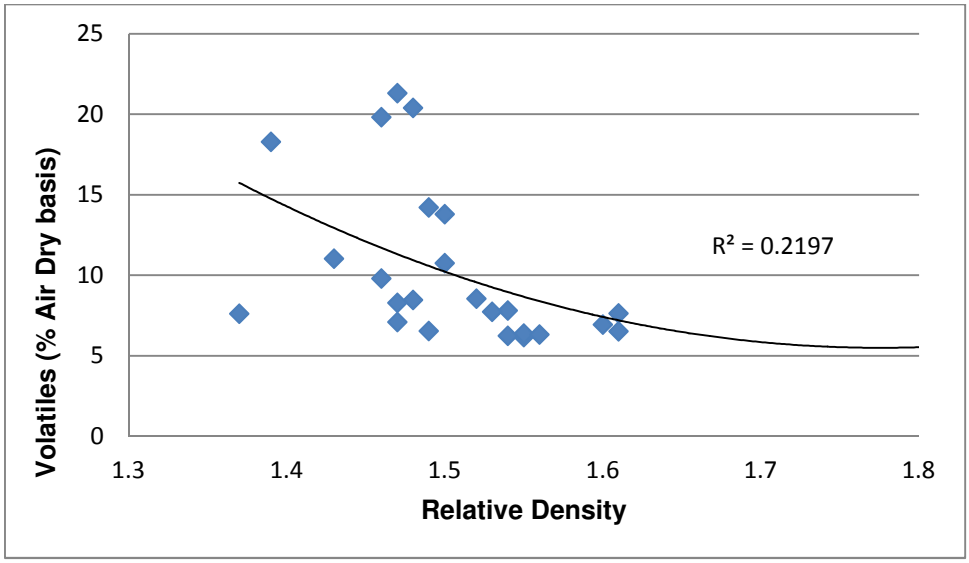

Figure 69. Correlation graph between volatile matter and the raw R.D

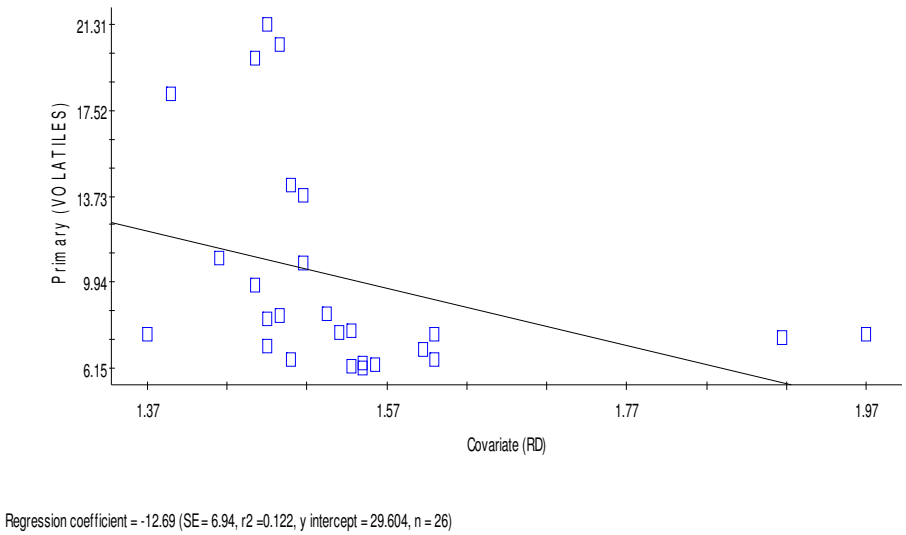

Figure 70. Regression plot for R.D and V.M

4.5. Variograms

Data was imported into the software, where model build is run prior to building the variogram model. Variograms have been built for Ash, C.V, V.M and R.D. Experimental variograms were determined through GS+ Geostatistics for Environmental Sciences.

The variogram of V.M displays “saw-toothing” where the data set does not follow a trend, no matter how the data is manipulated. The data thus does not fit into any of the four available models and R^2=0.00 for all.

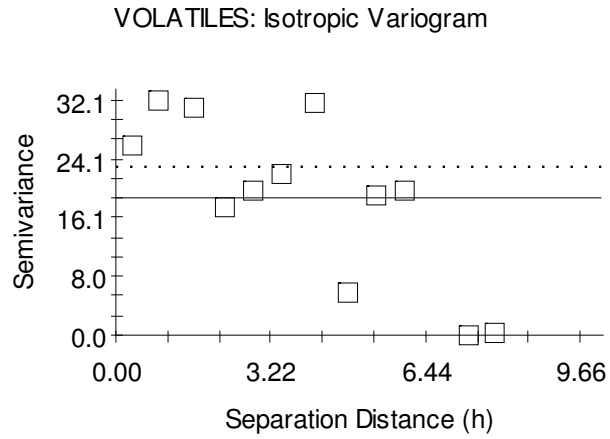

Figure 71. V.M variogram

To address the "saw-toothing", the automated lag distance is reduced to 12 and the uniform interval set at 2. The manipulation of the data has reduced the noise to produce a near linear model variogram with R^2 =0.73.

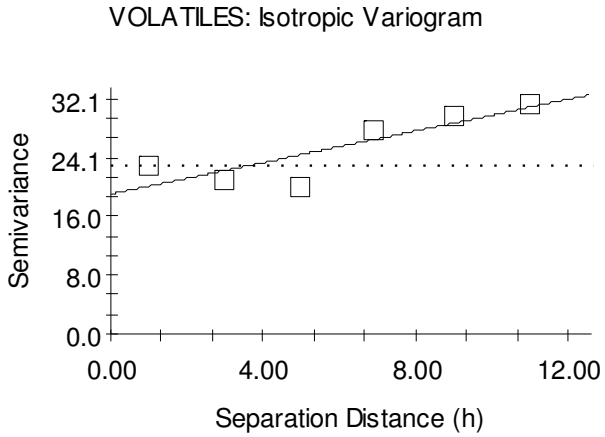

Figure 72. V.M variogram with lag distance reduced to 12 and intervals set to 2.0

Variogram is plotted for Ash. The data set fit into a Gaussian model with a R^2 =0.89. The fit is not perfect with data points lie off the slope of the variogram.

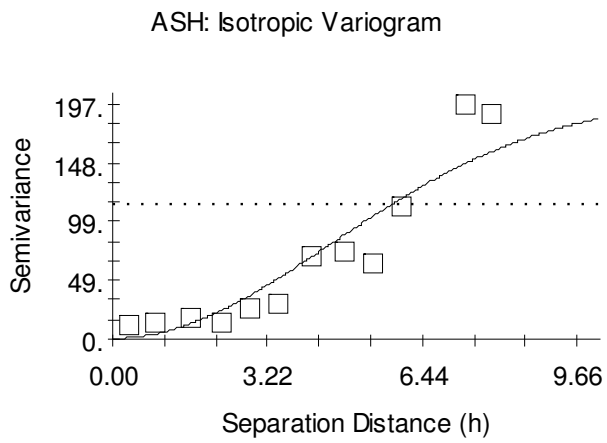

Gaussian model (Co = 0.70000; Co + C = 202.30000; Ao = 6.42; r2 = 0.886; RSS = 6044.)

Figure 73. Initial ash variogram automatically built

To circumvent the poor fit, the lag is manually manipulated in order to improve the fit of the experimental variogram. Therefore the lag distance has been reset to 18.50 with the uniform interval at 0.80. The final fit remains the Gaussian model, however the R^2 =0.97.

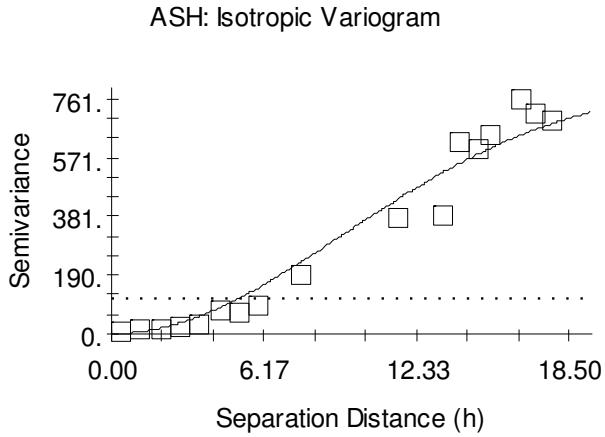

Gaussian model (Co = 1.00000; Co + C = 812.90000; Ao = 13.17; r2 = 0.967; RSS = 53806.)

Figure 74. Ash variogram after manipulation of the distance lag

C.V variogram is also plotted. The initial lag distance is 24.85 with a uniform interval of 1.66, which is automatically set by the software. The R^2 =0.74, which indicates deviation from the Gaussian model.

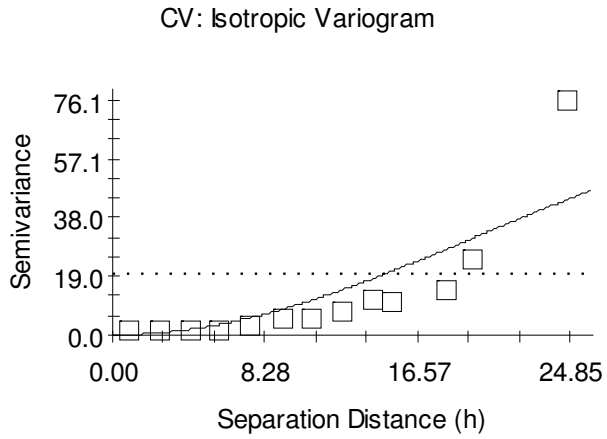

Gaussian model (Co = 0.10000; Co + C = 81.20000; Ao = 27.97; r2 = 0.738; RSS = 1503.)

Figure 75. Variogram plot for C.V using Gaussian model

In order to produce the closest fit of the experimental variogram the distance lag is adjusted from 24.85 and interval 1.66 to 18 at an interval of 1.40 to increase the R^2 =0.94.

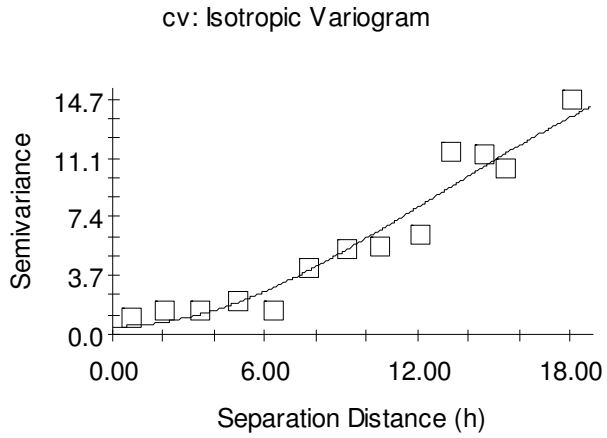

Gaussian model (Co = 0.50000; Co + C = 20.99000; Ao = 17.78; r2 = 0.942; RSS = 15.0)

Figure 76. C.V variogram after the distance was is reduced

Lastly the R.D variogram is automatically generated through model build in GS+ Geostatistics to produce a best fit experimental model for the data set. The result of which is a near fit of the data to a Gaussian model with an R^2 =0.94. The data however still deviates slightly from the model.

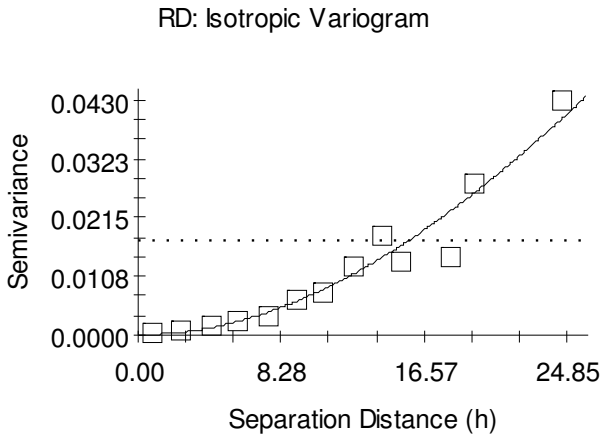

Gaussian model (Co = 0.00010; Co + C = 0.18060; Ao = 49.42; r2 = 0.942; RSS = 1.066E-04)

Figure 77. R.D Variogram plot for R.D using Gaussian model

The fit of the data is improved through reducing the distance lag from 26.62 to 24.85 with uniform interval of 1.66.The result of which the R^2 =0.94 increases to R^2 =0.99.

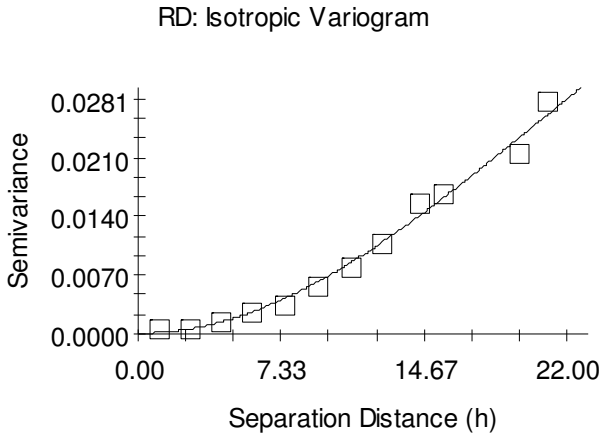

Gaussian model (Co = 0.00010; Co + C = 0.06350; Ao = 28.85; r2 = 0.990; RSS = 9.177E-06)

Figure 78. Manipulated variogram to achieve the best fit experimental variogram for R.D

4.6. Volatile matter relationships

Expected V.M qualities of the coal based on the ash are calculated using equation 3. The calculated values are plotted with the actual V.M values received (Figure 79.). The graph displays a relationship between the calculated and the actual measured V.M content.

The calculated V.M fluctuates between just 15% and 24%, as observed in the blue lines. Two points have the lowest values at or just below 15% V.M. The measured V.M, indicated as red in the graph below, display greater fluctuation. The greatest fluctuation is observed at points between 20% and 24% where the V.M is close to the calculated V.M.

In summary, the calculated V.M is greater than the actual V.M received.

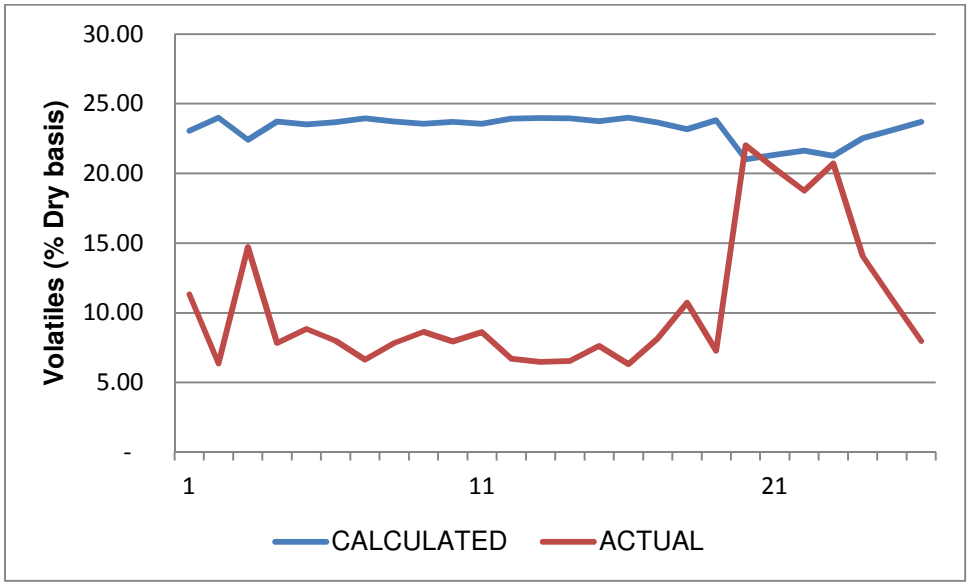

Figure 79. Graphical comparison between calculated V.M and measured V.M for study area B.

To further investigate the relationships involving the V.M, V.M versus ash is plotted (Figure 80.). A rapid change in V.M between Ash 10% and 20% is present. The V.M peak at values greater than 20% and follow to dropping to less than 10%. The fluctuation in V.M begins to taper off at Ash greater than 20%. Two outliers are present with Ash greater than 50%. Therefore maximum V.M is identified at 20% Ash.

The data points display a non-linear relationship; therefore an exponential trend line is superimposed as it had the closest fit. The R^2-value calculated is 0.15. Consequently the data is neither displaying an exponential trend nor linear trend and displays poor correlation to each other.

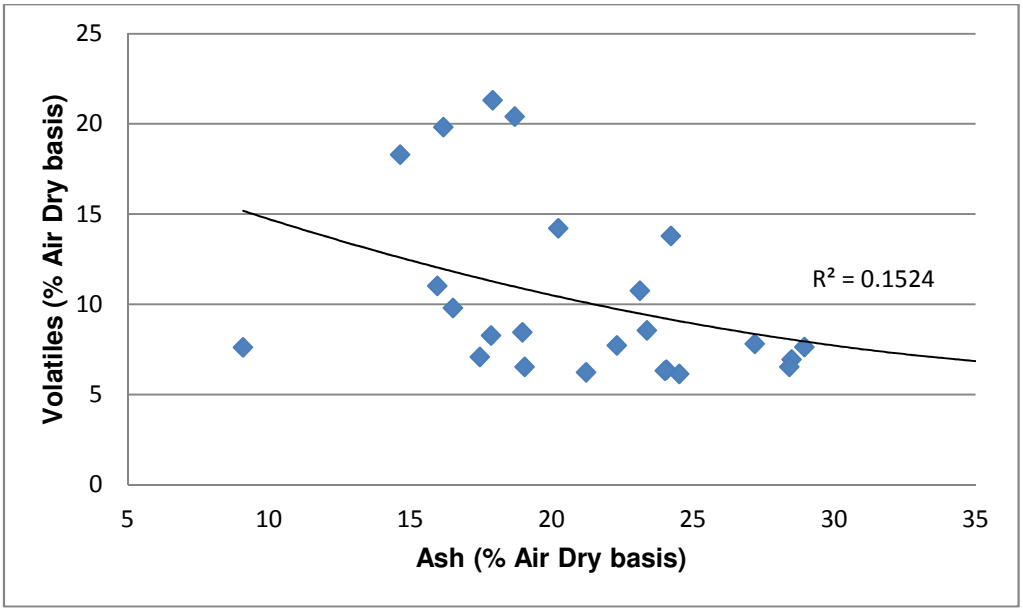

Figure 80. Cross correlation between V.M and Ash

5. Comparison between Study Area A and Study Area B

Study Area A has 51 samples, while Study Area B has 26 samples. Though the number of samples differs between the areas, comparison of relevant parameters will be done. Comparison will be conducted for the following:

- Volatile matter versus Ash;
- Measured V.M and calculated V.M;
- Volatile matter versus R.D;
- Ash versus R.D; and
- Calorific value versus R.D.

5.1. Volatile matter versus ash

In Study Area A poor correlation is observed between the V.M and the ash with exceptions at high ash. In Study Area B the correlation between the parameters is even lower, possibly due to the smaller dataset. Greatest variability is present at 10- 20% Ash, followed by a decrease which tapers off towards the outliers (Figure 81). This is further supported by the respective R^2 values of the areas which display a poor exponential relationship between V.M and Ash.

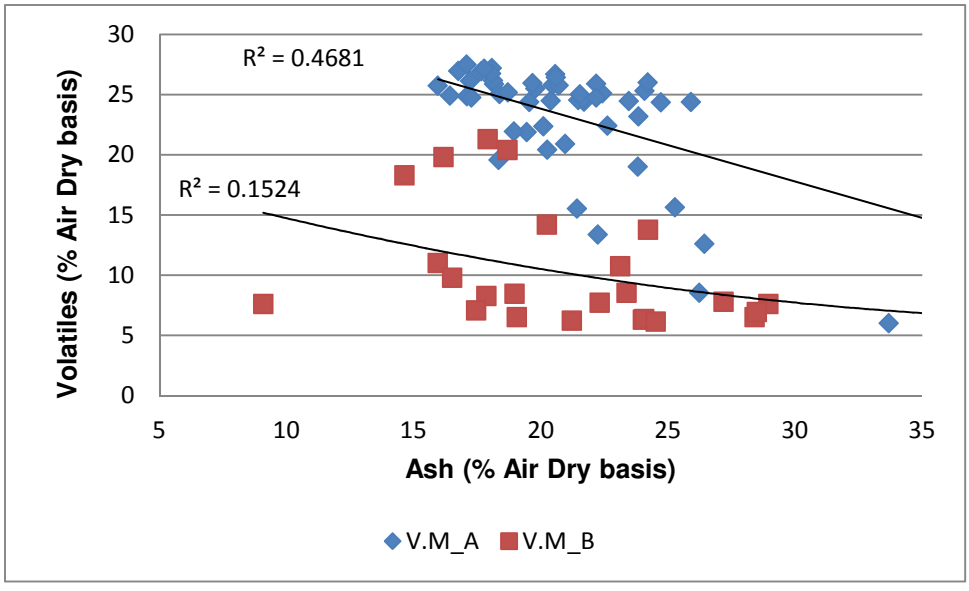

Figure 81. V.M versus Ash scatter plot of Study Area A and B

5.2. Measured volatile matter and calculated volatile matter

The two study areas (A and B) are compared in order to determine any similarities or discrepancies between the study areas. For Study Area A (Figure 82), the actual V.M from analysis is greater than that calculated from Equation 3 with six exceptions that are greater than the measured. Conversely, Study Area B displays an opposite trend to Study Area A (Figure 82), as the measured V.M is less than that which is calculated. This is true for all data points, with the exception of two which are nearly equal to the calculated V.M. Thus on comparison of the two areas, differing conditions prevailed which influenced the behaviour of the coal seam on the basis of the V.M.

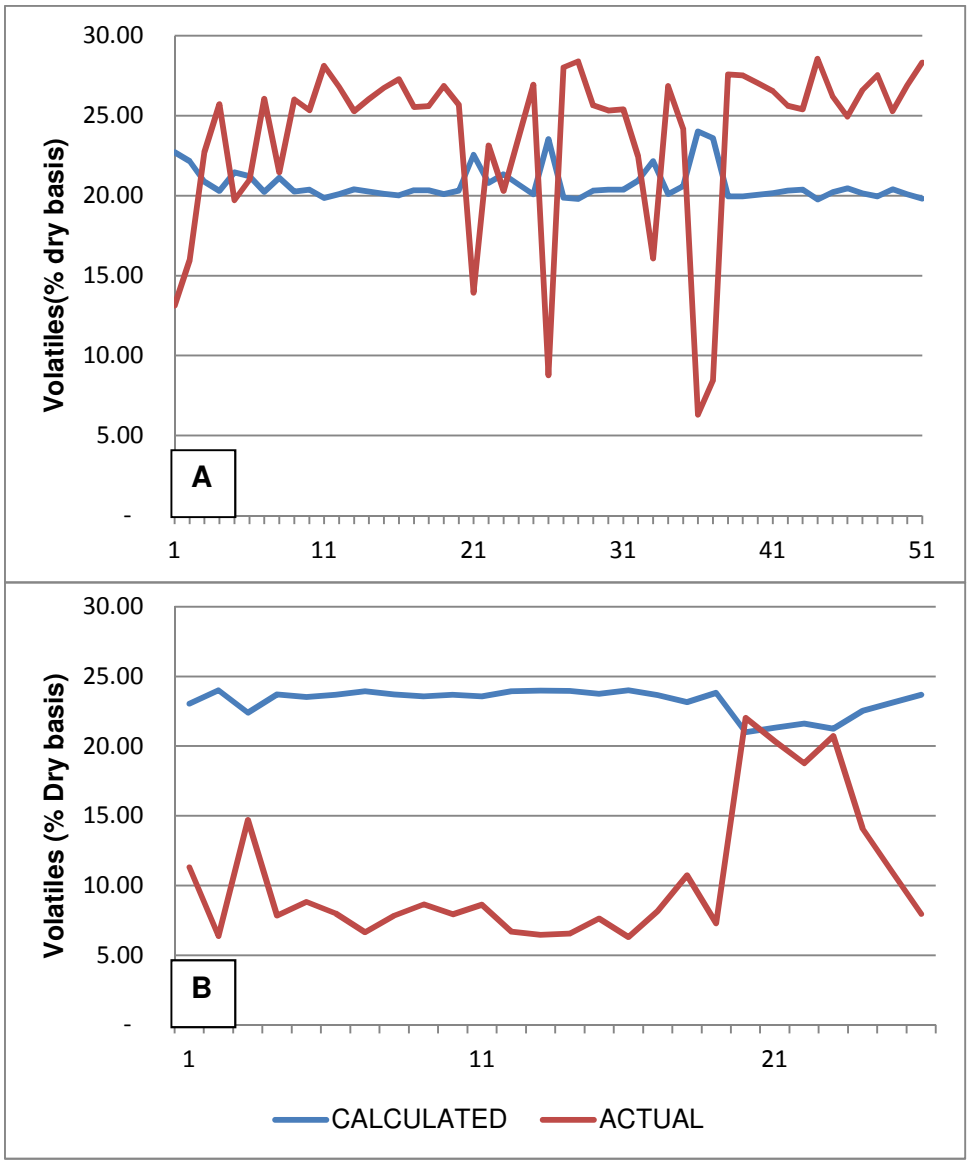

Figure 82. Measured and calculated V.M of Study Areas A and B

5.3. Volatile matter versus relative density

Figure 83 shows the relation between V.M. and R.D for both areas. Study Area A displays better correlation between these parameters than Study Area B, but this may be attributed with the differing sample sizes. The variability is supported by the R^2 values which are both low. Overall V.M displays no particular trend.

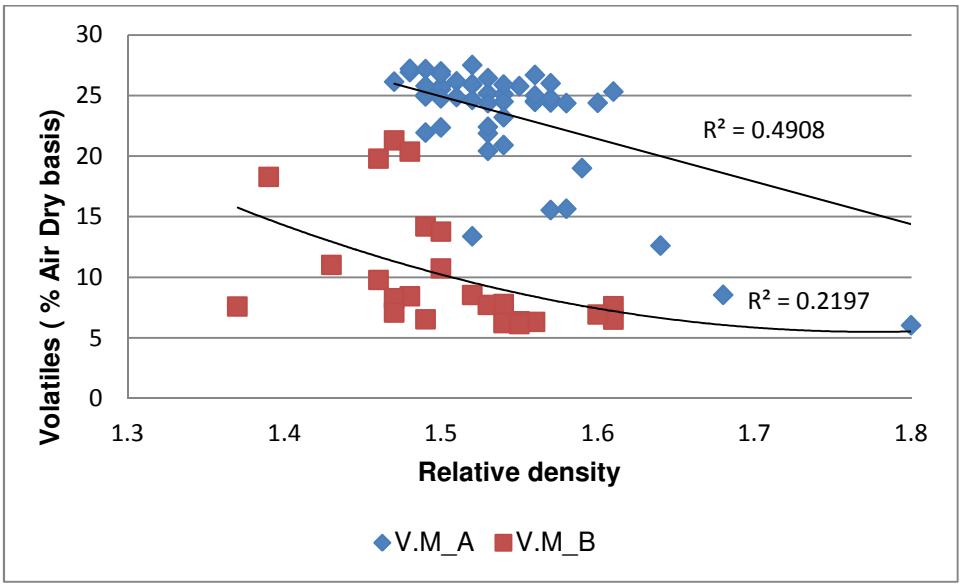

Figure 83. V.M versus R.D of Study Area A and B

5.4. Ash content versus relative density

In Study Area A, an R^2-value of 0.73 indicates some correlation between the density of the samples and their Ash (Figure 84.), a correlation which is even stronger for Study Area B, as shown by a R^2 -value very close to 1 (R^2=0.98)(Figure 84). This may be explained by the high ash content which is often silica rich(shale has a density of 2.4g/cm^3) and has a higher density than that of coal(1.5g/cm^3), which is richer in carbon and lower in ash (The South African Coal Processing Society, 2012).

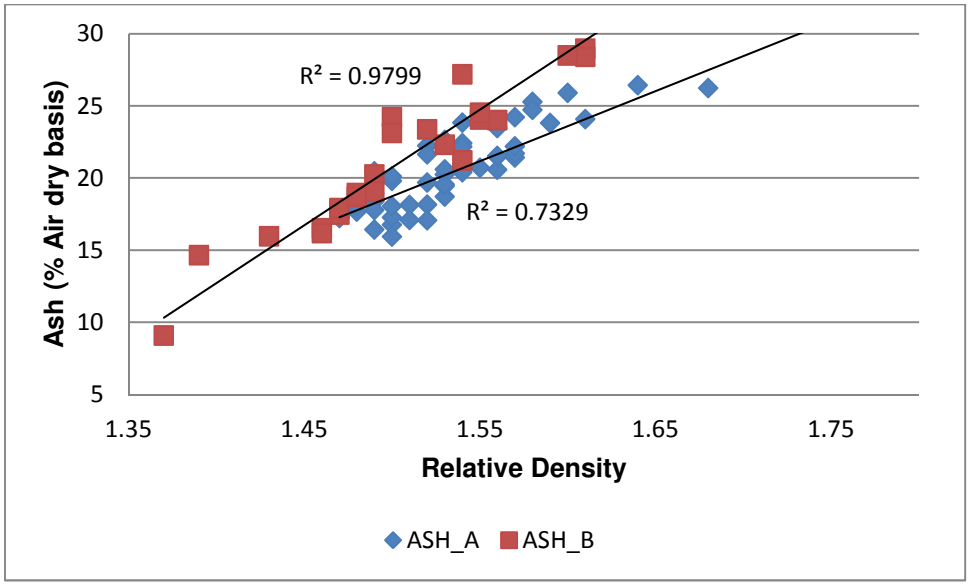

Figure 84. Ash versus R.D scatter plot of Study Area A and B

5.5. Calorific value versus relative density

On comparison, the two study areas indicate differing relationships between R.D and CV. In Study Area A with R^2 value equals 0.62 (Figure 85), whereas a better correlation is present in Study Area B (Figure 85). In both area the C.V decreases with increasing R.D. However the bias caused by unequal sampling should be considered in this comparison.

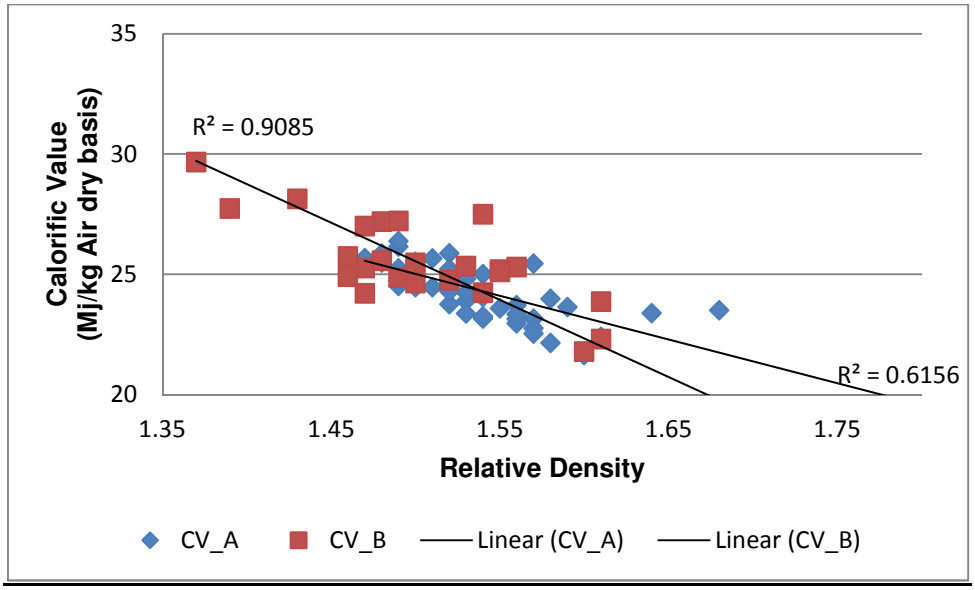

Figure 85. C.V versus R.D scatter plot of Study Area A and B

6. Previous studies on the interaction between coal seams and intrusions

6.1. Huaibei, Hongyang and Handan Coalfield (China)

An investigation was conducted in northern China by Yao et al. (2011) on Pennsylvanian-Permian coal formations in the locations highlighted in the map below (Figure 86). The formations experienced multiple phases of metamorphism which began in the Mesozoic era and culminated during the early Cenozoic era. The study was selected due to the age for formation which is close to the Permian coals of the study area as well as the coal rank (bituminous) and intrusion patterns.

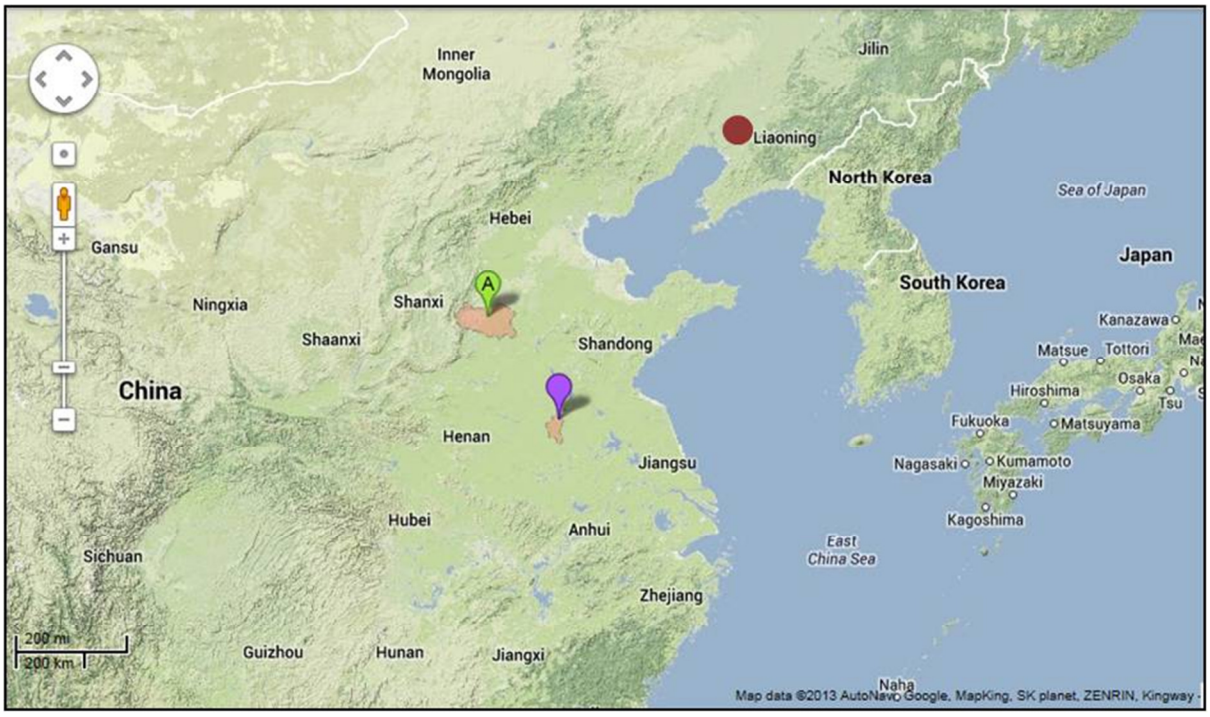

Figure 86 Location map of Huaibei and Handan, China (Google maps, 2013)

The purpose of the study was to investigate the influence of various sills with differing patterns on coal rank, quality and adsorption capacity. The study took place in 3 locations in active coal mines. Each location displayed one of the following patterns under investigation:

- Pattern I: Dyke cut through;
- Pattern II: Dyke cut in;
- Pattern III: Floor intrusion by sill;
- Pattern IV: Roof intrusion by sill; and
- Pattern V: Dual intrusion (roof and floor) by sill.

In total 24 samples were taken in 5 underground profiles. The samples were taken through grab sampling. An additional 2 samples were taken in an unaltered area which is 2km from the heat affected areas. Thin sections were made for reflectance investigation, proximate and ultimate analyses were conducted, and 16 samples were analysed for methane isothermal adsorption.

Results from the study reported that where the dyke cuts through the coal (Pattern I) the ultimate and proximate analyses indicated that the ash and carbon were noticeably affected by the intrusion, as both parameters were elevated in the affected samples relative to the unaltered samples. Numerous calcite occurrences were noted in veinlets in the altered samples, which increased the ash. Lastly no changes were observed in the V.M closer to the contact.

In pattern II, the dyke cuts into the coal. The results indicate the high volatile bituminous coal was altered to a meta-anthracite with Ash of ~25.55% and inherent moisture of ~5.13%, both of which were higher than the unaltered coal. The carbon content towards the coal/dyke contact also displayed an increase in content.

In pattern III, the dyke intrudes below the No. 3 coal seam of the Permian age Shihezi Formation. Results indicate that 0.5m towards the sill the ash increases to 19% and the V.M decrease to ~10% as well as the moisture to ~2.6%, whereas the furthest samples remain unchanged.

Pattern IV (Figure 87) was where the sill intruded above the No. 9 coal of the Pennsylvanian-Permian age Shanxi Formation. The seam has a sandy shale and black siltstone parting in the centre. Four samples were taken of which two were 0.80(E1) and 0.85m (E2) away from the coal/sill contact. The two samples with similar distance displayed differing results. The moisture content of the sample 0.80m from the sill, which lies above the parting has a higher moisture content in relation to the sample below the parting (0.85m), while E2 reported lower Ash to E1.

Lastly in pattern V (Figure 88), the sills intrude both the floor and roof of the coal seams. Samples close to either of the contacts, D1 (upper contact) and D5 (lower contact) reported that the lower contact produced more ash and less I.M than the above contact; however the V.M reported an inverse relationship where the upper contact had less Ash than the lower contact coal. This may be explained by the presence of the carbonaceous shale parting.

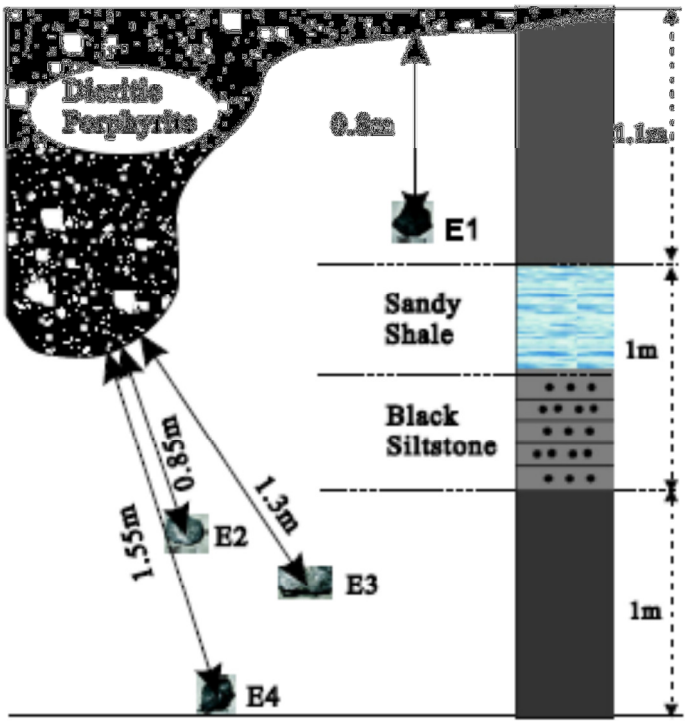

Figure 87. Schematic representation where the sill overlies the coal seam as well as an example of the presence of interburden lithology (Yao, et al., 2011)

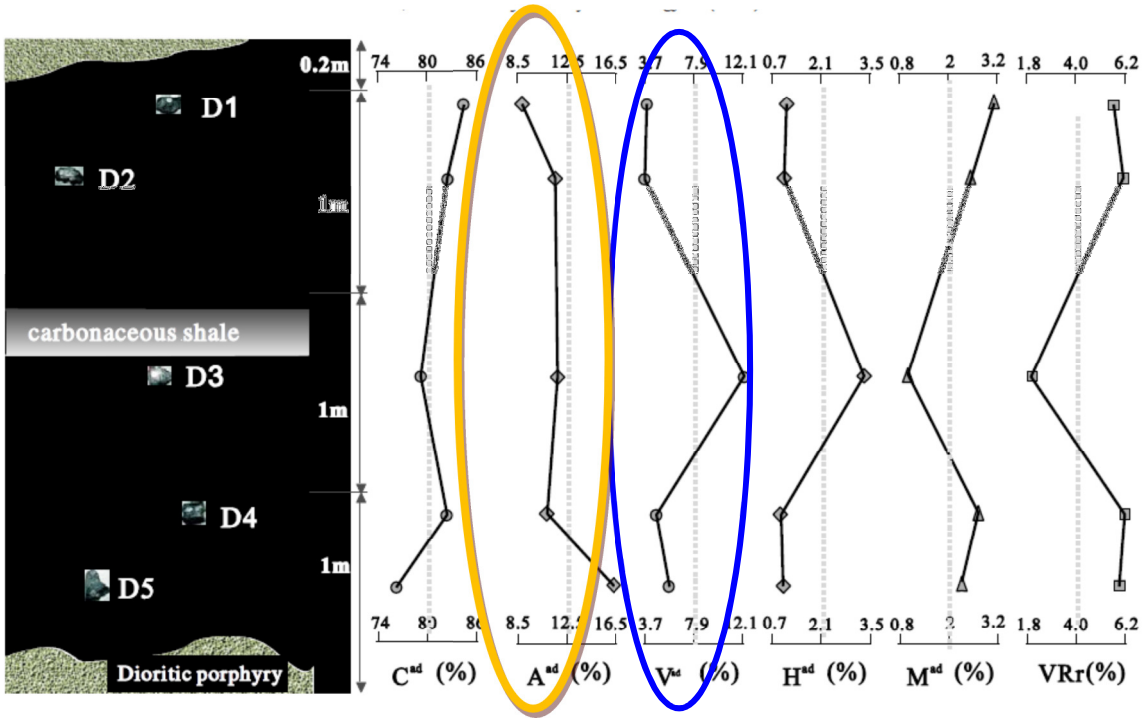

Figure 88. Schematic representation where there is an intrusion both in the roof and floor of the coal seam (Yao, et al., 2011)

In summary, five factors were found to influence the characteristics of thermal metamorphism:

- Rates and duration of heat conductivity;
- Heat conductivity/ convection model;
- Intrusion forms between dyke and sill and the size of the intrusions;
- Distance from the contact; and
- The thermal properties of the country rocks.

Comparing the sill and dyke intersections, the study found that sills have greater influence on the coal. Metamorphism is found to increase within one or two widths of the intrusion. Overall the ash showed an increase whereas the V.M showed a decrease with the exception to pattern V.

6.2. Kaierkan Deposit, Noril'sk District (Russia)

The study was conducted in the bituminous Kaierkan deposit which is found within the late Palaeozoic Tunguska series (Figure 89). The series has been intruded by a 6.75m thick dolerite dyke. Four samples from the Kaierken deposit, 24.50m, 0.30m and 0.05m away from the dyke/coal contact and one additional sample at the contact. Additional samples were also collected of Silurian age sapropelic coals as well as graphite samples from Kureiskii mine (Melenevsky et al., 2008). The purpose of the study was to understand the coal transformation of the coal seam under the influence of a dolerite dyke.

The investigation was selected as both areas had coal of similar rank and were both intruded by an igneous body.

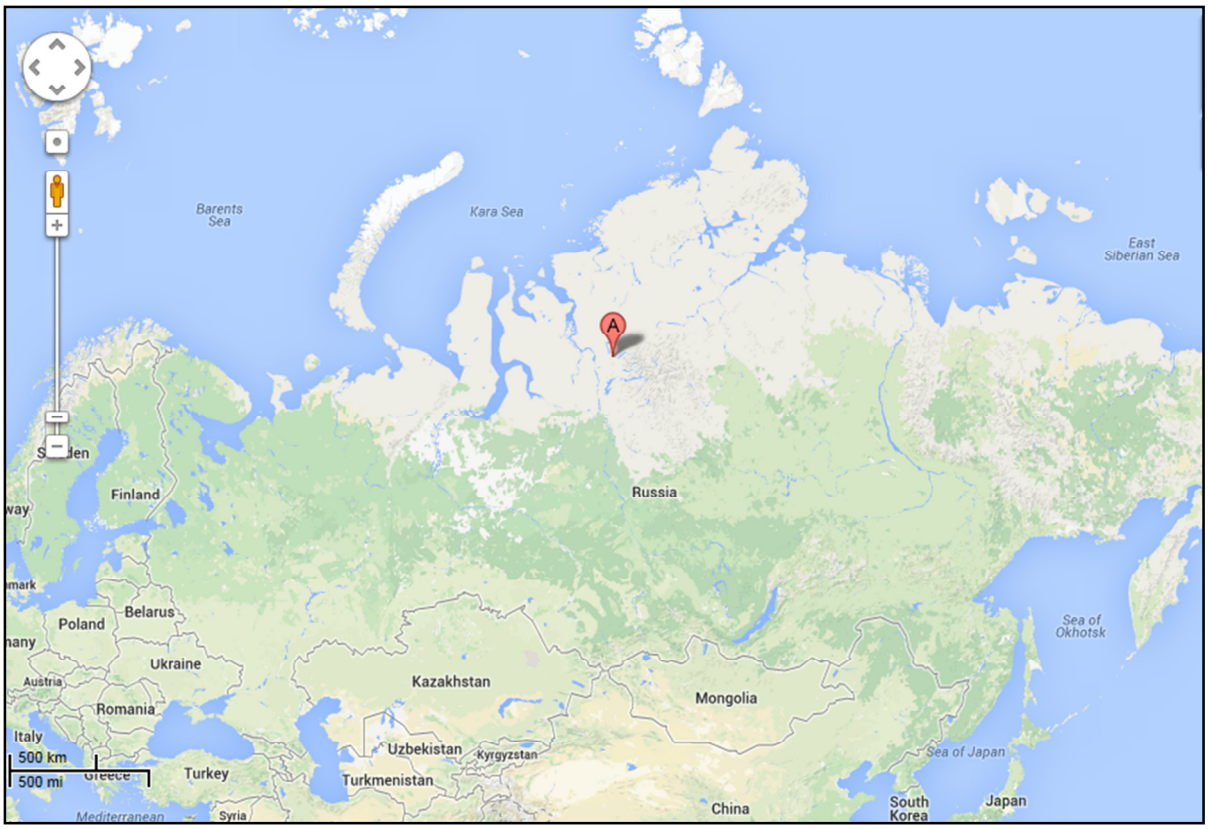

Figure 89. Location map of Noril'sk District, northern Russia (Google maps, 2013)

In order to achieve the above, pyrolysis analysis was conducted on the bituminous coals in order to determine the hydrocarbon (HC) content. Vitrinitic reflectance was measured and chemical kinetics modelling (CKM) was conducted to determine the dynamics involved in contact metamorphism.

Once the pyrolysis on the bituminous coal was completed, it was compared to the immature sapropelic coals and the metamorphosed graphite sample. Results indicate that the Hydrogen Index, calculated from the determination of HC, remained constant between 0.30m and 24.50m. However a decrease was noted from 0.05m to the contact. Between 0.30 m and 24.50 m, the vitrinite reflectance of the coal was 2.00-2.30%. Closer to the contact, less than 0.05 m from the contact, the vitrinite reflectance decreased to 4.80-5.30%. V.M at dry ash free was found to decrease during the process of metamorphism (catagenesis).

Organic transformation through CKM was carried out and it was found the coal was bituminous at distances far greater than the dyke's thickness implying that the coal was metamorphosed to bituminous prior to the dyke's intrusion by regional metamorphism. Taking this into consideration the thermal effect was calculated by the authors using Fourier's heat conductivity calculation at the following distances from the contact: 0.45m, 0.30m and 0.15m. Results reported 10% of V.M HC was lost, followed by 70% at 0.30m and

nearly 100% at 0.15m from the dyke Therefore the residual HC are released by 0.5m and culminate at 0.15m, however based on sample 2 (0.30m away from the contact) the range of influence should be less as the vitrinite reflectance showed no difference as mentioned above.

In summary, the Melevensky, et al. (2008), concluded that catagenesis in their study area experienced two metamorphic events, i.e. (1) Transformation to bituminous and (2) transformation from bituminous to anthracite due to the dolerite intrusion. Pyrolysis results indicate the most amount of HC was released at the 1st stage of metamorphism. Lastly CKM for coal cracking indicated that vitrinite reflectance alone cannot be used as a geothermometer and is best used as an estimation tool, as it has been found that the degree of transformation depended of the intrusion's thickness and temperature, which have an inverse relationship to each other. It is also known that the vitrinite reflectance is calculated by the degree of transformation, thus it cannot be employed as an absolute geothermometer.

6.3. Springfield coal (United States of America).

The study by Stewart et al. (2005) was conducted on the No. 5 seam of the Pennsylvanian age Carbondale Formation near Eldorado, Illinois (Figure 90). The coal seam is high volatile bituminous in rank and has been intruded vertically by a highly serpentinized 10.10m thick dyke intrusion (which is tentatively called a kimberlite). The study though not of the same age as the study area, was selected on the basis of it being a bituminous coal seam that had been intruded by an igneous intrusion.

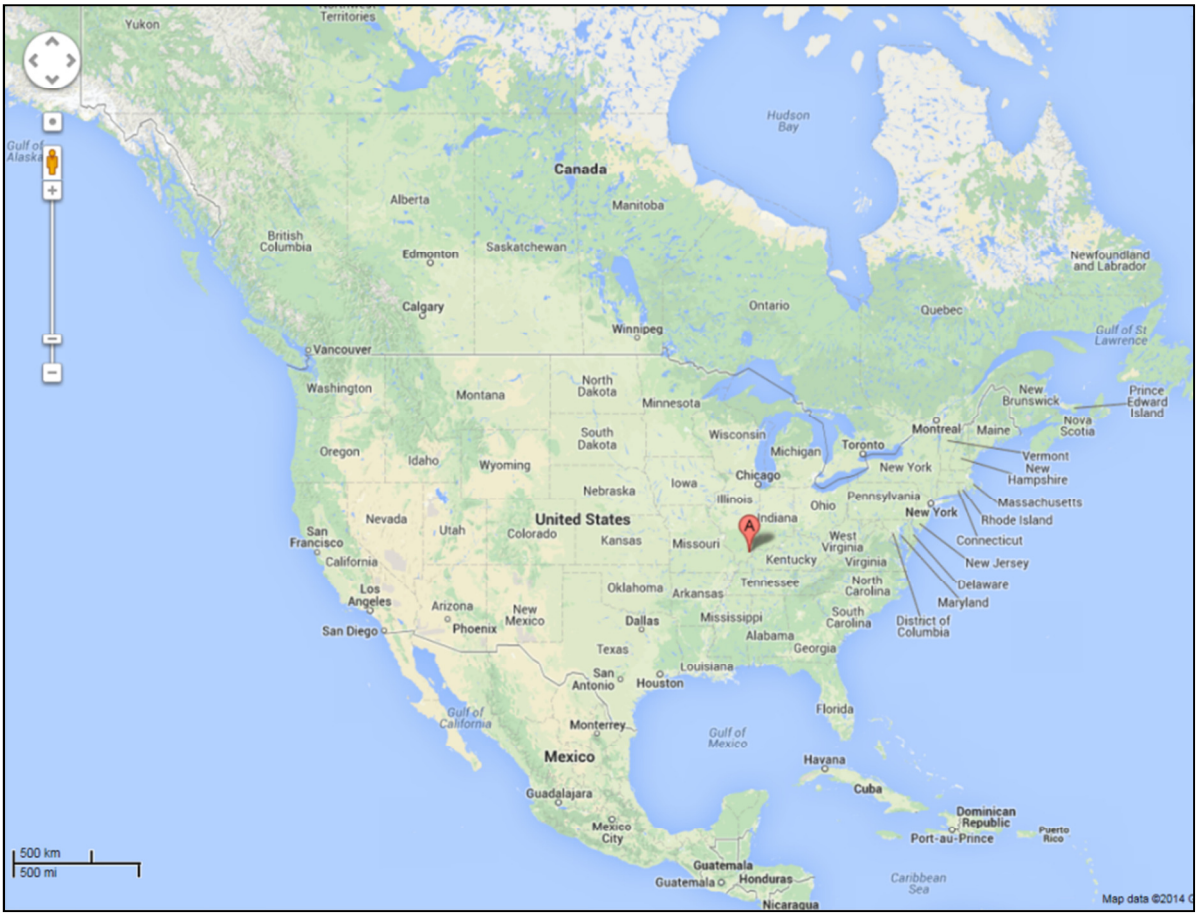

Figure 90. Location map of Eldorado, Illinois (United States of America)

The authors employed the following methodology in their study. They collected 15 samples along the mining face of the mine at increasing intervals which equated to approximately 60m from the sill. In addition seven samples were collected at the intrusion. The samples were collected with a hammer taking a portion of the seam and do not represent the entire seam, though all samples were collected along the same height. Some samples were prepared for vitrinite reflectance (8 samples), and the remaining samples sent for proximate and ultimate analyses.

Results from the analysis of inorganic components indicate that there was an increase in the Mg due to the continuous influx of serpentinization from the dyke, and simultaneously there was an increase in CaO and Mn. Adjacent to the intrusion, unstable sulphides decreased in abundance relative to the unaltered coals. Other elements hosted in inorganic minerals that showed a decrease were Ar and Hg, where the chalcophiles were found to have been driven off by the intrusion.

Results from the vitrinite reflectance showed that the coal returned to the high volatile bituminous at 120% of the dyke's thickness, thus moving from an anthracite/ meta-anthracite

at the contact to high V.M bituminous. This study, as well as that of Yao et al., (2011), highlight that the usage of vitrinite reflectance as a geothermometer is a speculative tool. This point was further re-enforced by the presence of hydrothermal fluid such as calcite veins and serpentine which implied that the initial temperature (T_o) was not the ambient temperature of the contact and thus the temperature of the intrusion's melt was higher than that calculated.

7. Discussion: Western Witbank Coalfield

7.1. Summary of results

The relationship of six parameters has been assessed in Study Area A. Correlation studies indicate that the thickness of the sill is poorly related to the distance, R.D and V.M., and very poorly with the ash and C.V. Distance between the sill and the coal is also poorly correlated with R.D, ash and C.V. However, the relationship between distance and V.M is clear, with a correlation coefficient of 0.75. Between 10-20m from the sill, the V.M displays rapid increase from the origin.

The proximate parameters display better correlations to each other than to thickness and distance, this is seen in the good relationship between R.D and V.M and the very good relationship between R.D and the ash. Lastly R.D has a poor correlation with the C.V (R^2=0.62) when compared to Study Area B. Lastly the V.M has a good correlation with the ash and a poor correlation with C.V, whereas Ash and C.V have a very strong correlation (0.94). Overall, the V.M display better correlation to both the distance from the sill and the thickness of the sill. Therefore the relationship of the V.M was further assessed through the empirical equation suggested by Van Alphen (2012).

Thus, there is no evidence that either the thickness of the sill or the distance between the sill and the coal seam have any effect on the coal quality in Study Area A.

For Study Area B, relationship between each of the measured parameters indicates that R.D has a strong inverse correlation (-0.95) to C.V, a strong positive relationship (0.98) to Ash, and a weak correlation (0.22) to the V.M. On the other hand, C.V negatively corresponds strongly with the Ash (-0.96) and not to the V.M. The ash shows poor correlation with the V.M.

Overall the following relationships are present in Area B:

- R.D and C.V;
- R.D and Ash; and
- C.V and ash.

Therefore the all the above have a linear relationship. This has been further supported by regression graphs of the parameters.

The experimental calculation from Van Alphen (2012) indicates the coal in Study Area B is devolatilised, as the measured V.M are less than those expected for coal of that nature.

Therefore Study Area A and Study Area B indicate differing results in the measured V.M of the samples. Study Area A displays no devolatilisation with an exception of 11 samples shown in the calculated V.M graph, while Study Area B displays all samples to be devolatilised. Therefore the additional factors are to be reviewed to determine what factor in Study Area A and Study Area B result in the differing results.

The two main differing conditions in the study areas are:

- The sill is overlying in Study Area A, while it is underlying in Study Area B; and
- In Study Area A, a thick sandstone layer is present as well as shale bands that separate the overlying coal seams from the sill (please refer to stratigraphic column). Underlying the bottom coal seam is Dwyka tillites which are consolidation of material in a sandy matrix.

7.2. Conductivity

According to Yao et al. (2011), different rock types have differing conductivity properties with coal being the lowest increasing to shale which itself has a much lower conductivity than sandstone which is known to have a very high conductivity. Conductivity is controlled by:

1. mineralogical composition;
2. degree of metamorphism;
3. porosity;
4. anisotropy; and
5. temperature (Jones, 2003)

Sandstone, shale and coal have differing conductivity due to the controlling factors mentioned above. Between sandstone and shale, studies by Jones (2003) and Railback(2011) indicate that shale has the lowest conductivity ranging from ~0.5 to 3.8 $Wm^{-1}K^{-1}$ whereas sandstone has more than double the conductivity of shale, with a conductivity range of between ~2-7.5 $Wm^{-1}K^{-1}$ (Figure 91).

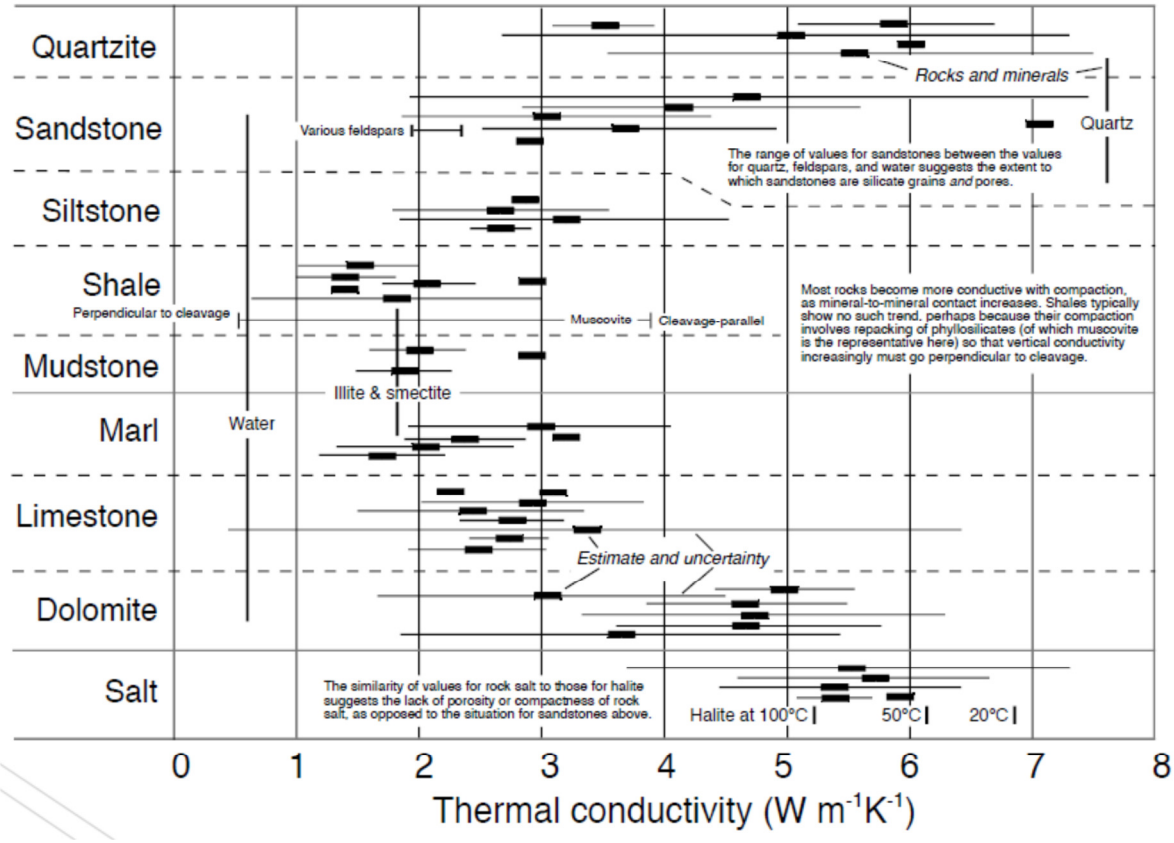

Figure 91. Thermal conductivity of sedimentary rocks (Railback, 2011)

In terms of the mineralogical composition of the rock types, the sandstones of the Ecca Group are mainly quartz, feldspar and slightly micaceous (Jones, 2003). From personal observation during core logging, the sandstone is quartz-rich with laminations of carbonaceous silty material. The grain size is coarsening downwards. Shale within the Ecca Group is characterised by clays, minor quartz, feldspar, muscovite and carbonaceous material which is all cemented by a silica matrix (Jones, 2003).

In relation to Study Area A, a sandstone layer with an average thickness of 10.91m and a maximum of 26.85m is located directly below the sill. The sandstone has the same composition as that described above. Simultaneously the coal seams are separated by variable shale bands which occur consistently in the study area.

Therefore in the conditions which prevail in Study Area A, the heat is transferred to the conductive sandstone layer underlying the sill intrusion and overlying all the coal seams. Progressing down the stratigraphy, the heat encounters poorly conductive coal seams as well as poorly conductive shale bands. As a result the heat of the sill undergoes good conduction through the sandstone and is barred and isolated from the bottom coal seam by the overlying poorly conductive lithology.

On the other hand the prevailing condition is Study Area B indicate a more conductive layer underlies the coal seam. From the regional geology, the Dwyka tillites are the obvious suspects. The intrusion underlies the tillite floor, which due to its clastic sediment composition supported conduction of the emanating heat produced by the sill or sill up to Seam 2.

In addition to the conductivity, the coal in Study Area A is bituminous with average V.M of 22.69 (30.29 *DAF*). This implies the coal had been upgraded from sub-bituminous by another mechanism besides direct heat. Such heat is postulated to be from hydrothermal activity which is supported by the presence of chlorite filled veins and fractures. However this was not further investigated as it extends beyond the scope of the investigation.

8. Summary

The aim of the study was to investigate the effect of the undulating sill on the coal within its immediate vicinity and the implications this relationship had on the V.M of the coal. Two study areas were selected for the study. In Study Area A the sill overlies the coal body where in which the sill is separated from the top coal seams by on average 10.91 m thick sandstone with intermittent bands of shale, siltstone and carbonaceous shale. Study Area B on the other hand is located where the same sill underlies the coal seams, and the parting between the sill and the bottom coal is postulated to be the Dwyka tillites only which is intersected during drilling.

51 composited samples were taken from Study Area A and 26 samples which were not composited were taken from Study Area B. The samples were selected based on the stratigraphic location of the seam and it's regularity in the coalfield. Therefore Seam 2 was selected for investigation in the study.

Correlation investigations in Study Area A indicate that a poor correlation is present between the V.M and the thickness of the intrusion and a better correlation between V.M and distance from the sill, whereas in Study Area B, a clearer trend was observed for V.M in relation to the other parameters through the variograms.

The V.M behaviour was further investigated through an experimental equation to determine if the coal seam had been devolatilised. The experimental calculation, based on a regression slope in relation to the South African baseline, indicated that two very different events had occurred in the two areas. In Study Area A, the calculation indicated that the coal in the area was not devolatilised, thus implying that the sill had no influence on the coal. The results of the experimental equation in Study Area B indicated that the V.M of the lower coal seam had been greatly reduced by an external factor. Therefore in the case of Study Area B the underlying sill is identified as the source of the devolatilisation, as the majority of the 26 samples displayed devolatilisation.

Studies from diverse locations were assessed to further understand the results. In all the studies, the V.M of coal was most affected by its relationship to nearby sills. The variability was governed by proximity to the sill, the shape of the intrusion, the thickness of the intrusion, orientation or location of the sill. Each study investigated different scenarios relating to the coal seam and sill relationship.

Of the multiple scenarios of sills intruding into coal seams, different examples from China's Shanxi formation match the relationships seen in Study Area A and Area B. In the two study

sites, the dolerite sill overlies the coal seam and the results indicated that the inherent moisture (IM) displayed little change and less ash was present where the coal was separated from the sill by shale. Another sample containing siltstone interlaying displayed higher ash and low IM. Overall the main factor controlling the measured parameters is the conductivity of different rock types.

In Study Area A results indicated that the bottom coal seam was not devolatilised. On further investigation of the stratigraphy, it was found that a +/-11m thick sandstone underlies the sill which is a highly conductive rock, but further down the stratigraphy poorly conductive rocks such as shales and mudstones are present. These rocks have been found to isolate heat which resulted in no devolatilisation of the seam by the intrusion.

In Study Area B, a sill was found to underlie the coal seams and results indicate that the limited sample group reported low moistures of 4.01 and actual V.M less than the calculated V.M, which is indicative of a devolatilised sample. However as the sample population is much smaller than that of Study Area A, some bias may be present in the results. Underlying the coal seam are Dwyka tillites consisting of upward fining clastic sediments (Catuneanu, 1998) which are variably conductive. Therefore it is postulated that more heat was transmitted to lower coal seam through the conductive lithological layer.

In conclusion, two study areas with differing intrusion conditions have been assessed in order to determine how the undulating sill affects the coal seam when it intruded above and below the lower coal seam.

The outcome of the study was that the coal seam was not affected where the sill was overlying the coal, due to the thermal characteristics of the country rock where the sandstone conducted the heat and the underlying shale, coal and siltstone layers behaved as barriers through their non-conductive characteristics; neither the distance from the sill nor the thickness of the sill affected the bottom coal seam in Study Area A.

Results indicated that where the sill is underlying the coal seam (Study Area B), greater influence on the bottom coal is observed, as the measured V.M is less than that is anticipated through modelling; an indication that the coal may have been devolatilised by an external feature, such as the sill. The influence of the country rock also played a role in the area where a more conductive sandstone rich tillite aided the transmission of the sill's heat.

9. Bibliography

Aarnes, I., Svensen, H., Polteau, S. and Planke, S., 2011. Contact metamorphic devolatilisation of shales in the Karoo Basin, South Africa and the effects of multiple sill intrusions, *Chemical Geology,* 281(3-4), 181-194.

Cairncross, B (1990)

Cairncross, B., 2001. An Overview of the Permian (Karoo) Coal Deposits of southern Africa, *Journal of African Earth Sciences,* **33**, 529-562.

Catuneanu, O, Hancox, P.J and Rubidge, B. S, 1998. Reciprocal flexural behaviours and contrasting stratigraphies: new basin development model for the Karoo retroarc foreland system, South Africa, *Basin Research*, 10, 417-439.

Clauser, C and Huenges, E, 1995. Thermal Conductivity of Rocks and Minerals, Handbook of Physical Constants, Shelf 3, 105-126.

Crelling, J. and Dutcher, R. R, 1968. A Petrologic Study of a Thermally Altered Coal from the Purgatoire River Valley of Colorado, *GSA Bulletin,* 79(10), 1375-1386.

Dekker, K. and van Wyk, D.(compiler) (2008, cited January 2014*). Independent Competent Persons Report: The Sterkfontein Project and Delmas Coal Projects* (Bibliogragraphy on the Internet), Available from: http://www.keatonenergy.co.za/im/files/CPR_2_Geology_01apr08.pdf

Du Plessis, G. P., 2008. The relationship between geological structures and dolerite intrusions in the Witbank Highveld Coalfield, South Africa, M.Sc thesis, Department of Geology, University of Free State.

Du Plessis, J.J., 2008. Petrochemical Characterization of Dolerites and their Influence on Coal in the Witbank Highveld Coalfield, South Africa, Department of geology, University of Free State.

Duncan, A. R and Marsh, J. S., 2006. The Karoo Igneous Province *in* Johnson, M. R, Anhaeusser, C.R and Thomas, R. J (Eds.), The Geology of South Africa. Geological Society of South Africa, Johannesburg/Council of Geoscience, Pretoria, 501-520.

Falcon, R. M. S., 1977 Coal in South Africa-Part 1: The Quality of South African Coal in Relation to Uses and World Energy Resources, *Minerals Science Engineering,* 9 (4), 198-216.

Falcon,R., 2012 Coal in South Africa: Coal Qualities(Types) Related to Combustion, presented at the Coal Quality course, University of the Witwatersrand, 13-17 February 2012

Google maps., 2013. *Handan, China,* viewed 10 October 2013, from https://maps.google.co.za/maps?q=huaibei,+china&oe=utf-8&client=firefox-a&ie=UTF-8&ei=5vbUUq3zAsWg7Aa2-YDoAw&ved=0CAoQ_AUoAg.

Google maps., 2013. Kaierkan (Kayerkan) *Noril'sk, Russia,* viewed 10 October 2013, from https://maps.google.co.za/maps?q=huaibei,+china&oe=utf-8&client=firefox-a&ie=UTF-8&ei=5vbUUq3zAsWg7Aa2-YDoAw&ved=0CAoQ_AUoAg.

Google maps., 2013. *Illinois, United States of America,* viewed 10 October 2013, from https://maps.google.co.za/maps?q=huaibei,+china&oe=utf-8&client=firefox-a&ie=UTF-8&ei=5vbUUq3zAsWg7Aa2-YDoAw&ved=0CAoQ_AUoAg.

Hamidreza, H, Esmaeil, J and Abbas, S., 2012. Evaluation of Mayer curve validity on feed blending at the Zarand coal washery plant*, International Journal of Mining Science and Technology,* 22, 19-22.

Johns, A., 2012 Milling and Coking Properties, presented at the Coal Quality course, University of Witwatersrand, 13-17 February 2012

Johnson, M. R, van Vuuren, C. J, Visser, J. N.J, Cole, D. I, de V Wickens, H, Christie, A. D. M, Roberts, D. L and Brandl, G., 2006. Sedimentary rocks of the Karoo Supergroup *in* Johnson, M. R, Anhaeusser, C.R and Thomas, R. J (Eds.), The Geology of South Africa. Geological Society of South Africa, Johannesburg/Council of Geoscience, Pretoria, 461-500.

Jones, M. Q. W., 2003. Thermal properties of stratified rocks from Witwatersrand gold mining areas, The Journal of The South African Institute of Mining and Metallurgy, 173-186.

Melenevsky, V. N., Fomin, A. N. , Konyshev, A. S. and Talibova, O. G.,. 2008 Contact coal transformation under the influence of dolerite dike (Kaierkan deposit, Noril'sk district), *Russian Geology and Geophysics,* 49*, 667-672.*

Railsback, L. B. (compiler) (2011, cited January 2014) *Petroleum Geoscience and Subsurface Geology, University of Georgia*, Available from: http://www.gly.uga.edu/railsback/PGSG/PGSGmain.html

Saghafi, A. , Pinetown, K. L, Grobler, P. G and van Heerden, J. H. P., 2008. CO2 storage potential of South African coals and gas entrapment enhancement due to sills, *International Journal of Coal Geology*, 73, 74-87.

Snyman, C.P. and Barclay, J., 1989. The coalification of South African coal, *International Journal of Coal Geology*, 13(1-4), 375-390.

Snyman, C. P., 1998. Coal *in* The Mineral Resources of South Africa (M. G. C. Wilson and C. R. Anhaeusser, eds): Handbook, Council of Geoscience, 16, 136-206.

South African National Standards, 2004, *South African guide to the systematic evaluation of coal resources and coal reserves*, (SANS 10320:2004), Standards South Africa, Pretoria.

SRK Consultancy., 2006. Independent Competence Persons Report on mining assets of Exxaro Resources Limited (Internet), Publisher Unknown, 99-116, Available from http://www.exxaro.com/pdf/icpr/u/pdf/section3_no.pdf

England, T, Hand, P.E, Michael, D. C, Falcon, L. M and Yell, A. D (Eds.) 2012, Coal Preparation in South Africa, The South African Coal Processing Society, Pietermaritzburg, 46-46.

Van Alphen, C., 2012. Coal Quality Impact, presented at the Coal Quality course, University of the WItwatersrand, 13-17 February 2012

Vann, J., 2008. Applied Geostatistics for Geologists and Mining Engineers, Quantitative Group, Fremantle

Yao, Y., Lui, D. and Huang, W., 2011. Influence of sills on coal rank, coal quality and adsorption capacity in Hongyong, Handan and Huaibei coalfields, North China, *International Journal of Coal Geology,*88(2-3), 135-146.

10. Appendix

FROM	TO	MAIN	SUB	SEAM	COLOUR	TEXTURE	WEATHER	MINERALS	REMARKS
0.00	20.60	CL							
20.60	21.62	SS			LBR	F	HW		CLAYISH
21.62	23.68	SS			CR	F-M			
23.68	26.45	SS5			BR/GY				CONTAIN GREY CARBONACEOUS SILTSTONE LAMINATIONS, 50:50 SANDSTONE, SILTSTONE
26.45	28.64	SS	ST		LGY	F			CONTAINS MINOR SILTSTONE THIN BANDS
28.64	28.73	SS			GY	F			
28.73	29.20	SS			W	M-F			
29.20	29.36	SS			DG	F		P	OCCASSIONAL PYRITE LENSES
29.36	29.77	SS			W	M-F	SW		
29.77	31.96	SS			W	F	SW		BURNT, BROKEN IN PARTS
31.96	36.88	SS			CR	M-F			RECRYSTALLIZED
36.88	39.86	DO			GGY	M-C		P	FRACTURES WITH CHLORITE INFILLING, PYRITE SPECKLES PRESENT, SHARP IREGULAR CONTACT
39.86	44.30	DO			DG-GY	C		CA	DARK GREEN HORIZONTAL CALCITE VEINS
44.30	44.75	DO			GGY	F			DOWNWARD FINING TOWARDS SANDSTONE CONTACT
44.75	46.37	SS			LGY	F			COARSE LENTICULAR SANDSTONE LENSES, MINOR SILTSTONE BANDS, BROKEN
46.37	47.64	SS5			GY				ALTERNATING LAMINATIONS
47.64	49.51	ST			GY				MINOR WHITE SANDSTONE BANDS, BROKEN CORE
49.51	49.56	S			GY				
49.56	63.18	SS	ST	OVB, LOW	LGY	M	SW		CRUMBLED TEXTURE AT TOP, COARSE AT TOP, BANDING, BECOMING GREY

									DOWNWARDS
63.18	63.83	CMD		S5	B		SW	P	BANDED, BROKEN, POSSIBLE CORE LOSS
63.83	64.39	ST		BB-SHALE	DGY				MINOR SANDSTONE BANDS
64.39	65.08	CMD		S4U	B			PS	
65.08	65.37	ST		S4U	GY				
65.37	65.48	CMD		S4U	B			PS	MINOR CALCITE PRESENT
65.48	65.82	CD		S4U	B				
65.82	66.01	CMD		S4U	B			PC	
66.01	66.38	SC		S4U	B				
66.38	66.70	CMD		S4U	B			PS	DIAGONAL CROSS CUTTING CALCITE VEINS
66.70	67.06	CD		S4U	B			C	FRACTURED, CALCITE VEINS
67.06	67.22	CMD		S4U	B			PS	MINOR CALCITE VEINS
67.22	67.85	CD		S4U	B				SLICKENSIDES AT TOP
67.85	68.25	S		X-SHALE	DGY				
68.25	68.52	CMD		S4L	B			P	
68.52	68.66	CD		S4L	B			CS	
68.66	68.95	S		S4L	DGY				
68.95	69.31	CMD		S4L	B			SP	
69.31	69.41	S		S4L	DGY				
69.41	69.55	CS	S	S4L	B				CONTAIN SHALE LENSES
69.55	69.80	CMD		S4L	B			PS	HIGH PRESENTS OF SIDERITE
69.80	72.91	SS	ST	O-SHALE	LGY	M			MINOR SILTSTONE BANDS, BROWN SANDSTONE BAND AT BOTTOM, SHARP CONTACT
72.91	73.05	CD		S2U	B				FRACTURES, SHARP CONTACT
73.05	73.19	SS		S2U	W	M			INTERMINGLED WITH COAL

73.19	73.38	CS		S2U	B				
73.38	74.10	S		S2U	DGY				
74.10	74.31	SC		S2U	B				
74.31	74.96	S	SS	S2U	DGY				BROWN SANDSTONE PATCHES
74.96	75.00	CS		S2U	B				SLICKENSIDES
75.00	75.16	CD		S2U	B				
75.16	75.34	SC	S	S2U	B				LIGHT GREY SHALE LENSES AT TOP, BRIGHT BAND IN CENTER
75.34	75.58	S		S2U	DGY				
75.58	75.61	CMD		S2L	B			PC	CALCITE VEINLETS
75.61	76.06	CD		S2L	B				SLICKENSIDES
76.06	76.18	CMD		S2L	B			PC	BROKEN
76.18	76.41	CD		S2L	B				
76.41	76.45	CS	S	S2L	B				LIGHT GREY SHALE LENSES
76.45	76.48	CMD		S2L	B				
76.48	77.07	CD		S2L	B			P	PYRITE PATCHES
77.07	77.19	CMD		S2L	B			C	
77.19	77.23	CD		S2L	B				
77.23	77.28	CS		S2L	B			C	OCCASSIONAL SHALE LENSES
77.28	79.35	CD		S2L	B			C	CALCITE VEINS, SLICKENSIDES
79.35	80.00	CMD		S2L	B			PC	CALCITE VEINS, SLICKENSIDES
80.00	80.77	CD		S2L	B			C	SHALE LENSES, SLICKENSIDES WITH CALCITE INFILLING
80.77	81.26	CMD		S2L	B			PC	BROKEN
81.26	81.36	CD		S2L	B				
81.36	81.45	CMD		S2L	B				
81.45	81.51	CD		S2L	B				
81.51	81.58	CMD		S2L	B				
81.58	81.68	CD		S2L	B				

81.68	82.40	CMD		S2L	B			PS	FEW CALCITE VEINLETS
82.40	82.47	CD		S2L	B				
82.47	82.87	CMD		S2L	B			P	SHALE BANDS AT BOTTOM
82.87	82.95	SS		S2L	LGY				LAMINATED, WITH SHALE INTERMINGLED
82.95	83.10	CMD		S2L	B				
83.10	83.15	SS		S2L	GY				
83.15	83.36	CD		S2L	B			P	BRIGHT BANDS
83.36	83.46	CS		S2L	B				LIGHT GREY SHALE LENSES
83.46	85.38	T			LGY				END OF HOLE